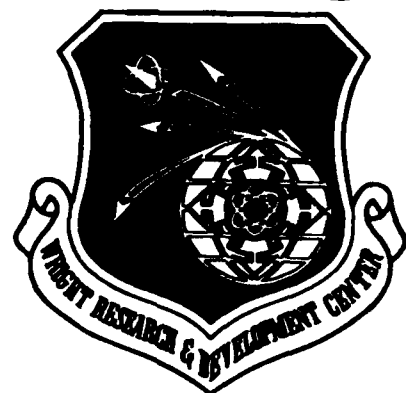WRDC-TR-89-3067
VOLUME I

AD-A221 970

DAMAGE TOLERANCE ANALYSIS FOR MANNED HYPERVELOCITY VEHICLES

VOLUME I - FINAL TECHNICAL REPORT

D.M. HARMON
C.R. SAFF

McDonnell Aircraft Company
McDonnell Douglas Corporation
P.O. Box 516
St. Louis , Missouri 63166

September 1989

Final Report For Period
September 1986 - September 1989
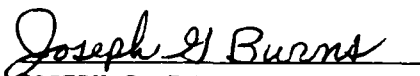
DTIC
MAY 2 1990

NOTICE

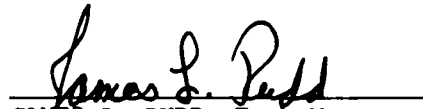When Government drawings, specifications, or other data are used for any purpose other than in connection with a definitely Government-related procurement, the United States Government incurs no responsibility or any obligation whatsoever. The fact that the government may have formulated or in any way supplied the said drawings, specifications, or other data, is not to be regarded by implication, or otherwise in any manner construed, as licensing the holder, or any other person or corporation; or as conveying any rights or permission to manufacture, use, or sell any patented invention that may in any way be related thereto.

This report is releasable to the National Technical Information Service (NTIS). At NTIS, it will be available to the general public, including foreign nations.

This technical report has been reviewed and is approved for publication.
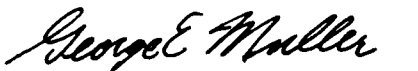

JOSEPH G. BURNS
Project Engineer

JAMES L. RUDD, Tech Manager
Fatigue, Fracture & Reliability Group
Structural Integrity Branch

FOR THE COMMANDER

GEORGE E. MULLER, Chief
Structural Integrity Branch
Structures Division

If your address has changed, if you wish to be removed from our mailing list, or if the addressee is no longer employed by your organization please notify WRDC/FIBE, WPAFB, OH 45433-6553 to help us maintain a current mailing list.

Copies of this report should not be returned unless return is required by security considerations, contractual obligations, or notice on a specific document.

REPORT DOCUMENTATION PAGE

1a. REPORT SECURITY CLASSIFICATION UNCLASSIFIED		1b. RESTRICTIVE MARKINGS		

2a. SECURITY CLASSIFICATION AUTHORITY N/A	3. DISTRIBUTION/AVAILABILITY OF REPORT
2b. DECLASSIFICATION/DOWNGRADING SCHEDULE N/A	Approved for public release; Distribution is unlimited.

4. PERFORMING ORGANIZATION REPORT NUMBER(S)	5. MONITORING ORGANIZATION REPORT NUMBER(S) WRDC-TR-89-3067, Vol I

6a. NAME OF PERFORMING ORGANIZATION McDonnell Aircraft Co.	6b. OFFICE SYMBOL (If applicable)	7a. NAME OF MONITORING ORGANIZATION Flight Dynamics Laboratory (WRDC/FIBEC) Wright Research and Development Center

6c. ADDRESS (City, State, and ZIP Code) P.O. Box 516 St. Louis, MO 63166	7b. ADDRESS (City, State, and ZIP Code) WRDC/FIBEC Wright-Patterson AFB, OH 45433-6553

8a. NAME OF FUNDING/SPONSORING ORGANIZATION	8b. OFFICE SYMBOL (If applicable)	9. PROCUREMENT INSTRUMENT IDENTIFICATION NUMBER F33615-86-C-3208

8c. ADDRESS (City, State, and ZIP Code)	10. SOURCE OF FUNDING NUMBERS			
	PROGRAM ELEMENT NO 62201F	PROJECT NO. 2401	TASK NO 01	WORK UNIT ACCESSION NO. 99

11. TITLE (Include Security Classification)

Damage Tolerance Analysis for Manned Hypervelocity Vehicles, Volume I - Final Technical Report

12. PERSONAL AUTHOR(S)
D. M. Harmon

13a. TYPE OF REPORT Final	13b. TIME COVERED FROM Sept 86 TO Sept 89	14. DATE OF REPORT (Year, Month, Day) 1989 September	15. PAGE COUNT 176

16. SUPPLEMENTARY NOTATION

17. COSATI CODES			18. SUBJECT TERMS (Continue on reverse if necessary and identify by block number)
FIELD	GROUP	SUB-GROUP	CRACK GROWTH, THERMOMECHANICAL FATIGUE
11	06	01	METALS, HYPERVELOCITY VEHICLES,
01	03	12	

19. ABSTRACT (Continue on reverse if necessary and identify by block number)

The objective of this program was to provide a fracture mechanics based life prediction procedure for hypersonic airframe structures subjected to combined mechanical loadings and thermal profiles. Existing routines were used along with element test data to develop this procedure. The accuracy of the procedure was determined by predicting the crack growth under thermomechanical load histories typical of advanced fighters and aerospace vehicles, and then comparing those predictions with test results. Limitations in the ability of this procedure to predict the test results were used to formulate recommendations for further modeling efforts and research.

A fracture mechanics based life prediction procedure was developed for hypersonic airframes subjected to thermomechanical load profiles. The analysis that was developed models crack growth behavior in metals, accounts for the effects of temperature on yield strength and fracture toughness, and includes the effects of sustained loads at elevated temperature on crack growth rate. The analysis was incorporated into a computer (cont'd)

20. DISTRIBUTION/AVAILABILITY OF ABSTRACT ☒ UNCLASSIFIED/UNLIMITED ☐ SAME AS RPT ☐ DTIC USERS	21. ABSTRACT SECURITY CLASSIFICATION UNCLASSIFIED	
22a. NAME OF RESPONSIBLE INDIVIDUAL Joseph G. Burns	22b. TELEPHONE (Include Area Code) (513) 255-6104	22c. OFFICE SYMBOL WRDC/FIBEC

DD Form 1473, JUN 86   *Previous editions are obsolete.*   SECURITY CLASSIFICATION OF THIS PAGE

19. ABSTRACT (Cont'd)

routine named DAMAGE. Predictions made with the DAMAGE routine were within 20 percent of the test lives for 67 percent of the combined thermomechanical load history tests performed. *Keywords:*

FOREWORD

This report was prepared by McDonnell Aircraft Company (MCAIR), St. Louis, Missouri, for the Structural Integrity Branch, Structures Division, Flight Dynamics Laboratory, Wright Research and Development Center, Wright-Patterson Air Force Base, Ohio under contract F33615-86-C-3208, Project 2401, Work Unit, 24010199, "Damage Tolerance Analysis for Manned Hypervelocity Vehicles." The contract monitor was Joseph G. Burns, WRDC/FIBEC. The period of performance for this contract was September 1986 through September 1989.

The Structural Research Department of McDonnell Aircraft Company was responsible for the performance of this program. The Program Manager was Charles R. Saff. Principal Investigator and principal author of this report was David M. Harmon.

Dr. Stephen D. Antolovich, of Georgia Institute of Technology, was a primary subcontractor, contributing creep and fatigue testing.

Accession For		
NTIS GRA&I	☒	
DTIC TAB	☐	
Unannounced	☐	
Justification		
By		
Distribution/		
Availability Codes		
Dist	Avail and/or Special	
A-1		

TABLE OF CONTENTS

TABLE OF CONTENTS - Continued

LIST OF ILLUSTRATIONS

LIST OF ILLUSTRATIONS - Continued

SECTION I

INTRODUCTION

Implementation of the Air Force structural integrity philosophy as defined in MIL-STD-1530A requires efficient, accurate, and cost effective prediction of crack growth behavior under complex combinations of mechanical loading and chemical/thermal environments. Current Air Force airframe structural life predictions are based on isothermal analyses, because the short times at high temperatures have little effect on life prediction. At most a "worst case" temperature is selected for limited testing and to generate allowables for high temperature areas of the structure.

In the aircraft engine industry, life analyses emphasize other parameters. The engine environment dictates that temperature, load frequency, and stress ratio effects be modeled accurately, while the mechanical load interaction effects are either ignored or simplified. Temperature variations have been much more accurately modeled, analyzed, and tested for engine environments than for airframes.

For the airframe structures engineer the ever-increasing mission requirements for Air Force hypervelocity and high Mach number aircraft is bringing temperature effects into increased prominence. Tests have shown that the thermal-mechanical load profiles experienced by such vehicles can produce lives considerably shorter than those predicted by "worst case" isothermal test data and analyses. Currently, no universally accepted analysis technique predicts this effect. Therefore, the goal of this program was to use the experience of the engine and airframe communities to provide a viable engineering tool to design "hot structures". Further research may later provide a more accurate tool for predicting crack growth in structures subject to thermo-mechanical loadings.

The objective of this program was to provide a fracture mechanics based life prediction procedure for hypersonic airframe structures subjected to combined mechanical loadings and thermal profiles. Existing routines were used along with element test data to develop this procedure. The accuracy of

1

the procedure was determined by predicting the crack growth in inconel and titanium test specimens subject to thermo-mechanical load profiles typical of those to be experienced by advanced fighters and advanced aerospace vehicles. We then compared the predictions with test results. Limitations in the ability of this procedure to predict the test results were used to recommend further modeling and research.

SECTION II

EXECUTIVE SUMMARY

A five task program was performed to develop a fracture mechanics based life prediction procedure for hypersonic airframe structures subjected to combined mechanical and thermal loadings. The five tasks were: 1) selection of a baseline procedure, 2) development of a combined thermal/mechanical model, 3) incorporation of this model into a state-of-the-art computer code for life prediction, 4) verification of the life prediction procedure, and 5) recommendations for future modeling efforts. The program was conducted over a period of 30 months.

In the first task, literature was surveyed and crack growth life prediction methods at elevated temperatures were documented. The literature survey is summarized in the Appendix. Based on this survey, a baseline crack growth life prediction methodology was selected for further development. CRKGRO was selected because of its familiarity to the aerospace community, its widely available and well-written documentation, and its modular coding style which easily permits modifications.

The Model Development Task was divided into two parts: analytical model development and supporting experimental work. The analytical model development efforts included incorporation of a temperature dependent version of the Modified Walker equation for fitting crack growth data, the Wei-Landes approach for time dependent crack growth acceleration under aggressive environments, Larson-Miller data for the effect of time at temperature on yield strength reduction, techniques for determining the instantaneous effect of temperature on yield strength and fracture toughness, and a method for predicting the effect of temperature on crack growth retardation. The resulting routine was named DAMAGE, Damage Analysis of Metals subjected to AGgressive Environments.

The test program was shared between McDonnell Aircraft Company (MCAIR) and Georgia Tech Research Corporation, under the guidance of Dr. Stephen Antolovich. In general, baseline constant amplitude crack growth testing

under a wide variety of elevated temperatures and frequencies was performed by Georgia Tech, and static and combined mechanical-thermal load spectrum tests were performed by MCAIR. Inconel 718 (IN 718) and 6Al-2Sn-4Zr-2Mo titanium (6-2-4-2 Ti) were selected for this testing because they can withstand temperatures up to 1000°F. Also, the two materials exercise different aspects of the crack growth model.

The objectives of the third task were to incorporate into CRKGRO all of the analysis techniques identified in Task 2 as required to predict the growth of cracks under combined mechanical and thermal loadings. Another objective is to make the routine user-friendly for the interactive computer user. The computer routine modules were simplified and were documented within the routine so that the user will not have to continually reference the user's manual. The input module was expanded to allow input of thermal history data along with the mechanical loading history and additional crack growth rate data for elevated temperatures. Additional error trapping was performed in the input module to minimize the chance that typing errors would prematurely terminate the program. All of these enhancements to the code are documented in the User's Manual, Reference 1.

The new computer code was used in the Verification Task to predict the crack growth in IN 718 and 6-2-4-2 titanium test specimens subject to combined mechanical and thermal load profiles typical of an advanced fighter aircraft and an advanced aerospace vehicle. Predictions were made for both of these spectra to determine the primary parameters affecting crack growth life. The predictions explored stress level effects, temperature effects, and load truncation effects. All of these effects were evaluated in a series of verification tests. Both the 6-2-4-2 titanium and IN 718 materials were tested. While the majority of the predictions matched the test lives within 20 percent, trends in the correlation suggest that the simple techniques in this routine cannot be used to extrapolate the test data extensively.

The limitations of the analysis methods, materials, and test data evaluated within this program lead to six recommendations for further study of the prediction of crack growth under combined thermal and mechanical load histories. These include: 1) a more comprehensive investigation of different

crack growth rate models (such as those being developed by the engine community), 2) a better method for incorporating creep effects on the crack growth rate, 3) enhancement of the Wei-Landes method to investigate load and temperature phasing effects on sustained load crack growth, 4) investigation of a closure model for the prediction of load interaction effects, 5) further testing of environmentally sensitive materials, and 6) additional spectrum testing for further analysis correlation.

SECTION III

BASELINE PROCEDURE SELECTION

1. <u>Literature Review</u> - Over 250 abstracts of papers summarizing tests and analyses of elevated temperature crack growth for various metals were reviewed prior to selection of a baseline analysis procedure. Our objective was to summarize test results to provide a background for the testing to be performed in this program. A catalog containing each paper pertinent to the type of testing performed in this contract resides on a computer file. Each listing includes the paper's title, author, and a brief summary. This catalog is provided in the Appendix.

The listing has been divided into three separate categories: Analysis Methods, Test Data, and Test Methods. The Analysis Methods section includes papers which model crack growth of metals at elevated temperatures. Methods are discussed which predict crack growth rate at elevated temperatures, determine the effects of frequency, creep, and stress ratio on crack growth, predict crack growth retardation due to creep, and determine crack growth acceleration due to environmental conditions. A variety of elevated temperature fatigue tests have been performed on inconel and titanium specimens. Data on these materials, as well as on titanium aluminide, was emphasized in the Test Data section. Only two papers are listed in the Test Method section. These papers discuss the use of the electric potential drop method and the crack opening displacement method for measuring crack growth.

2. <u>Baseline Computer Program Selection</u> - CRKGRO was selected as the baseline crack growth life prediction procedure because of its completeness, accuracy, simplicity, familiarity to investigators, and available documentation. CRKGRO is a room temperature crack growth prediction routine developed by Rockwell International. It is clearly and concisely documented in Reference 2. This model is well known by investigators researching or designing analyses for Air Force aircraft. It contains all of the analytic tools necessary for room temperature crack growth analysis of metals subjected to spectrum loading.

7

There are many ways to perform each step of a crack growth analysis. Investigators do not agree as to which technique is best for any particular analysis step. For example, to input dc/dN data and accommodate stress ratio effects, one could use equations or tables and interpolation. The industry's familiarity with CRKGRO, together with its sound analytical capabilities, presented a logical foundation upon which we added elements describing material and structural behavior under a full range of thermal environments.

3. <u>CRKGRO Summary</u> - The CRKGRO program is summarized in the flow chart presented in Figure 1, duplicated from Reference 2. There are four major components of the CRKGRO program: 1) the crack growth rate model, 2) the load interaction model, 3) the damage accumulation routine, and 4) the stress intensity library.

a. <u>Crack Growth Rate Model</u> - The baseline fatigue crack growth rate equation in CRKGRO combines the Modified Walker equation for positive stress ratios and the Chang equation for negative stress ratios:

for $R \geq 0$ and $\Delta K > \Delta K_{th}$

$$dc/dN = C \, [\Delta K \, (1-R)^{M-1}]^N$$

for $R < 0$ and $\Delta K > \Delta K_{th}$

$$dc/dN = C \, [(1+R^2)^Q K_{max}]^N$$

and for $\Delta K \leq \Delta K_{th}$

$$dc/dN = 0$$

where C and N are growth rate constants for R=0, and M and Q are empirical exponents based on tests at other stress ratios.

The threshold value of ΔK is determined by

$$\Delta K_{th} = (1 - A \, R) \, \Delta K_{th0}$$

8
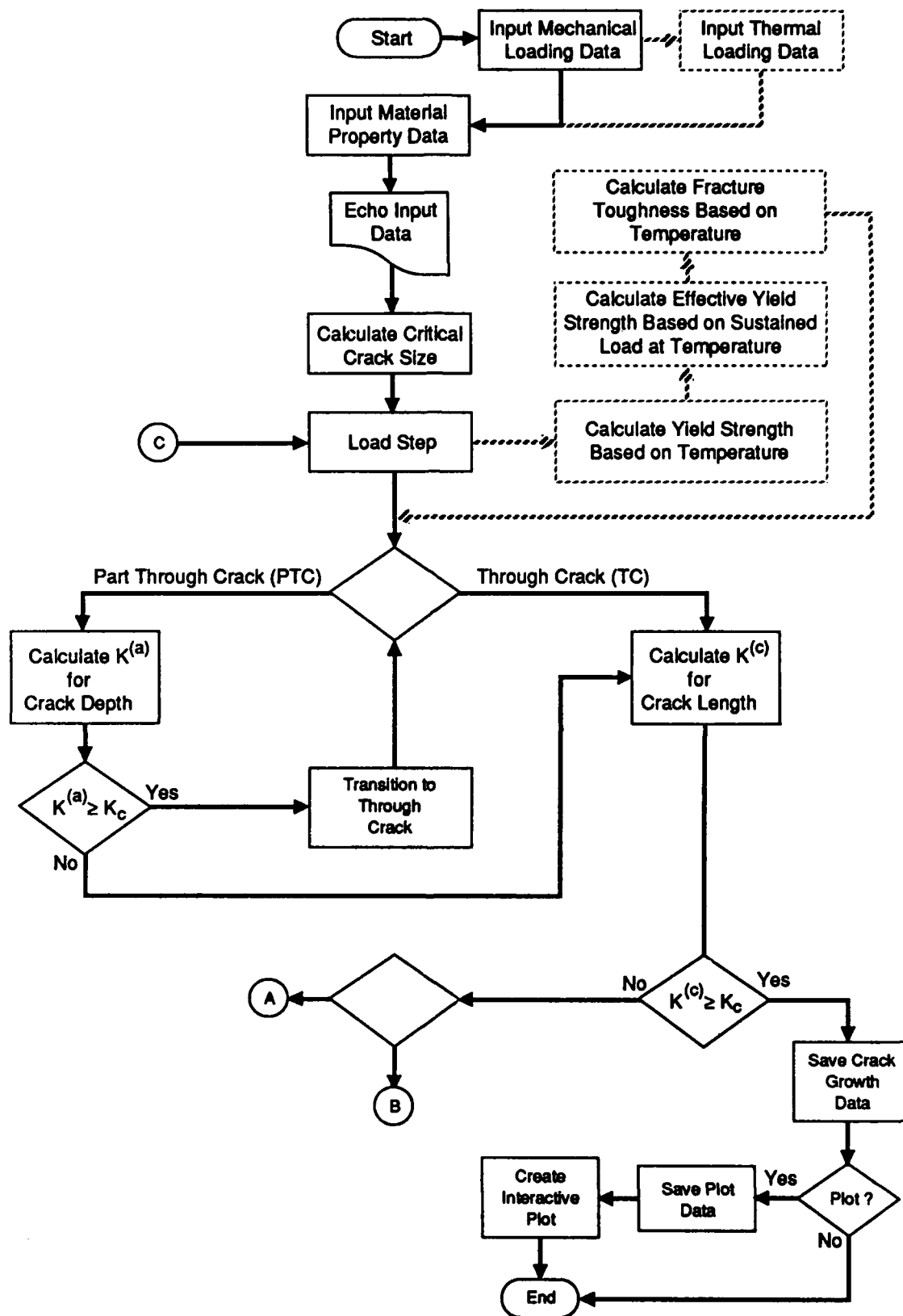
Figure 1. CRKGRO/DAMAGE Flow Chart

9

Calculate $R^{(a)}$ and $\Delta K^{(a)}$

Calculate Pastic Zone, $\rho_i^{(a)}$

$a_i + \rho_i \geq a_{OL} \rho_{OL}$

Yes (No Retardation)

No (Retardation)

$a_{OL} = a_i$
$\rho_{OL}^{(a)} = \rho_i$

Willenborg Model
$\Delta K^{(a)} = \Delta K_{eff}^{(a)}$
$R^{(a)} = R_{eff}^{(a)}$

$R^{(a)} \geq 0$

No

Chang Acceleration Scheme
$\rho_{OL}^{(a)} = [1 + R^{(a)}] \, \rho_{OL}^{(a)}$

Yes

Wei-Landes
Calculate Sustained
Load Crack
Growth Rate
da/dT

$R^{(a)} \geq 0$

Chang Equation
Calculate Cyclic Crack
Growth Rate
da/dN

No

Yes

Walker Equation
Calculate Cyclic Crack
Growth Rate
da/dN

Calculate Total Crack
Growth Rate
$$\frac{da}{dN} = \frac{da}{dN} + \frac{da}{dT}\left(\frac{dT}{dN}\right)$$

Vroman Method
Calculate Δa

Calculate Crack Depth
$a_i = a_{i-1} + \Delta a$

A

B

GP93-0418-109-D

Figure 1. (Cont.) CRKGRO/DAMAGE Flow Chart
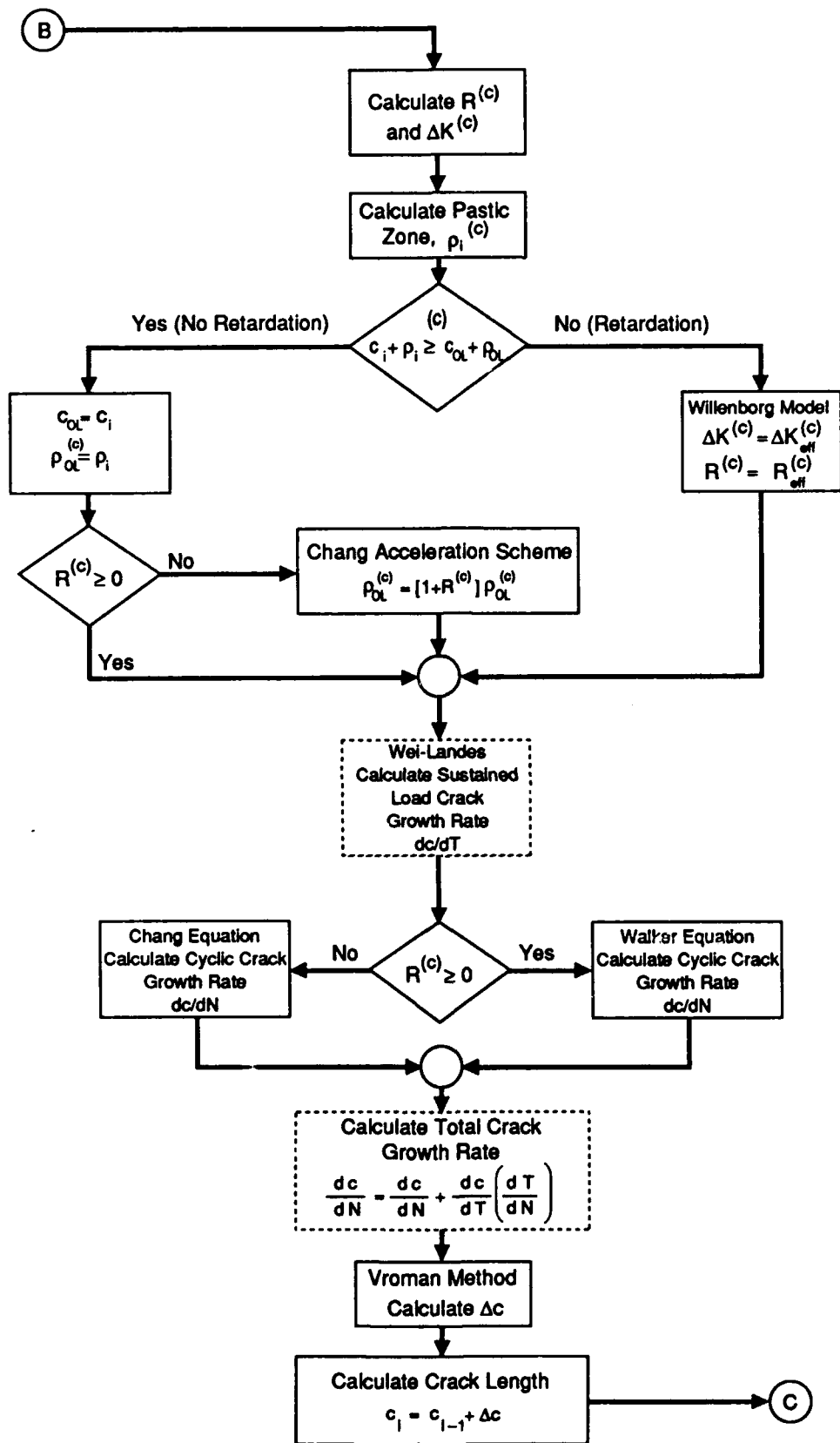
Figure 1. (Concluded) CRKGRO/DAMAGE Flow Chart

11

where ΔK_{th0} is the threshold value obtained from R = 0 constant amplitude tests and A is an empirical constant obtained from constant amplitude data with various stress ratios.

b. **Load Interaction Model** - The load interaction model in CRKGRO combines the Generalized Willenborg model for tensile overloads, with a reduction in overload zone size proposed by Chang for compressive underloads. Both of these models are described thoroughly in References 3 - 8.

The original Willenborg model predicts crack growth retardation due to overload cycles in the load spectrum. Figure 2 presents a drawing of a crack and its associated enclave of plastically deformed material following an overload. The crack length at which the overload occurred and the plastic zone created by the overload are c_{ol} and ρ_{ol}, respectively. The crack length associated with a load cycle following the overload is represented by c_i. Similarly, the instantaneous plastic zone associated with the same load cycle is designated as ρ_i.
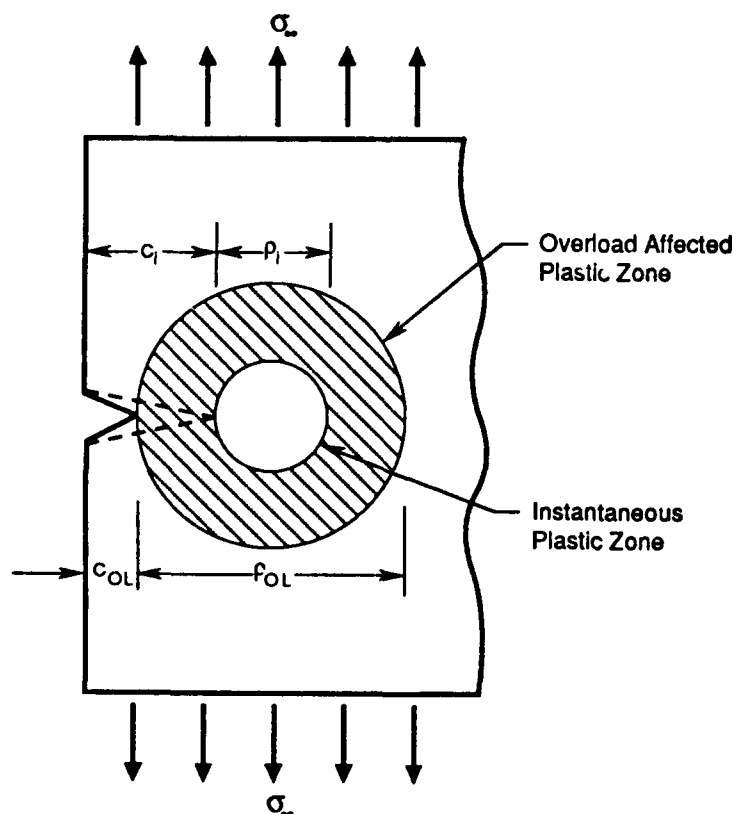
GP93-0418-16-D

Figure 2. Plastic Zone at Crack Tip

The underlying principle of the Willenborg model is that crack growth retardation will occur after an overload as long as:

$$c_i + \rho_i < c_{ol} + \rho_{ol}.$$

These sums are defined as the instantaneous interaction zone, z_i, and the overload interaction zone, z_{ol}, respectively. The model calculates an effective stress intensity, ΔK_{eff}, and an effective stress ratio, R_{eff}, to reduce the crack growth rate while the crack is growing under the influence of the overload.

The applied stresses, $\sigma_{\infty max}$ and $\sigma_{\infty min}$, for load cycles after the overload cycle, are reduced by an amount equal to the additional applied stress, σ_{red}, required to extend the instantaneous interaction zone to that created by the overload.

$$\sigma_{eff-max} = \sigma_{\infty max} - \sigma_{red}$$
$$\sigma_{eff-min} = \sigma_{\infty min} - \sigma_{red}$$

By definition, therefore,

$$\sigma_{red} = \sigma_{req} - \sigma_{\infty max}$$

where σ_{req} is the total stress required to stop the retardation effect. The effective stress intensity, ΔK_{eff}, is calculated using the standard fracture mechanics formulae.

$$K_{eff-max} = \sigma_{eff-max} (\pi c)^{1/2} \beta;$$

for $\sigma_{eff-min} > 0$

$$K_{eff-min} = \sigma_{eff-min} (\pi c)^{1/2} \beta;$$

for $\sigma_{eff-min} \leq 0$

$$K_{eff-min} = 0.$$

The effective stress intensity range is calculated as:

$$\Delta K_{eff} = K_{eff\text{-}max} - K_{eff\text{-}min} = (\sigma_{eff\text{-}max} - \sigma_{eff\text{-}min}) \, (\pi c)^{1/2} \, \beta = \Delta K$$

and the effective stress ratio is calculated as:

$$R_{eff} = K_{eff\text{-}min}/K_{eff\text{-}max}$$

Thus the Willenborg model reduces the stress ratio below that which was applied, but does not change the stress intensity range. The model will retard crack growth until the current load interaction zone extends to the end of the overload interaction zone.

An expression for σ_{req} is obtained through the plastic zone size equation, which differs for plane stress and plane strain conditions. In CRKGRO, the plane strain plastic zone size is used at the depth of a part-through crack. The plane stress plastic zone size is used along the length of through cracks and part-through cracks. The plane stress and plane strain plastic zone sizes for any load cycle are:

$$\rho = \gamma \, (K_{\infty max}/F_{ty})^2/(2\pi)$$

where

$$\gamma = 1 - \text{plane stress}$$
$$\gamma = 1/3 - \text{plane strain}$$

F_{ty} is the material tensile yield strength and $K_{\infty max}$ is the maximum applied stress intensity factor. At the point where crack growth retardation stops, one can express the interaction zone as:

$$z_{ol} = c_{ol} + \rho_{ol} = c_i + \rho_{req} = z_{req}$$

Substituting in the plastic zone expression, the following is obtained:

$$z_{ol} - c_i = \rho_{req} = \gamma \, (K_{req}/F_{ty})^2/(2\pi)$$

14

Finally, the equation for σ_{req} is derived by substituting in the actual expression for K_{req} and rearranging terms.

$$\sigma_{req} = F_{ty} [2(c_{ol} + \rho_{ol} - c_i)/(c_i \ \gamma)]^{1/2}/\beta$$

or

$$\sigma_{req} = F_{ty} [2(\rho_{ol} - \Delta c)/(c_i \ \gamma)]^{1/2}/\beta$$

This expression can also be written in terms of the overload stress, σ_{ol}, by rewriting the expression for the plastic zone as:

$$F_{ty} = K_{ol-max} [\gamma/(2\pi\rho_{ol})]^{1/2} = \sigma_{ol-max} \ \beta \ [\gamma \ c_i/(2\rho_{ol})]^{1/2}$$

where K_{ol-max} is the stress intensity corresponding to the overload. Substitution into the expression for σ_{req} then gives

$$\sigma_{req} = \sigma_{ol-max} (1 - \Delta c/\rho_{ol})^{1/2}$$

Because the Willenborg model truncates applied loads at zero, the model predicts that crack growth will be shut-off when $K_{eff-max} = 0$. When crack growth is shut-off, $\Delta c = 0$. Mathematically, shut-off will occur when the ratio of $K_{ol-max}/K_{\infty max}$ (known as the overload shut-off ratio, R_{SO}) equals 2. This is shown by substituting the expression for σ_{red} into the equation for $K_{eff-max}$.

$$K_{eff-max} = (\sigma_{\infty max} - \sigma_{red}) (\pi c)^{1/2} \beta = (2\sigma_{\infty max} - \sigma_{req}) (\pi c)^{1/2} \beta$$

Substituting in the stress intensity terms, this equation can be expressed as:

$$K_{eff-max} = K_{\infty max} - [K_{ol-max} (1 - \Delta c/\rho_{ol})^{1/2} - K_{\infty max}]$$

When shut-off occurs, $K_{eff-max} = 0$ and $\Delta c = 0$ and:

$$0 = 2 K_{\infty max} - K_{ol-max}$$

15

Research has shown that for some materials the overload shut-off ratio can be greater than 2 (References 5 and 6). The Generalized Willenborg model was developed by Gallagher and Hughes (Reference 7) to address this issue.

The Generalized Willenborg model predicts that when crack growth is shut-off, $K_{eff-max}$ equals the maximum threshold stress intensity of the material, K_{th-max}. The expressions for the effective stress intensities become:

$$K_{eff-max} = K_{\infty max} - \phi \left[K_{ol-max} (1 - \Delta c/\rho_{ol})^{1/2} - K_{\infty max}\right]$$

$$K_{eff-min} = K_{\infty min} - \phi \left[K_{ol-max} (1 - \Delta c/\rho_{ol})^{1/2} - K_{\infty max}\right]$$

where

$$\phi = (1 - K_{th-max}/K_{\infty max})/(R_{so} - 1)$$

$$R_{so} = K_{ol-max}/K_{\infty max}$$

The overload shut-off ratio, R_{so}, is obtained from test data. The variable, ϕ, is introduced in CRKGRO when σ_{red} is calculated.

$$\sigma_{red} = (\sigma_{req} - \sigma_{\infty max}) \phi$$

The reduction of the overload retardation effect caused by a compressive underload is accounted for through the "effective overload interaction zone" concept proposed by Chang (Reference 8). In this model, the plastic zone size is modified in terms of the negative effective stress ratio ($R_{eff} \leq 0$) as:

$$\rho_{eff} = (1 + R_{eff}) \rho$$

c. <u>Damage Accumulation Technique</u> - Damage accumulation in CRKGRO is based on the Vroman Linear approximation method. In this method, the crack growth for a given stress step is assumed to be 1 percent of the current crack

16

length. The stress steps are input by the user and consist of a number of constant amplitude cycles, N, in which the stress varies from the maximum stress in the cycle, σ_{max}, to the minimum stress in the cycle, σ_{min}.

For a given stress step, the crack growth rate, dc/dN, is calculated using the Modified Walker equation. The crack growth for the step is assumed to be $\Delta c = 0.01c$, where "c" is the instantaneous crack length. The number of cycles in the stress step, N, is then compared to the actual number of cycles required to achieve the assumed crack growth:

$$N_{act} = 0.01\ c\ /\ (dc/dN)$$

If $N_{act} > N$, then

$$\Delta c_{act} = N\ dc/dN$$

$$c = c + \Delta c_{act}$$

The analysis then proceeds to the next stress step.

If $N_{act} \leq N$, then
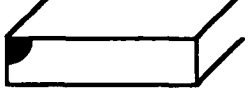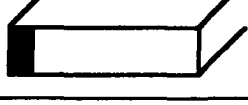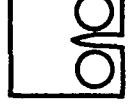
$$\Delta c_{act} = \Delta c = 0.01\ c$$

$$c = c + \Delta c$$

One must then examine the remaining cycles in this stress step, $N_{rem} = N - N_{act}$. The procedure described above is repeated until all of the cycles in the step have been examined. At that point, the analysis proceeds to the next stress step.

d. <u>Geometric Capabilities</u> - An extensive library of stress intensity factor solutions is available in CRKGRO, summarized in Figure 3. The CRACK library module consists of ten subroutines, each containing one stress intensity solution. For part-through cracks, shape change is predicted based on the assumption that growth in the two directions can be characterized by

the stress intensities at the extreme points. Compound solutions expressed in polynomial form are typically used in these routines to summarize the effects of width, thickness, crack depth, crack length, and crack aspect ratio.

Code No.	Description	Geometry
1010	Center Surface Crack	
1030	One Corner Crack from Center Open Hole	
1050	Two Corner Cracks from Center Open Hole	
1070	One Corner Edge Crack	
2010	Center Crack	
2020	One Crack from Center Open Hole	
2030	Two Cracks from Center Open Hole	
2040	One Edge Crack	
2050	Two Edge Crack	
2060	ASTM Compact Tension Specimen	

GP93-0007-663-D

Figure 3. Stress Intensity Factor Solutions
CRKGRO

18

SECTION IV

MODEL DEVELOPMENT TESTING

1. Testing Summary - The purpose of the model development testing is to gain an understanding of the effects of temperature and environment on the strength and fatigue properties of metals. To exercise the analytical models, two metals were chosen for testing which possess different elevated temperature characteristics. These materials were Inconel 718 (IN 718) and 6Al-2Sn-4Zr-2Mo titanium (6-2-4-2 Ti).

Static and creep tests were performed to determine the maximum temperature capability of the materials. Constant amplitude fatigue crack growth tests provided crack growth rate vs. stress intensity data at room temperature and at two elevated temperatures. These tests examined the effect of stress ratio, environment, and hold time at peak load on the crack growth behavior. Constant amplitude tests with occasional overloads were also performed to determine the retardation effects on crack growth. Some of the overloads were immediately followed by an underload. Finally, a series of spectrum load crack growth tests were conducted to examine the effects of a random load profile on crack growth. These tests were conducted under constant temperature.

The testing was completed by McDonnell Aircraft Company (MCAIR) and Georgia Institute of Technology (Georgia Tech). MCAIR performed the static tension tests, two constant amplitude fatigue tests per material, and all of the spectrum load fatigue tests. Georgia Tech, under the supervision of Dr. S. D. Antolovich, was responsible for the creep tests, the majority of the constant amplitude fatigue tests (including all vacuum tests), and all of the overload and overload/underload fatigue tests. The few constant amplitude tests performed by MCAIR were also run at Georgia Tech for comparison.

2. Material Selection - Two readily available test materials were chosen for this program: Inconel 718 (IN 718) and 6Al-2Sn-4Zr-2Mo titanium (6-2-4-2 Ti). These materials were selected because they have different sensitivities to temperature (Figure 4). Also, both materials already had an extensive data
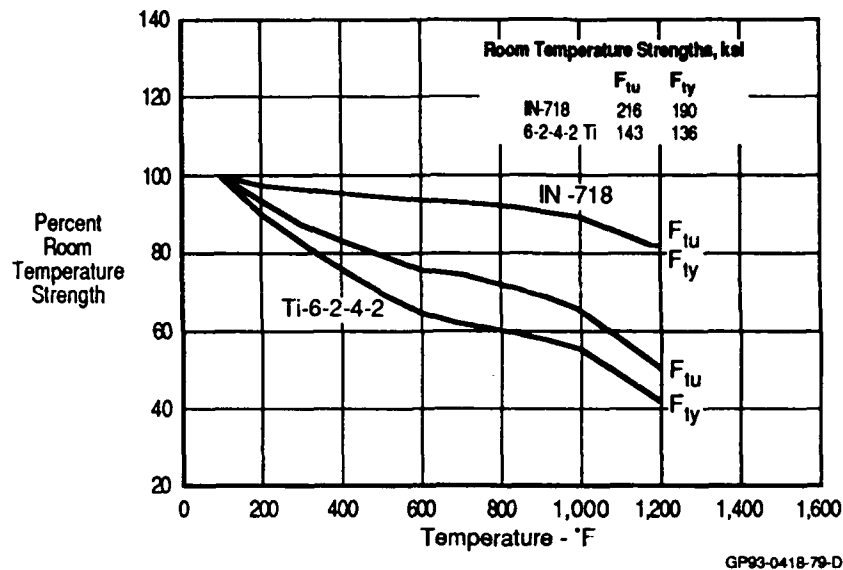
Figure 4. Material Strength at Temperature

base, as noted in Figure 5, and therefore required minimal testing. These materials respond to elevated temperatures, hold times, and changes in environment, and as a result, thoroughly test the predictive model. Model development is discussed in Section V.

IN 718 has many applications in the engine industry, due to its excellent strength at elevated temperatures. Still, it does creep under sustained load at high temperatures as shown in Figure 6. In addition, crack growth in IN 718 under sustained loads at high temperatures is sensitive to chemical environments. Figure 7 shows the effect of air and vacuum environments on sustained load crack growth at 1200°F.

6-2-4-2 Ti is the best readily available titanium for high temperature applications. With a room temperature structural efficiency (strength/ density) greater than that of IN 718 (~1.4:1), 6-2-4-2 Ti is suitable for many applications. Its strength and creep behaviors are more sensitive to temperature than IN 718's (Figures 4 and 6). However, 6-2-4-2 Ti is much less sensitive to changes in the environment while under sustained loads at high temperatures. The differences in the behaviors of IN 718 and 6-2-4-2 Ti made them excellent materials for model evaluation. They allow independent evaluation of creep and environmental sensitivity effects on crack growth.

20

Material	Useful Temp Range – °F Based on 100 hr Exposure at Temp	Strength Properties			Residual Strength After High Temp Exposure	Creep	Fracture Toughness			Fatigue			Effect of Service Environment	Physical Properties		
		Low Temp	Room Temp	High Temp			Low Temp	Room Temp	High Temp	Low Temp	Room Temp	High Temp		Low Temp	Room Temp	High Temp
Aluminum Alloys	423 to 400	●	●			●	●	●			●		●	●	●	●
Titanium Alloys																
6Al-4V, 6Al-4V ELI	423 to 750	●	●		●			●			●				●	●
5Al-2 5Sn, 5Al-2 5Sn ELI	423 to 600	●	●					●			●				●	●
Ti-6242	? to 1,100		●									●			●	●
Ti-5522S	? to 1,100															
Ti-11	? to 1,100			●												
Ti-5621S	? to 1,200															
Titanium Aluminides	? to 1,400															
Superalloys																
A-286	320 to 1,200		●								●	●				●	●
Inconel 718	423 to 1,300	●	●								●	●					●
Rene' 41	423 to 1,600	●	●								●					●	●
Udimet 500	? to 1,600		●								●					●	●
L-605	423 to 1,800	●	●													●	●
Hastelloy X	? to 1,800		●								●	●				●	●
HS-188	423 to 2,000	●	●								●					●	●
Cabot No. 214	? to 2,000		●													●	
Refractory Alloys																
TZM (Molybdenum Base)	70 to 2,400		●				●									●	●
FS-85 (Columbium Base)	320 to 2,400		●													●	●
T-222 (Tantalum Base)	320 to 2,800		●													●	●

Legend

● Substantial amount of data available. Little or no additional testing required.

·· Significant amount of data available. Additional testing required.

: Preliminary data only.

· No significant amount of data available.

| MCAIR Choices |

GP93-0418-1-T

Figure 5. Data Base of Different Materials
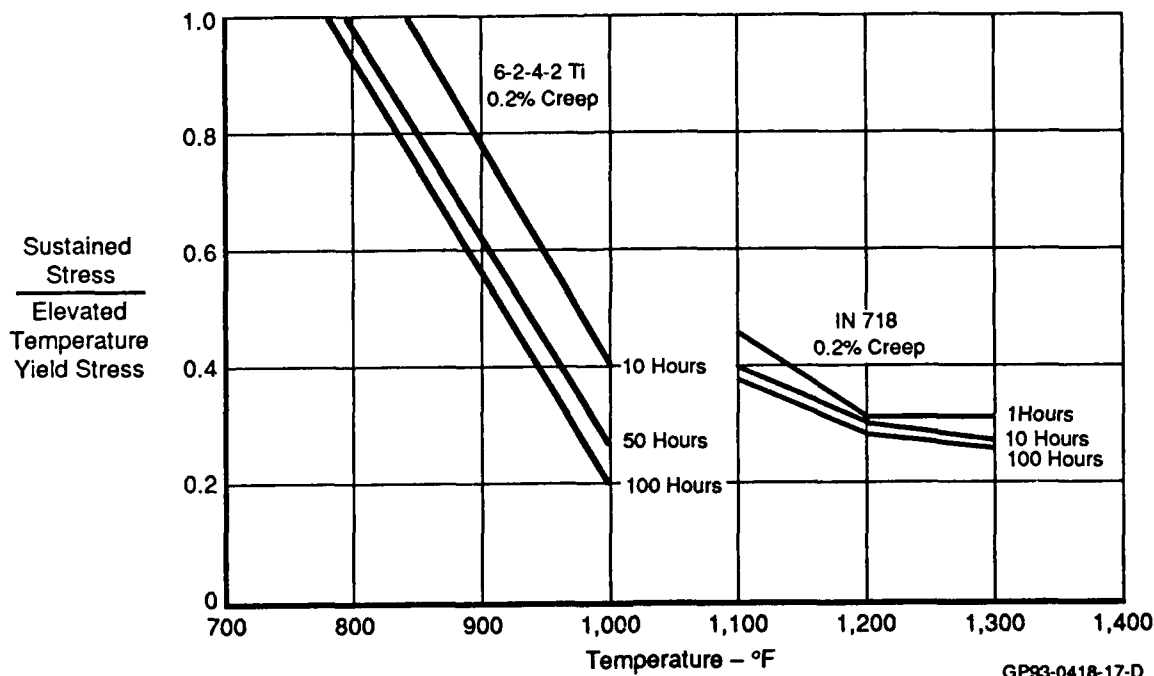
Figure 6. Creep Characterization of IN 718 and 6-2-4-2 Ti

GP93-0418-17-D

21
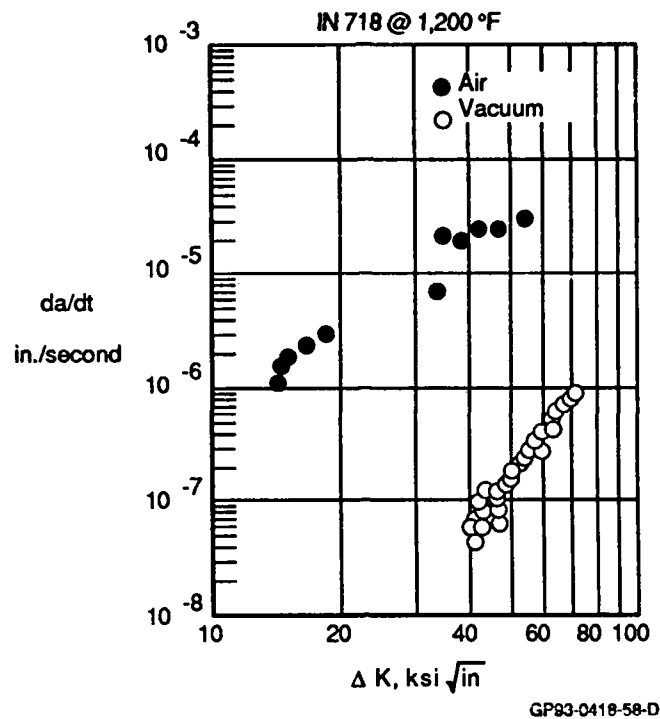
Figure 7. Environmental Sensitivity of IN 718 to Sustained Load Crack Growth
(Strucke, Khobiab, Majumdar, and Nicholas; 1984)

3. <u>Temperature Selection</u> - The model development test matrix is shown in Figure 8. The test temperatures for both IN 718 and 6-2-4-2 Ti were originally specified as room temperature (78°F), 700°F, and 1200°F. 700°F and 1200°F represent extreme temperatures for advanced fighter and aerospace vehicle applications, respectively.

After the initial static and creep tests, we decided to reduce the maximum temperature for the 6-2-4-2 Ti material to 1000°F. It had become evident that this material is not capable of carrying substantial structural load at 1200°F. This temperature choice was reviewed with personnel from the Flight Dynamics Lab and the Materials Lab at Wright Research and Development Center (WRDC), Wright-Patterson Air Force Base.

22

Test Type	Specimen Type	Model Development Test Program				Total Tests
		IN 718		6-2-4-2 Ti		
		Temperature	Tests	Temperature	Tests	
Static						
Tension	ST	R.T.	1	R.T.	1	2
	ST	700	1	700	1	2
	ST	1,200	1	1,200	1	2
Creep	DB	700	1	700	1	2
	DB	1,200	1	1,200	1	2
Constant Amplitude						
R = 0.02	CT	R.T.	1	R.T.	1	2
R = 0.02	CCT	R.T.	2	R.T.	2	4
R = 0.50	CCT	R.T.	1	R.T.	1	2
R = 0.3	CCT	R.T.	1	R.T.	1	2
R = 0.02	CCT	700	1	700	1	2
R = 0.02	CCT	1,200	2	1,000	2	4
R = 0.50	CCT	1,200	1	1,000	1	2
3 sec Hold Time						
R = 0.02	CCT	1,200	2	1,000	2	4
30 sec Hold Time						
R = 0.02	CCT	1,200	2	1,000	2	4
R = 0.50	CCT	1,200	1	1,000	1	2
R = 0.3	CCT	1,200	1	1,000	1	2
Vacuum						
No Hold Time						
R = 0.02	CT	R.T.	1	R.T.	1	2
R = 0.02	CT	1,200	1	1,000	1	2
30 sec Hold Time						
R = 0.02	CT	1,200	1	1,000	1	2
Alternating Rapid Cycling/Hold Time						
1,000 Cycles/30 sec Hold Time	CCT	1,200	1	1,000	1	2
Overload						
No Hold Time	CCT	1,200	1	1,000	1	2
	CCT	700	1	700	1	2
30 sec Hold Time	CCT	1,200	1	1,000	1	2
	CCT	700	1	700	1	2
Over/Underload						
No Hold Time	CCT	1,200	1	1,000	1	2
	CCT	700	1	700	1	2
30 sec Hold Time	CCT	1,200	1	1,000	1	2
Aerospace Vehicle Load Spectrum						
No Hold Time	CCT	R.T.	1	R.T.	1	2
	CCT	1,200	1	1,000	1	2
30 sec Hold Time	CCT	1,200	1	1,000	1	2
Total			34		34	68

ST   Static Test   CT   Compact Tension
DB   Dog Bone   CCT Center Cracked Tension

GP93-0418-2-T

Figure 8. Model Development Test Program

4. Specimen Layout and Configuration - The 6-2-4-2 Ti was purchased from the RMI Company in Niles, Ohio. It was ordered to specification MIL-T-9046H TY-3 COMP-G. The material was annealed at 1450°F for 1 hour and then air cooled.

The IN 718 material was purchased from Aerospace Specification Metals in Ft. Lauderdale, Florida. This material was ordered to specification AMS-5596. It was annealed at 1800°F for 1 hour and then air cooled. Subsequently, this material went through an aging cycle at MCAIR consisting of:

1) heating the panel to 1325°F;
2) holding at temperature for 8 hours;
3) cooling the panel at a rate of 100°F/hour to 1150°F;
4) holding at this temperature for 8 hours;
5) air cooling.

Both materials were cut into a 0.75 inch thick slab with an area of 36 inches by 60 inches. The grain direction was along the 60 inch dimension.

Static tensile strength tests were performed using 0.50 inch diameter round bar specimens, as shown in Figure 9. The creep tests were conducted on dog bone specimens, as shown in Figure 10. Center cracked tension (CCT) specimens (Figure 11) were selected for all crack growth tests performed at MCAIR. Georgia Tech used CCT specimens and compact tension (CT) specimens (Figure 12). CT specimens were required for testing in the vacuum chamber. All of the flat test specimens were 0.187 inch thick.

The test specimens were cut from the panel as shown in Figure 13. The static test and dog bone specimens were oriented such that the long dimension was cut parallel to the material grain dimension. The center cracked tension and the compact tension specimens were oriented such that the crack would grow perpendicular to the grain direction. Two flat test specimens were cut at the quarter thicknesses (Figure 14).

D = 0.750 ± 0.005
16-UNF-3A Threads

5.00 ± 0.06

D = 0.505 ± 0.005

All dimensions in inches

R = 0.50
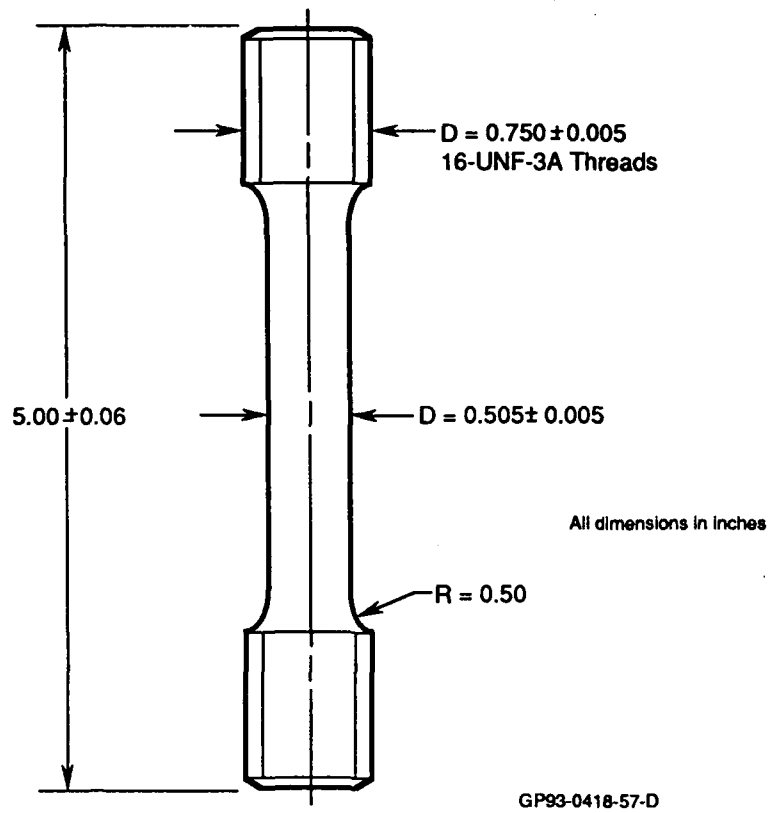
GP93-0418-57-D

Figure 9. Static Test Specimen (ST)

1.00

0.500

2.00

1.50

0.25

3.00

8.00

0.50

0.50

0.187

All dimensions in inches

2.00
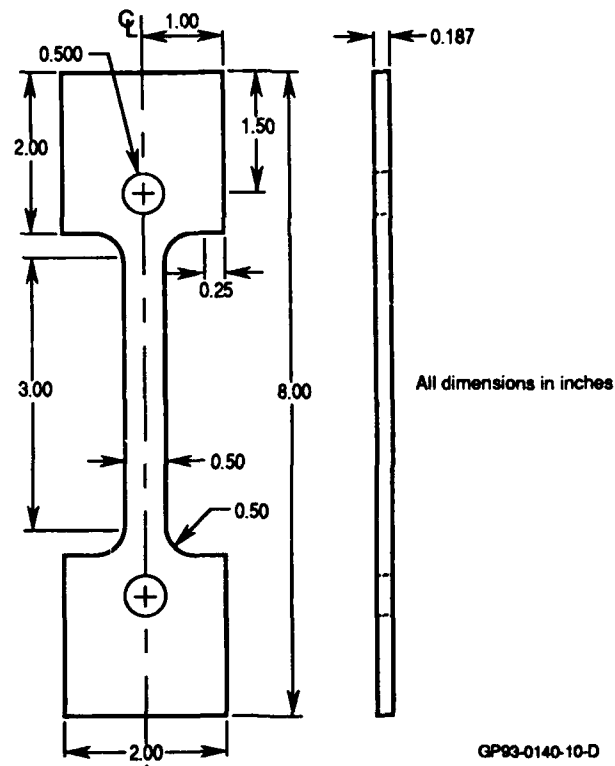
GP93-0140-10-D

Figure 10. Creep Specimen (Dog Bone, DB)

25
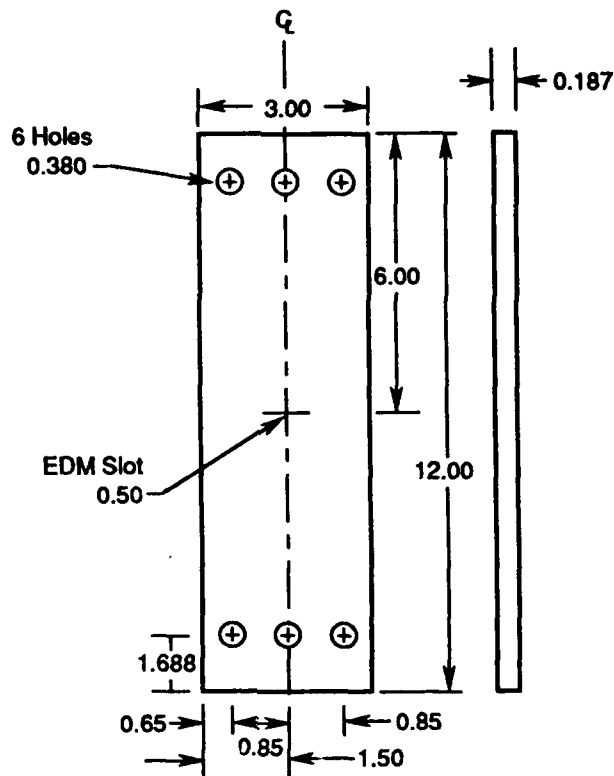
Note: All dimensions in inches.

GP93-0140-11-D

Figure 11. Center Cracked Tension Specimen (CCT)
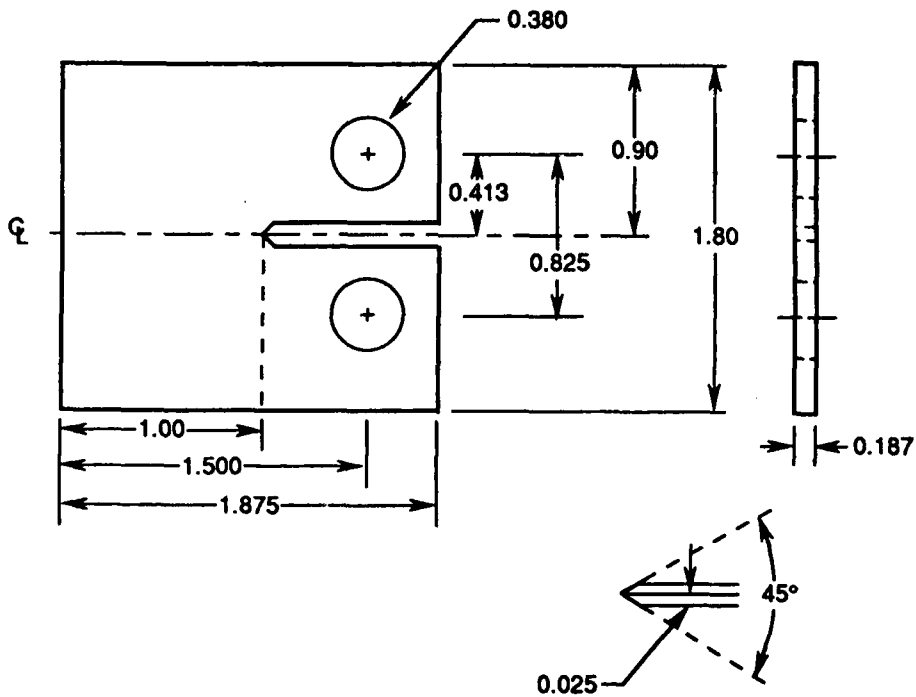
Note. All dimensions in inches.

Notch Detail - Straight Thru

GP93-0418-18-D

Figure 12. Compact Tension Specimen (CT)

26
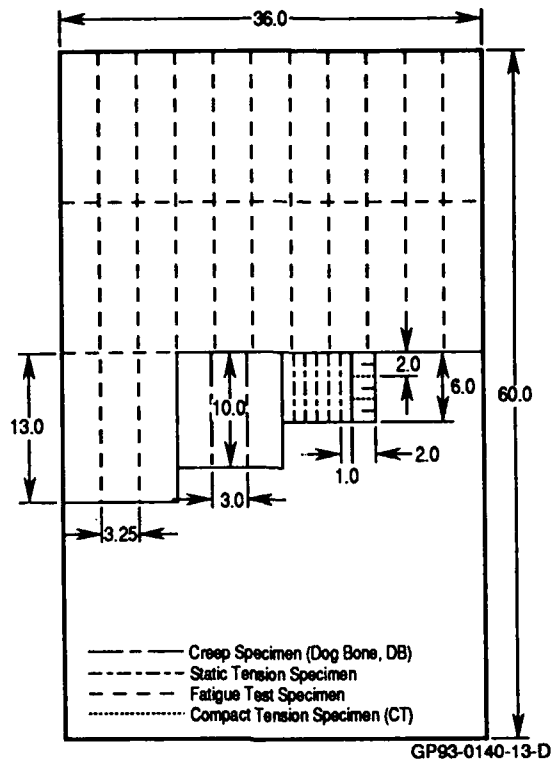
Figure 13. Specimen Layout

Legend (Figure 13):
- ── ── ── Creep Specimen (Dog Bone, DB)
- ──·──·── Static Tension Specimen
- ── ── ── Fatigue Test Specimen
- ············ Compact Tension Specimen (CT)

GP93-0140-13-D

Creep Specimen (Dog Bone, DB)

Center Cracked Tension Specimen (CCT)

Open Hole Tension Specimen (OHT)

Compact Tension Specimen (CT)

Static Tension Specimen (ST)

GP93-0418-19-D
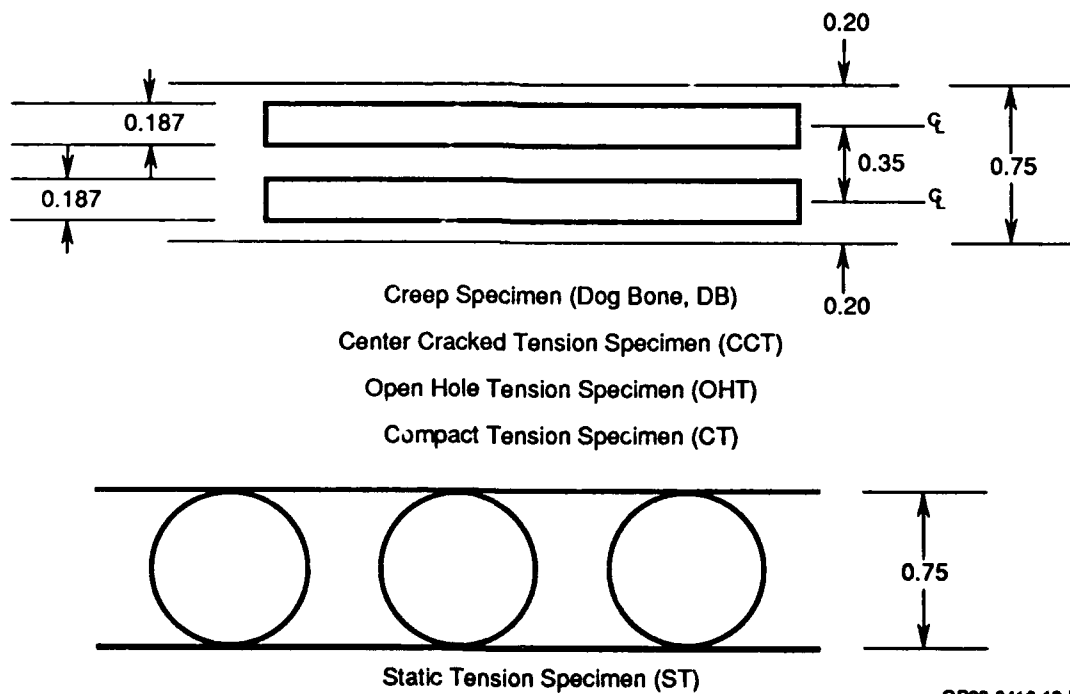
Figure 14. Specimen Layout (Cross-section)

27

5. <u>Test Methods</u> - The model development tests were performed by MCAIR and Georgia Tech. Certain fatigue tests were performed by both contractors for comparison. The main differences between MCAIR and Georgia Tech's test methods were in the load transfer, specimen heating, and crack measurement. The test procedures at each facility are described below.

a. <u>Tests Performed at MCAIR</u> - MCAIR conducted all of the static tension tests, 4 constant amplitude fatigue tests, and all of the spectrum load fatigue tests. These tests were all performed at constant temperatures: room temperature and 700°F for both 6-2-4-2 Ti and IN 718, 1000°F for 6-2-4-2 Ti, and 1200°F for IN 718.

All of the static test specimens were manufactured according to ASTM standards. A round bar tensile specimen (Figure 9) was manufactured to a 2 inch gage length and a 0.50 inch diameter. The specimens were heated to temperature using quartz lamp banks. The tests were displacement controlled at a rate of 0.05 inch per minute. The elastic modulus, yield strength, ultimate strength, and elongation were measured for each test. In addition, plots of head deflection vs. load were recorded.

Center cracked tension (CCT) specimens were used for all of MCAIR's constant amplitude fatigue and spectrum load fatigue tests. The center slot in the CCT specimen was electrically discharge machined (EDM). The slot width varied from 0.005 inch to 0.01 inch. The slot length was 0.50 inch. Crack length vs. cycles or flight hours were recorded for each test.

All specimens were loaded through self-aligning hydraulic grips in MTS, Inc. test equipment. The specimens were gripped along the upper and lower 1.50 inches. Tabs were not necessary due to the EDM slots. Cracks initiated at the slot at applied stress levels well below those that would cause failure at the edge of the grips. The six pin loading holes, shown in Figure 11, were not drilled in the specimens tested at MCAIR.

Buckling guides were not required for negative stress ratio fatigue tests. Compression stress levels were too low to cause specimen buckling.

High frequency fatigue tests were conducted at 15-20 Hertz. Some tests had 30 second hold times at peak load which corresponded to a test frequency of approximately 0.032 Hertz.

MCAIR performed all elevated temperature tests in the test fixture shown in Figure 15. The elevated temperature fixture is a radiant heating system made up of quartz lamp banks, a SCR power supply, and a digital programmable controller. The lamp banks consist of four 12 inch 1000 watt lamps spaced on 1.25 inch centers. They are positioned on each side of the specimen and are enclosed in a water cooled copper reflective shield which has a center slot for specimen observation and measurement of crack length. Using thermocouple feedback, the temperature can be held constant with setpoint control or varied with a 51 segment digital programmable controller. A cooling line for dry air or nitrogen is provided for rapid cooling. This facility generates temperatures up to 2000°F for static tests and 1500°F for fatigue tests. It accommodates specimens up to 4 inches wide and 0.75 inch thick.

GP93-0140-5

Figure 15. MCAIR Elevated Temperature Test Facility

Crack growth measurements were made using microscopes attached to a calibrated slide. Crack length readings were made after a specified number of cycles or flight hours for constant amplitude and spectrum load fatigue tests.

b. Tests Performed at Georgia Tech - Georgia Tech performed all of the creep tests, the majority of the constant amplitude fatigue tests, and all of the overload and overload/underload fatigue tests. These tests were all performed at constant temperatures: room temperature (78°F), 700°F, 1000°F for 6-2-4-2 Ti, and 1200°F for IN 718.

The creep tests were conducted on the dog bone (DB) specimen shown in Figure 10. This specimen had a 2 inch gage length and was 0.50 inch wide. The DB specimen had 0.50 inch holes drilled at the top and bottom for pin loading. Strain vs. time was recorded for each test.

Center cracked tension (CCT) specimens (Figure 11) were used or the majority of the constant amplitude fatigue tests and all of the overload and overload/underload fatigue tests. This specimen had a 0.50 inch long EDM slot in the center. The slot varied in width between 0.005 inch and 0.01 inch, specimen to specimen. Three 0.38 inch holes were drilled in the top and bottom of the specimen for pin loading. Compact tension (CT) specimens (Figure 12) were required for tests conducted in the vacuum chamber. Crack length vs. cycles was recorded for these tests. All testing was performed with a MTS Model 810 closed loop servo-hydraulic machine.

Crack growth was monitored in the CCT and CT specimens using the electric potential drop method (EPD). This required that 18 inch long x 0.03 inch diameter stainless steel wires be butt welded to each specimen at four locations (Figure 16). A current of approximately 3 Amperes was sent to the specimen. The input voltage was recorded on a strip chart and entered into a computer file as a basis for the crack growth propagation rates. At specific intervals during the tests, the number of cycles and the voltage output from the specimen was recorded. The potential difference was then converted to crack length using Johnson's equation (Reference 9).

$$c = 2W/\pi \cos\text{-}1\{ch/\cosh[V/V_0 \cosh^{-1}(ch \cos(\pi c_0/2W))]\}$$

where

$$ch = \cosh(\pi Y/2W)$$

In these equations, c and c_0 are the initial and current crack length, V and V_0 are the initial and current electric potentials, W is the specimen width, and Y is the spacing between output leads attached to the specimen.

X - S.S. 316 wire butt welded at these locations.

EDM Slot
0.50

Note: All dimensions in inches.

GP93-0418-111-D
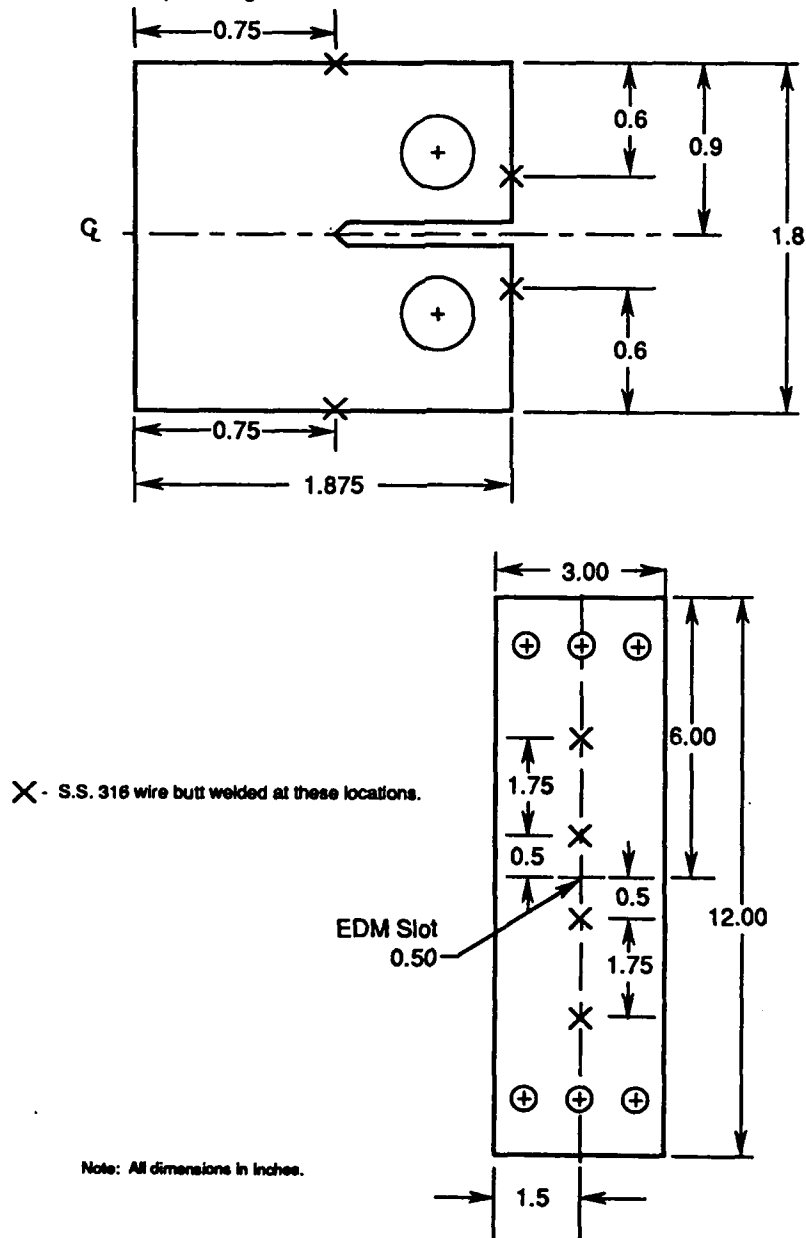
**Figure 16. Location of Stainless Steel Wires on
Specimens for EPD Method**

31

Damage monitoring was completely automated. Crack growth measurements were made using the EPD method and were recorded onto a personal computer. Visual measurements were made randomly for comparison.

Georgia Tech's high temperature capability was supplied by resistance furnaces obtained from Marshal and ATS. Their internal capacity is 5 inches in diameter and 15 inches long. The length is divided into 3 zones each with its own temperature controller. This furnace is pictured in Figure 17.

GP93-0140-6

Figure 17. Georgia Tech's High Temperature Furnace

A special Perkin-Elmer vacuum chamber has been incorporated into an MTS testing frame, providing Georgia Tech with "oxide free" testing (Figure 18). The vacuum chamber is capable of achieving 10^{-10} torr. To achieve this level of vacuum, an overnight bake of the system and specimen was required. Only the compact tension (CT) specimens (Figure 12) could be tested in this system. The maximum load for the system is 5000 pounds. The maximum demonstrated temperature for the high vacuum system is 2012°F (1100°C), provided by an auto tune induction heater assembly. Specimen material and outgassing must be compatible with the requested temperature and vacuum level.

32

GP93-0140-4

Figure 18. Georgia Tech's Vacuum Chamber

The vacuum system is monitored by a UTI residual gas analyzer. This self-contained mass spectrometer is used to assure that the hydrogen and oxygen levels are kept low during the test, and to measure the partial pressures of other elements in the material being tested.

6. <u>Model Development Test Program</u> - To guide the development of a high temperature crack growth prediction methodology, a test matrix (Figure 8) was designed which progressed from high frequency constant amplitude loading at room temperature through spectrum loading at elevated temperature. The testing systematically introduced and evaluated the effects of pertinent variables.

The matrix extensively investigated the effects of temperature and environment on strength and crack growth for the two chosen materials. These materials had extensive data bases for comparisons.

33

It is difficult to draw specific conclusions from any of the tests performed in this program because only one test was performed per condition. However, basic trends in the data are discussed, and possible explanations are provided. In some cases, however, the data scatter may hide the true explanation.

Georgia Institute of Technology was a subcontractor to MCAIR. They performed creep and constant temperature fatigue tests. Testing, at Georgia Tech, was under the supervision of Dr. Stephen Antolovich and Mr. Richard Brown. MCAIR conducted static and spectrum load fatigue tests. Testing at MCAIR was supervised by Mr. Russell Bill.

a. Static Tension Tests - MCAIR performed all of the static tension tests. Results of both the IN 718 and 6-2-4-2 Ti tests were compared to data published in the Aerospace Structural Materials Handbook (Reference 10).

Three static tension tests were performed on the 6-2-4-2 Ti. Tests results are shown in Figure 19. The ultimate strength, yield strength, and elongation compared well with expected values. There was a 27 percent reduction in strength at 700°F and a 46 percent reduction in strength at 1200°F.
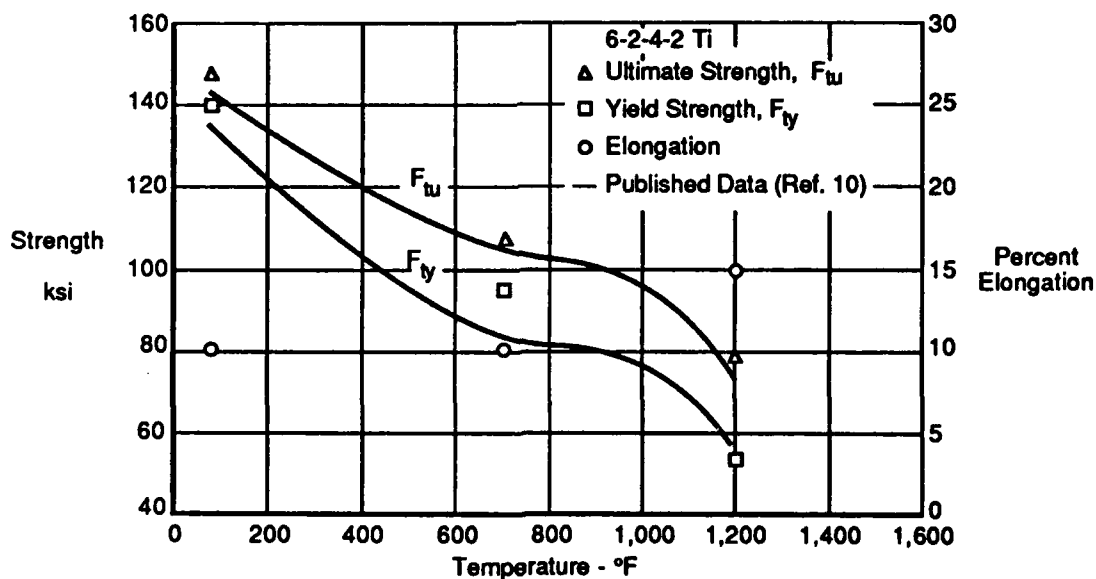
Figure 19. 6-2-4-2 Ti Static Tension Test Data and Published Results

GP83-0418-76-D

34

A total of six static tests were conducted on the IN 718 material: three tests on as-received material and three tests on aged material. The as-received IN 718 was ordered according to AMS 5596 which included an annealing process, but no aging process. IN 718 was selected for model development testing because of its environmental sensitivity. Without the aging cycle however, this sensitivity was not expected to be as pronounced. This was found to be true for 300M steel in which underaged material was not nearly as sensitive to aggressive environments as peak aged material.

The aging cycle consisted of an eight hour hold at 1325°F, a 100°F per hour cool down to 1150°F, and an additional hold of 8 hours at 1150°F. The material was aged at MCAIR.

The data from the as-received material agrees well with published data for un-aged material (Figure 20). The strengths of the aged material most

GP93-0418-20-D
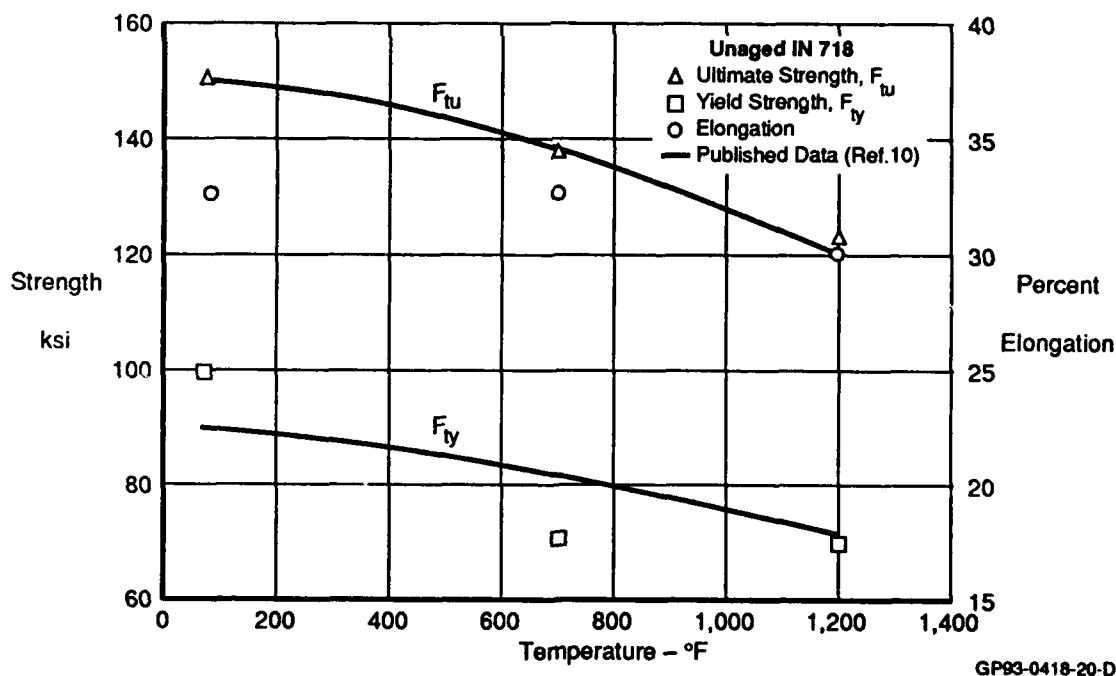
Figure 20. Static Tension Results of As–Received IN 718

35

closely match those of material which has been 15 percent cold worked and aged (Figure 21). The AMS 5596 specification specifies that plate material be hot rolled. However, since our specimens were cut from the center of this plate, these specimens would have been cooler than the surface, and therefore may have undergone cold working.

Rockwell hardness tests also support the conjecture that the IN 718 material was cold-worked. Hardness tests were conducted on the un-aged and aged IN 718. The results of these tests (Figure 22) imply that the material had undergone approximately 15 percent cold working.

b. Creep Tests - Georgia Tech performed five creep tests, two on IN 718 and three on 6-2-4-2 Ti. The objective of these tests was to determine for a given stress level the time required to achieve 0.2 percent strain. The stress required to obtain 0.2 percent creep was referred to as the effective yield stress. The tests were conducted at 700°F and 1200°F.

The 6-2-4-2 Ti creep test results are shown in Figure 23. These results indicate that at 1200°F, 6-2-4-2 Ti is not capable of withstanding any substantial structural loads. After reviewing this data in-house and with personnel from Wright-Patterson AFB, it was decided to lower the maximum temperature for the 6-2-4-2 Ti fatigue tests from 1200°F to 1000°F. The 1200°F and 700°F (Figure 23) creep data was compared to data from the Aerospace Structural Metals Handbook (Reference 10) in Figure 24. In this figure, the time to obtain 0.2 percent strain is plotted for different temperatures and stress levels.

IN 718 is less susceptible to creep than is 6-2-4-2 Ti. After 100 hours of testing at 1200°F with a stress level of 60 ksi, the IN 718 specimen had strained just less than 0.2 percent (Figure 25). At 700°F and 85 ksi, virtually no creep was measured after 125 hours. Data from the Aerospace Structural Metals Handbook (Reference 10) is compared to our data in Figure 26.
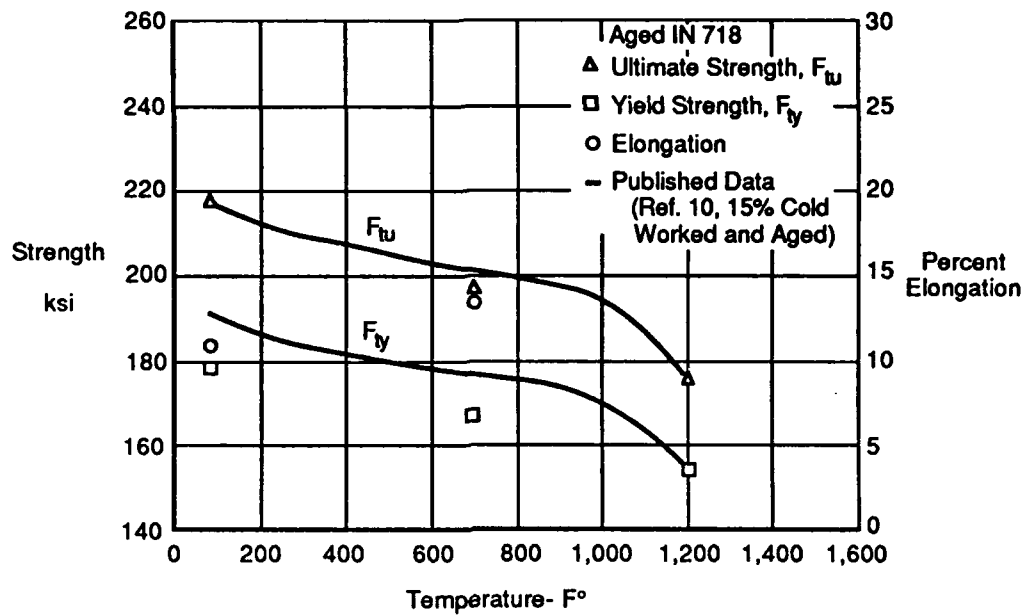
Figure 21. Static Tension Results of Aged IN 718
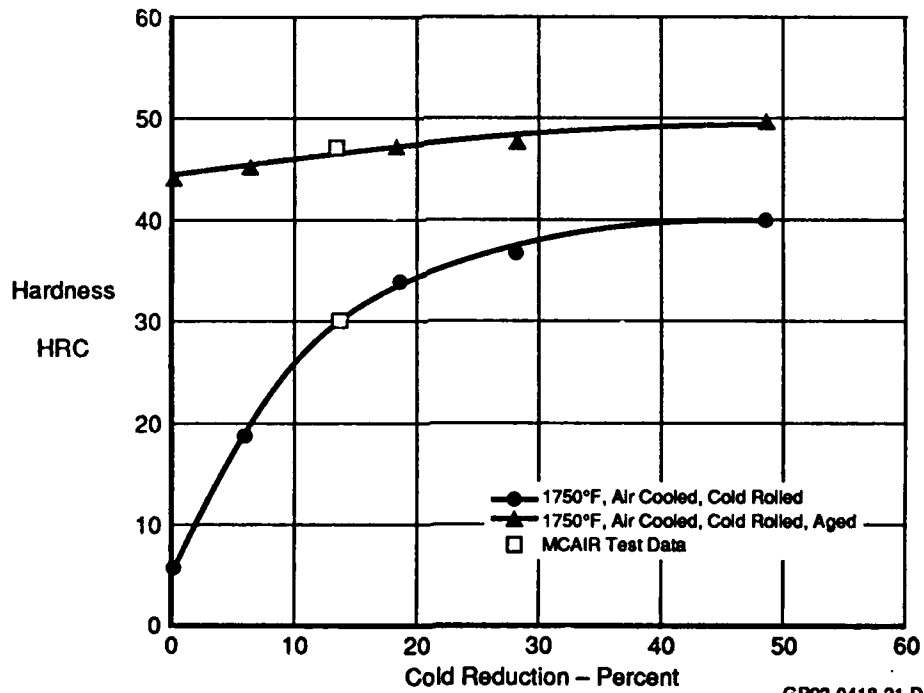
Figure 22. Rockwell Hardness Tests of 15% Cold Worked IN 718

37
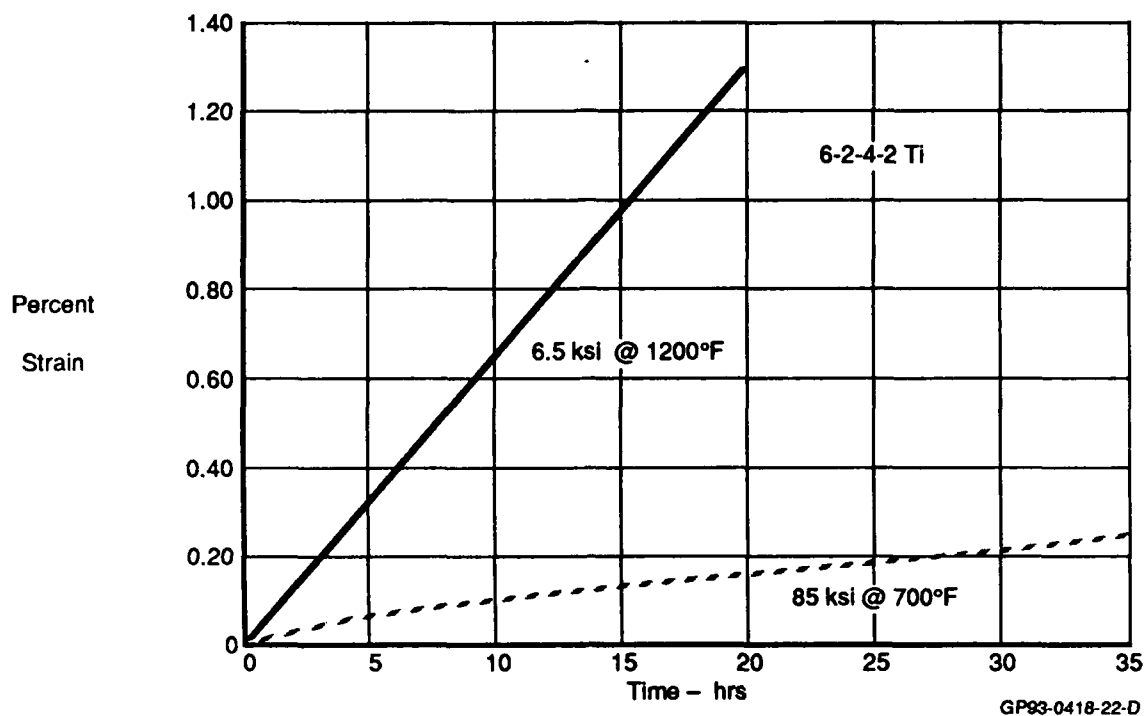
Figure 23. 6-2-4-2 Ti Creep Properties at 700°F and 1200°F
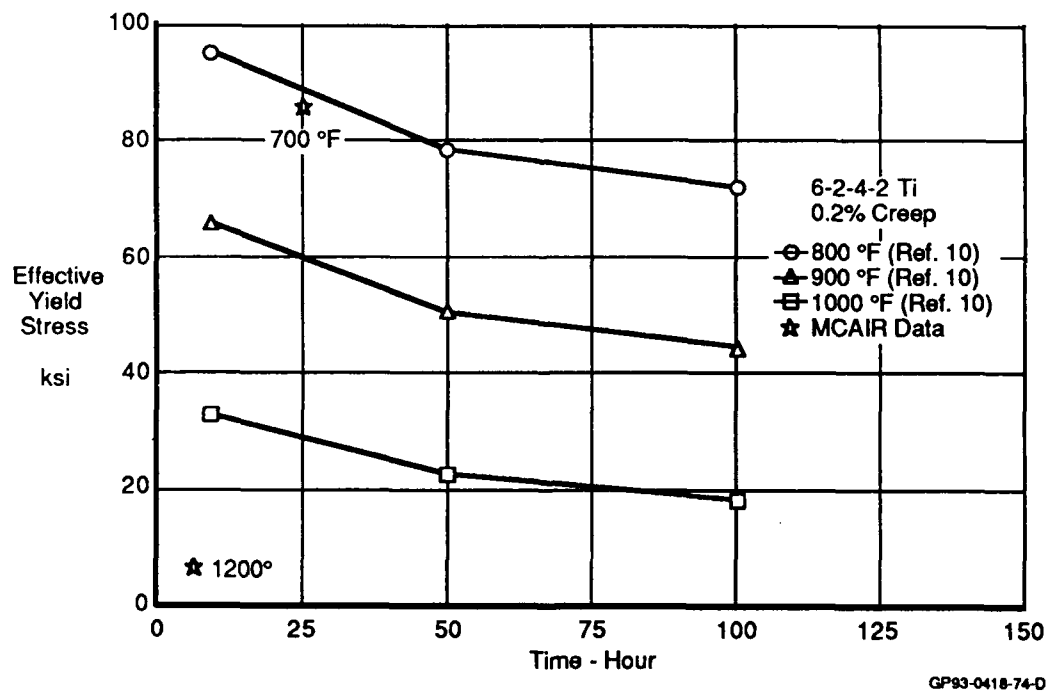
Figure 24. 6-2-4-2 Ti Effective Yield Stress

38
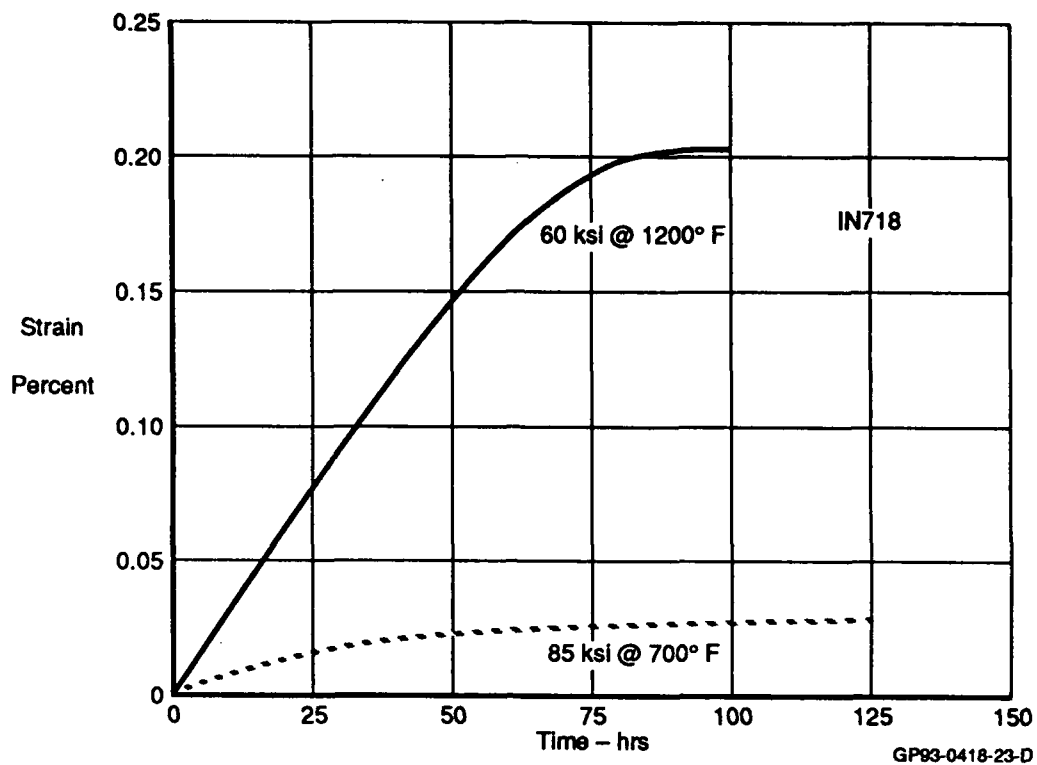
Figure 25. IN 718 Creep Properties at 700°F and 1,200°F
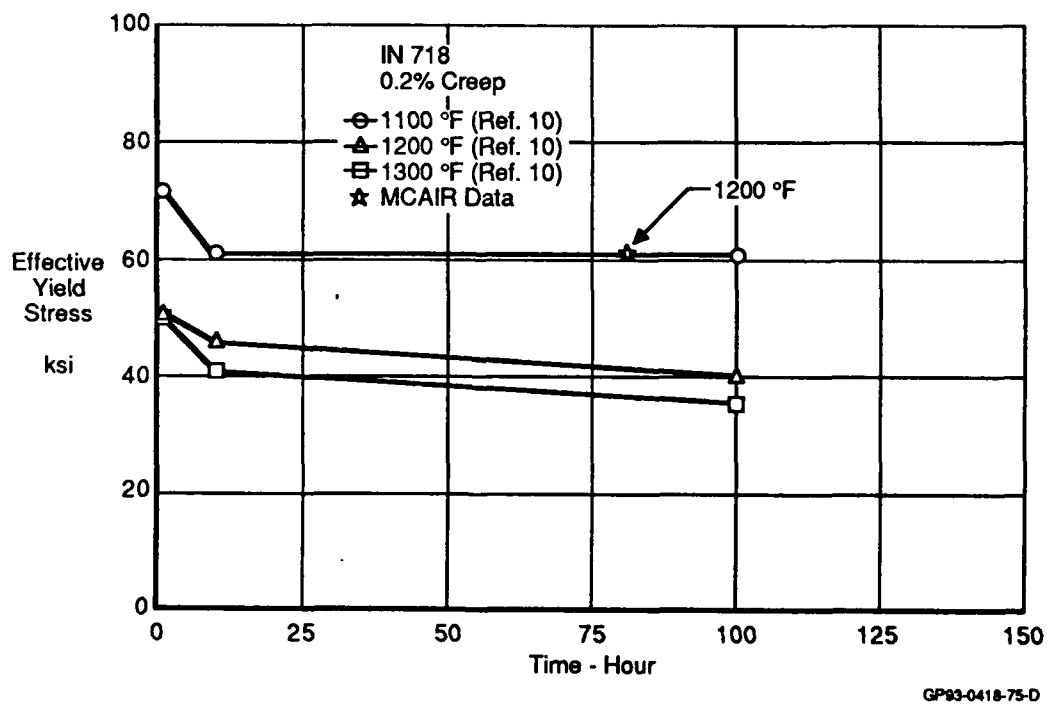
Figure 26. IN 718 Effective Yield Stress

39

The results obtained from our tests confirm the trends documented in the literature. IN 718 and especially 6-2-4-2 Ti are susceptible to creep. Creep could play an important role in fatigue crack growth when the applied spectrum has cycles in which loads are held for a long time at temperature. Creep needs to be considered for 6-2-4-2 Ti when temperatures are above 700°F, and for IN 718 for temperatures above 1000°F.

c. <u>Constant Amplitude Fatigue Tests</u> - Tne purpose of these tests was to investigate the effects of temperature on the crack growth rate for various stress ratios. All of the tests were conducted at frequencies of approximately 10 Hz. These tests were performed primarily by Georgia Tech.

Duplicate room temperature, R=0.02 tests were run by both Georgia Tech and MCAIR for comparison. Consistent trends in the crack growth rate data were found for both the 6-2-4-2 Ti and the IN 718 materials (Figures 27 and 28).

Increasing positive stress ratios increased crack growth rates at room temperature and at 1000°F in 6-2-4-2 Ti (Figures 29 and 30). The room temperature R=-0.3 data resulted in higher initial crack growth rates than the room temperature R=0.02 data.

Stress ratio effects on crack growth were more pronounced at room temperature than at 1200°F for IN 718 (Figures 31 and 32). The room temperature, R=0.50 crack growth rate data was more severe than the R=0.02 data. The negative stress ratio (R=-0.20) data showed no effect on crack growth as compared to the R=0.02 data. When plotting negative stress ratio data, the minimum stress intensity, K_{min} was not allowed to be below zero.

High temperatures appeared to reduce the crack growth rates of 6-2-4-2 Ti. The R=0.02 and R=0.50 data showed small changes in the crack growth rate at elevated temperatures (Figures 33 and 34). At 700°F, the material softens and the crack tip may not be as sharp, producing slower crack growth rates. The same is true at 1000°F, however, at this temperature the material is reaching its maximum capability. As a result, a degradation of the material properties may produce faster crack growth at low stress intensities at 1000°F than those found at 700°F and room temperature.

40
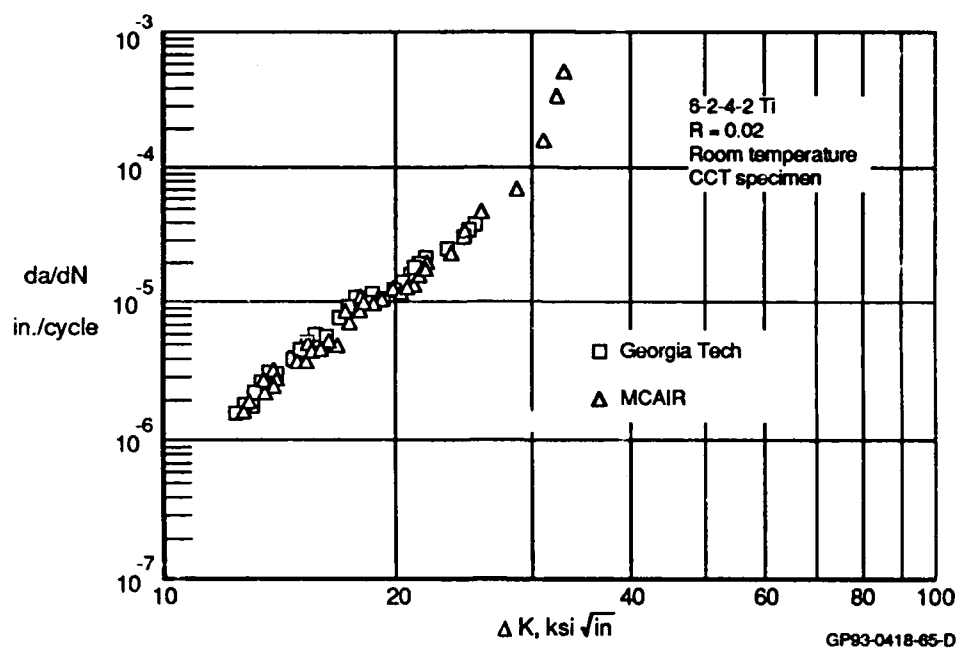
Figure 27. Room Temperature Crack Growth Rate Data for 6-2-4-2 Ti
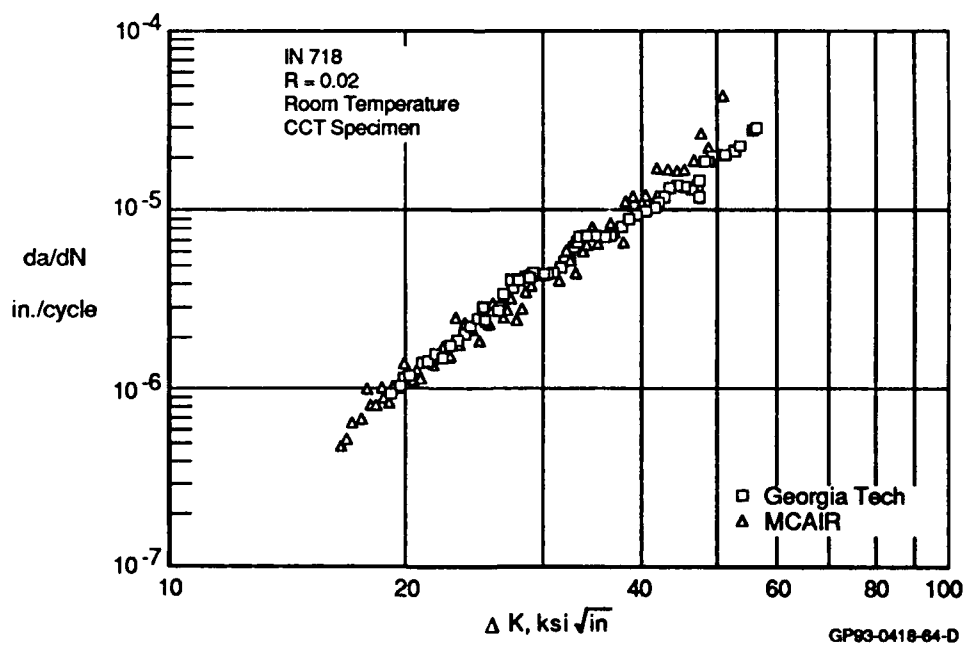
Figure 28. Room Temperature Crack Growth Rate Data for IN 718

41
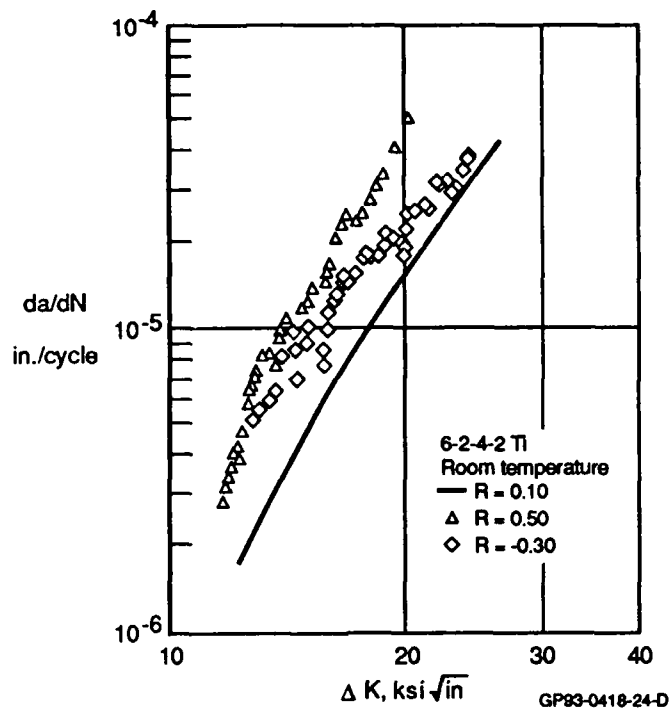
Figure 29. Stress Ratio Effects on Crack Growth
Rate in 6-2-4-2 Ti at Room Temperature
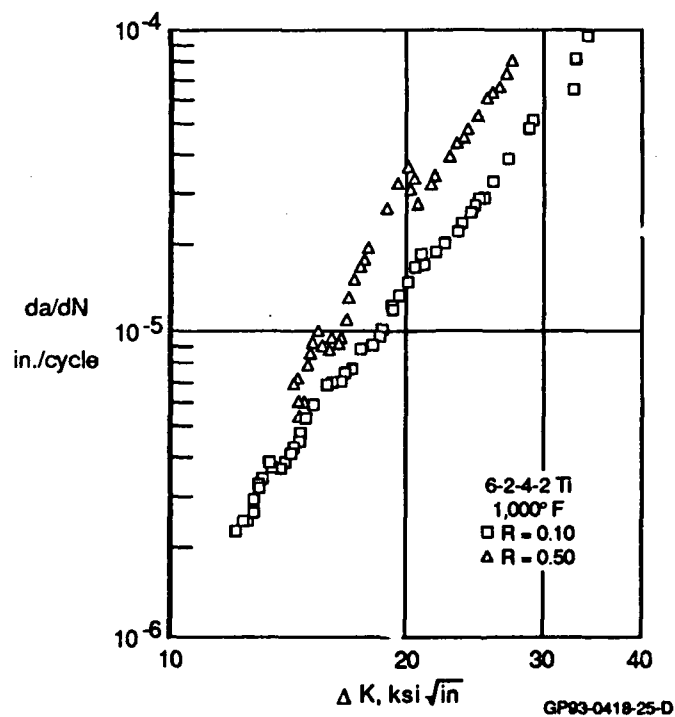
Figure 30. Stress Ratio Effects on Crack Growth
Rate in 6-2-4-2 Ti at 1,000° F

GP93-0418-26-D
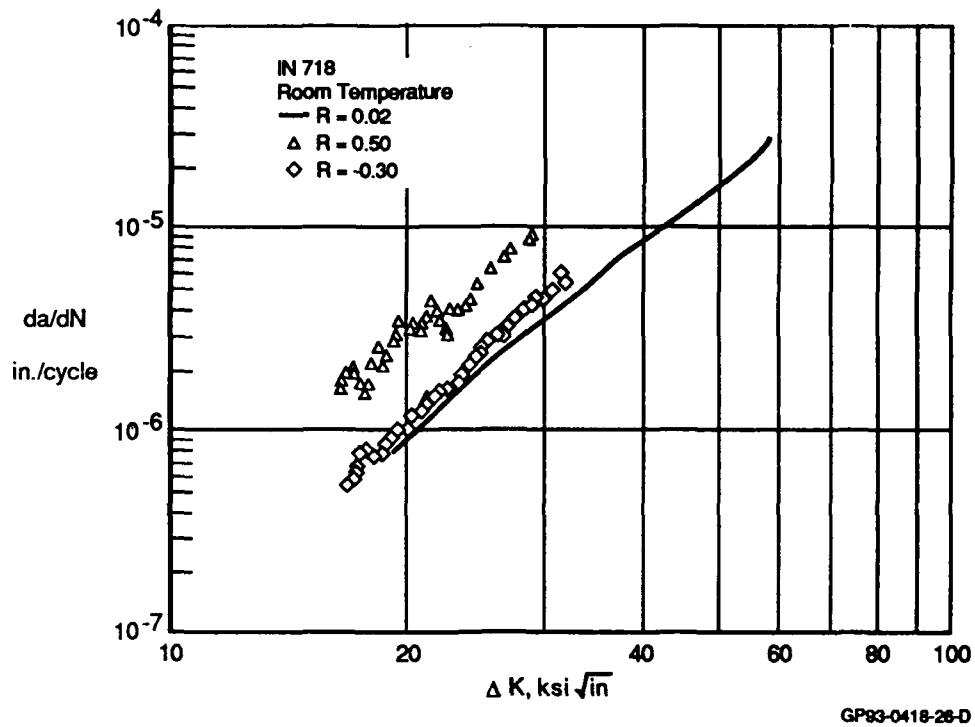
**Figure 31. Stress Ratio Effects on Crack Growth Rate
in IN 718 at Room Temperature**

GP93-0418-27-D
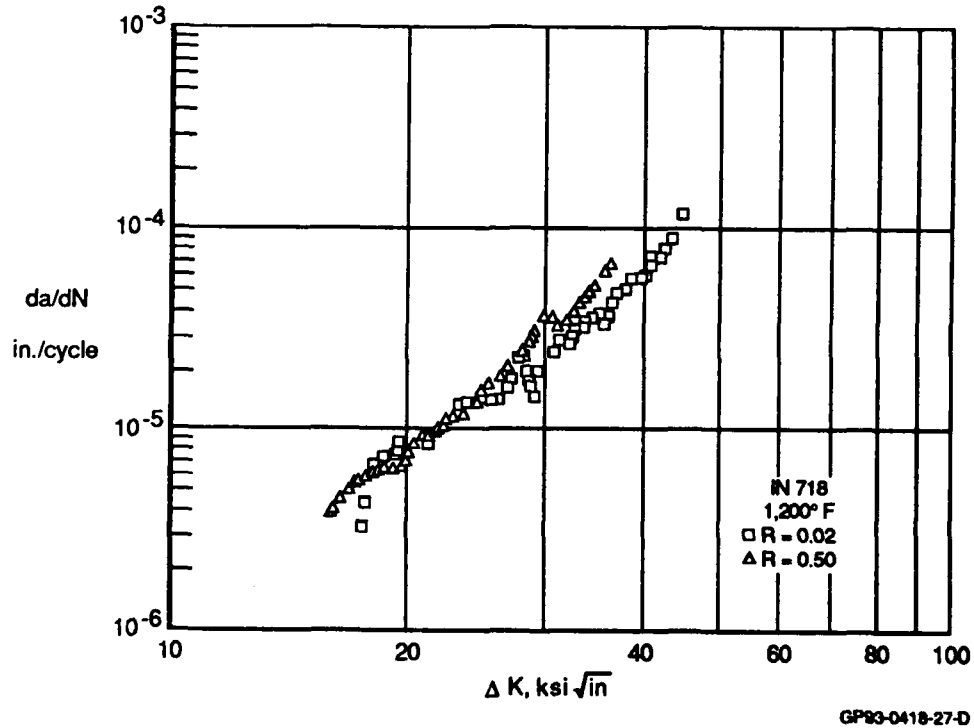
**Figure 32. Stress Ratio Effects on Crack Growth Rate
in IN718 at 1,200° F**

43
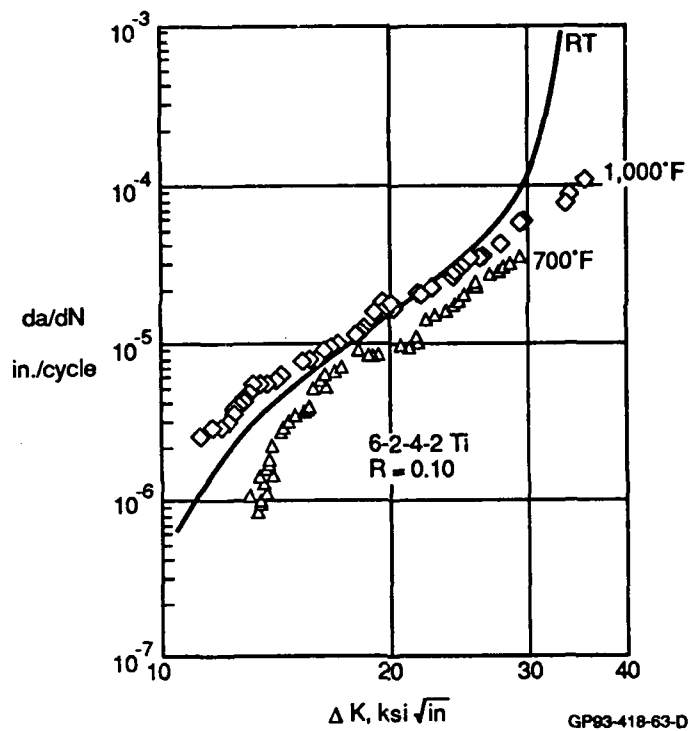
Figure 33. Temperature Effects on Crack Growth Rate of 6-2-4-2 Ti (R = 0.10)
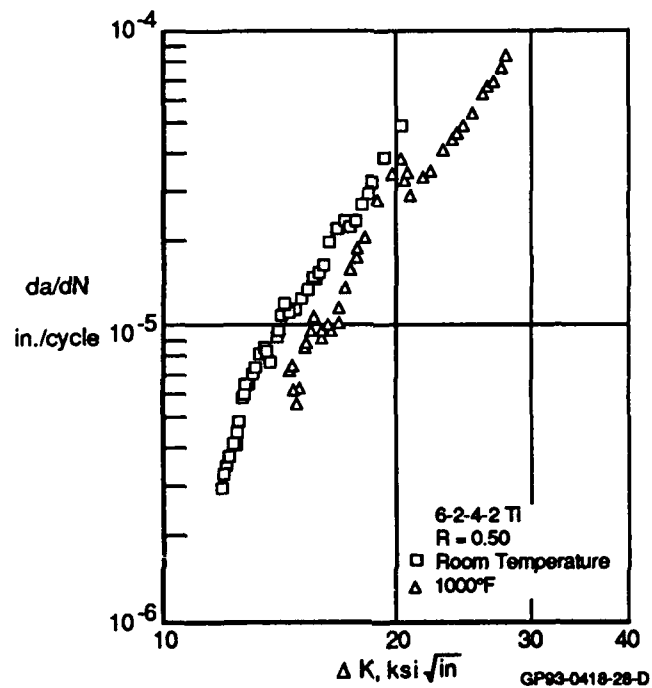
Figure 34. Temperature Effects on Crack Growth Rate of 6-2-4-2 Ti (R = 0.50)

44

IN 718 experienced accelerated crack growth at temperatures above 700°F. At 1200°F, the R=0.02 and R=0.50 crack growth data was significantly higher than the room temperature data (Figures 35 and 36). These tests were performed in lab air. IN 718 is sensitive to the environment. At elevated temperatures, IN 718 will react with the environment to produce faster crack growth.

d. <u>Hold Time Fatigue Tests</u> - Constant amplitude fatigue tests were also run with hold times during peak loads to determine the effects of environmental acceleration and creep in the plastic zone on crack growth. Hold times of 3 seconds and 30 seconds were used. All of the tests were conducted at the maximum temperature for each material: 1000°F for 6-2-4-2 Ti and 1200°F for IN 718. Tests were also conducted in which 1000 high frequency cycles were followed by a single 30 second hold time cycle. The purpose of these tests was to demonstrate the effects of creep and sustained load on crack growth behavior.

Data for the hold time fatigue tests was difficult to obtain simply because of the amount of time required to run a complete test. Only 3000 cycles per day are accumulated on a test with 30 second hold times at peak loads. As a result, tests were conducted in two different manners. Some tests were run at three or four different stress levels. This provided a discontinuous, yet full-ranged crack growth curve. Other tests were started at high stress intensities and run till failure. This provided a continuous, but incomplete crack growth curve.

Figures 37 and 38 compare hold time data (3 seconds and 30 seconds) to data without hold times in 6-2-4-2 Ti at two stress ratios of R=0.02 and R=0.50. The hold time appears to retard crack growth. This is probably because the crack tip blunts with the additional plasticity and creep induced during sustained loads at 1000°F. This effect is more pronounced in R=0.02 data than in the R=0.50 data.
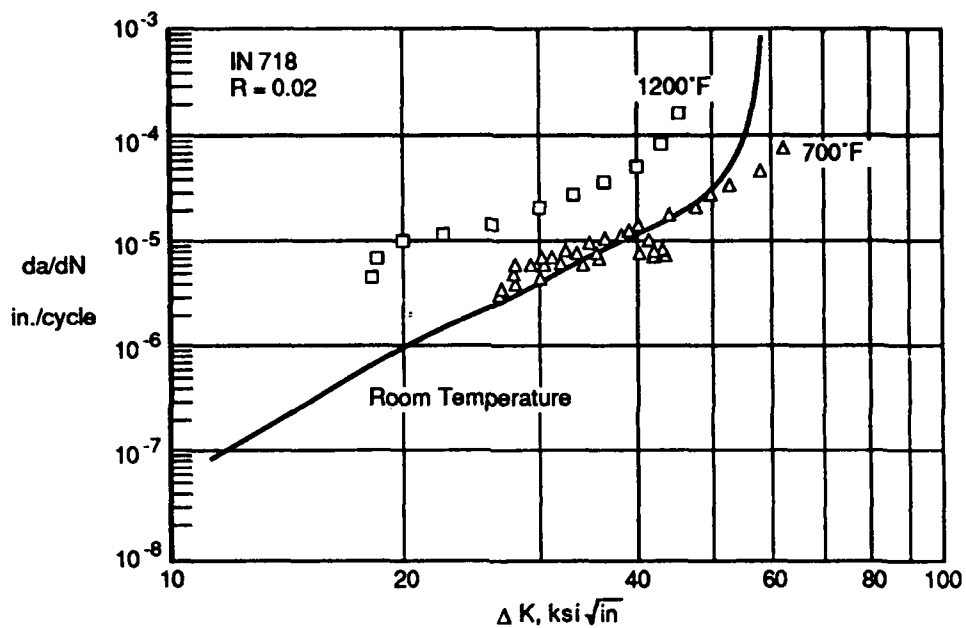
Figure 35. Temperature Effects on Crack Growth Rate of IN 718 (R=0.02)
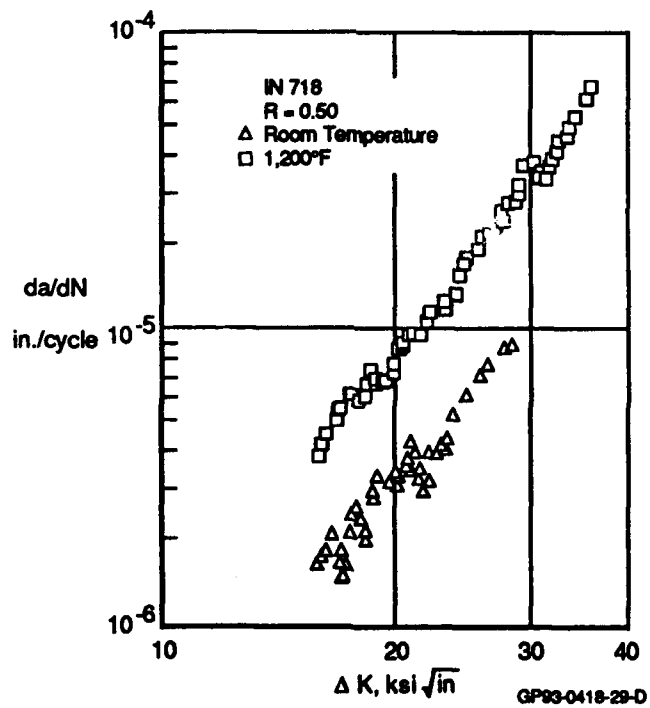
**Figure 36. Temperature Effects on Crack
Growth Rate of IN 718 (R=0.50)**

46
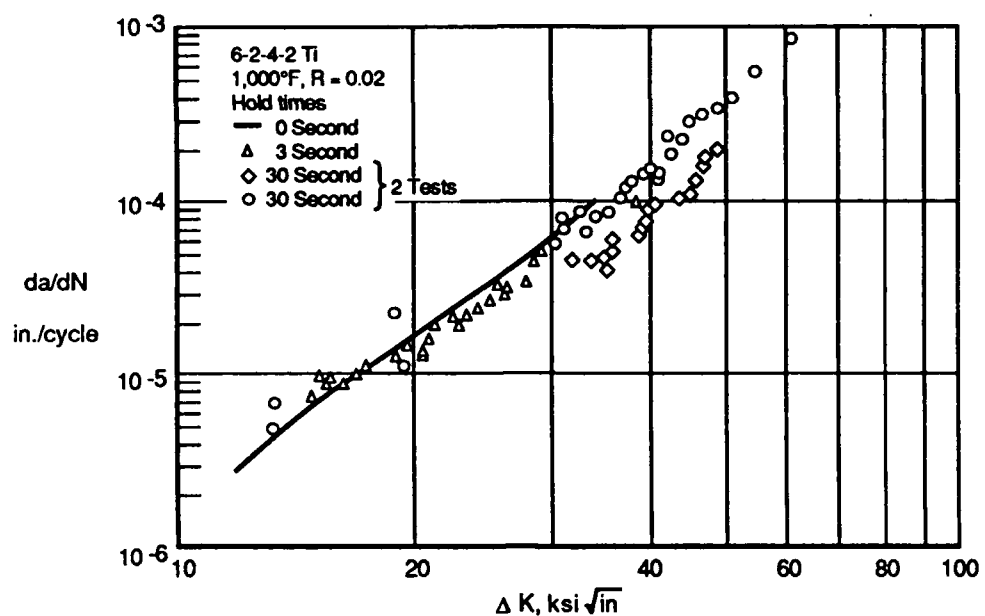
**Figure 37. Hold Time Effects on Crack Growth
Rate of 6-2-4-2 Ti (R = 0.02)**
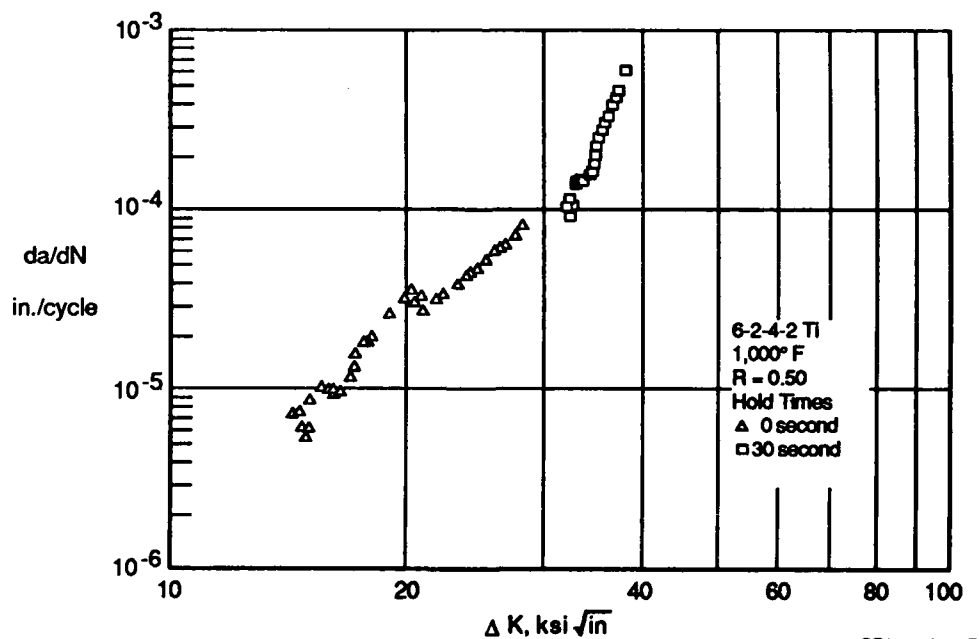
**Figure 38. Hold Time Effects on Crack Growth
Rate of 6-2-4-2 Ti (R = 0.50)**

A similar high frequency vs. hold time comparison is made for IN 718 at 1200°F. The data is plotted in Figures 39 and 40. This data indicates that crack growth per cycle is slowed by increasing hold times. This is the same trend found in 6-2-4-2 Ti. However, this is the opposite trend found by Larsen (Figure 41 and Reference 11). His data indicate that the crack growth rate in IN 718 increased almost linearly with hold time. Apparently, the crack growth of IN 718 material used in this program is not as sensitive to the environment as the material tested by Larsen. The exact reason for this difference is not known.

Hold times were also applied in the elevated temperature negative stress ratio tests (Figures 42 and 43). IN 718 showed a substantial decrease in crack growth rate as compared to a hold time R=0.02 fatigue test; while 6-2-4-2 Ti showed little difference in crack growth rates for the same two tests. The decrease in the crack growth rate seemed to indicate that the IN 718 was more affected by creep and blunting of the crack tip than it was by the environment. In these plots, the minimum stress intensity, K_{min} was not allowed to be less than zero.

Two tests were performed which consisted of 1000 high frequency constant amplitude cycles followed by a single 30 second hold time cycle. These tests were conducted at maximum temperature: 1000°F for 6-2-4-2 Ti and 1200°F for IN 718. This data is plotted against high frequency data and 30 second hold time/cycle data in Figures 44 and 45. Crack growth retardation was more evident in IN 718 than in 6-2-4-2 Ti. In fact, at low ΔK values, the crack growth rate was higher in 6-2-4-2 Ti compared to the high frequency test. This would indicate that at low ΔK, environmental sensitivity influences the crack growth rate of 6-2-4-2 Ti, while at high ΔK values, crack tip blunting due to creep slows the growth rate. IN 718 showed no crack growth acceleration due to environmental attack. Rather, crack tip blunting appears to slow crack growth at all ΔK ranges.

e. Vacuum Fatigue Tests - High frequency vacuum fatigue tests were conducted at Georgia Tech. The chamber is capable of pulling a vacuum on the order of 4.0E-8 torr. All tests were performed on compact tension (CT) specimens (Figure 12).

48
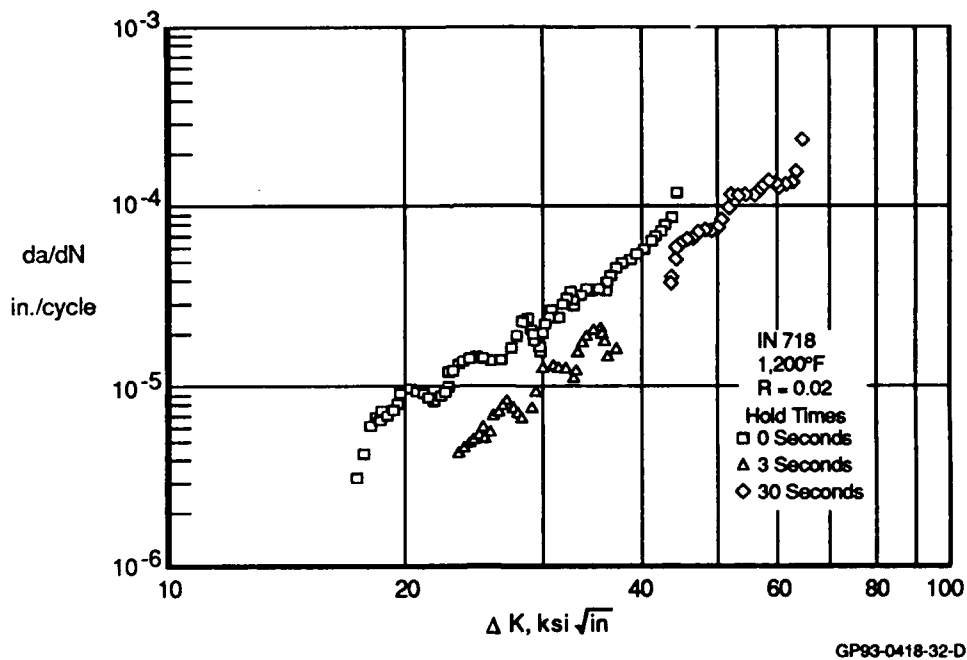
Figure 39. Hold Time Effects on Crack Growth Rate of IN 718 (R = 0.02)
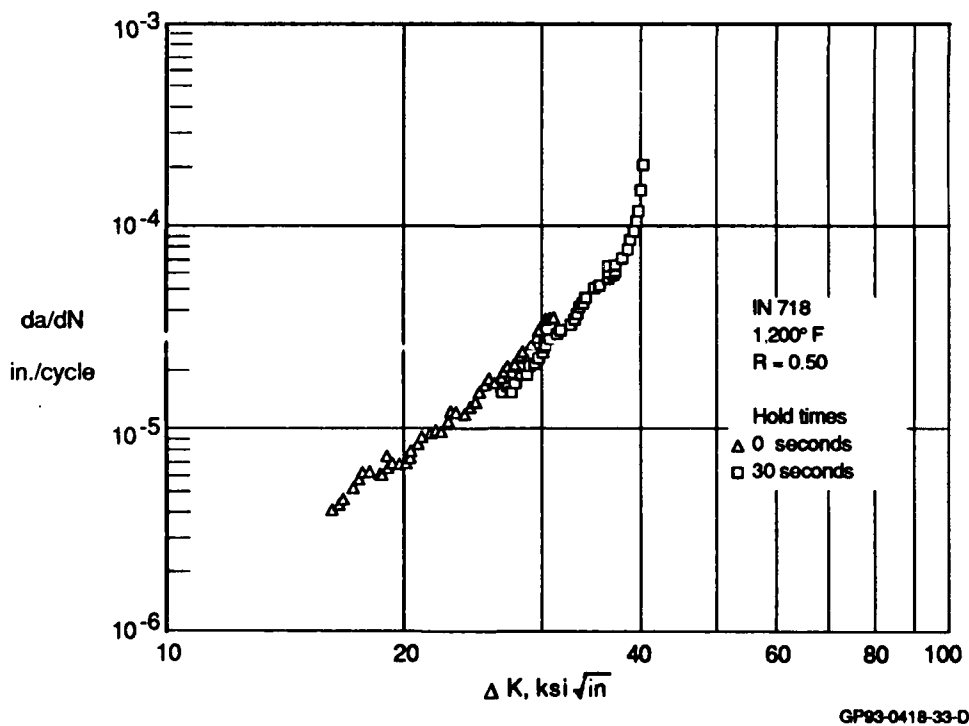
Figure 40. Hold Time Effects on Crack Growth Rate of IN 718 (R = 0.50)

49
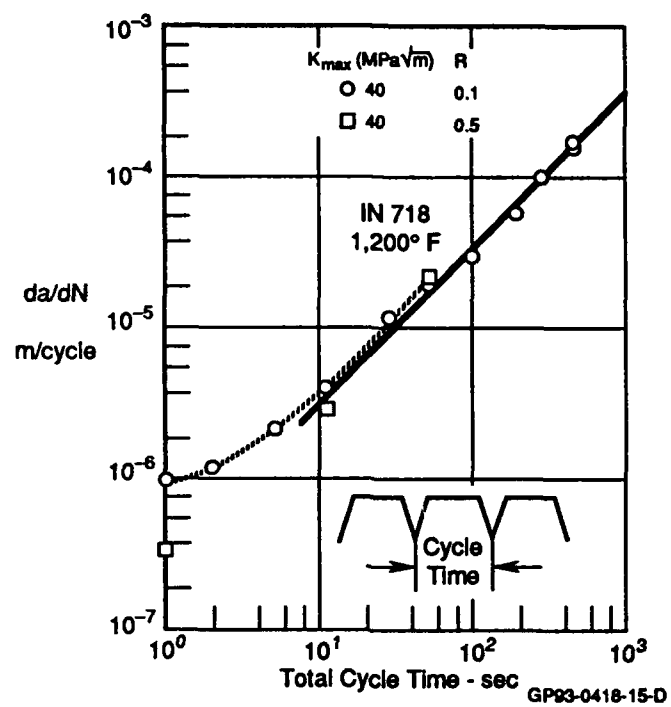
**Figure 41. Hold Time Effects on Crack Growth
Rate of IN 718 at 1,200°F**
Larsen, Nicholas
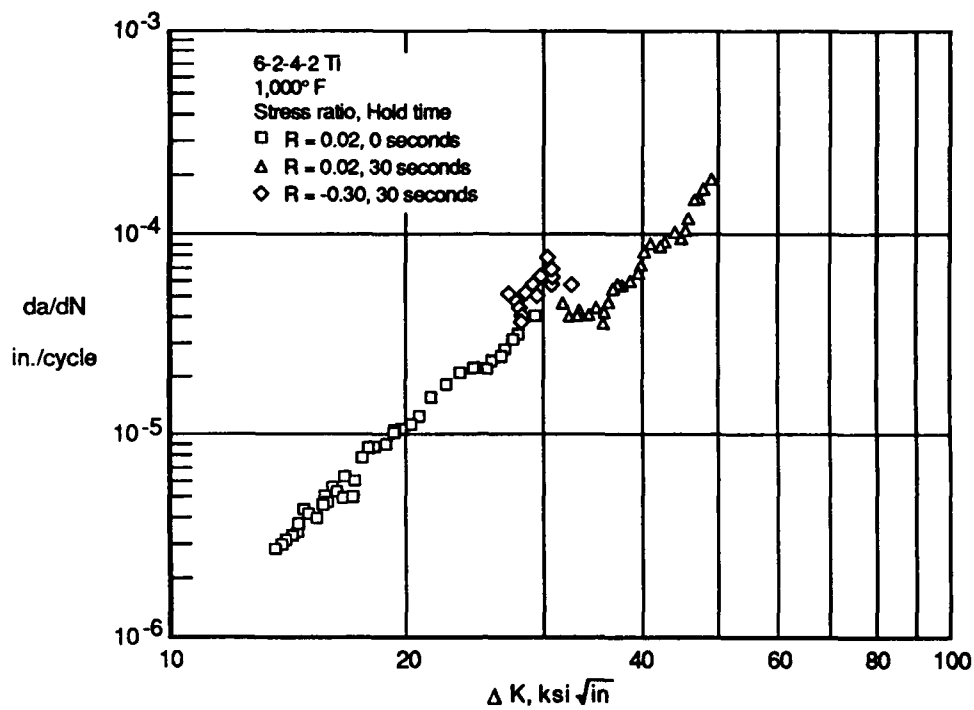
Figure 42. Hold Time Effects on Crack Growth Rate
of 6-2-4-2 Ti at 1,000° F
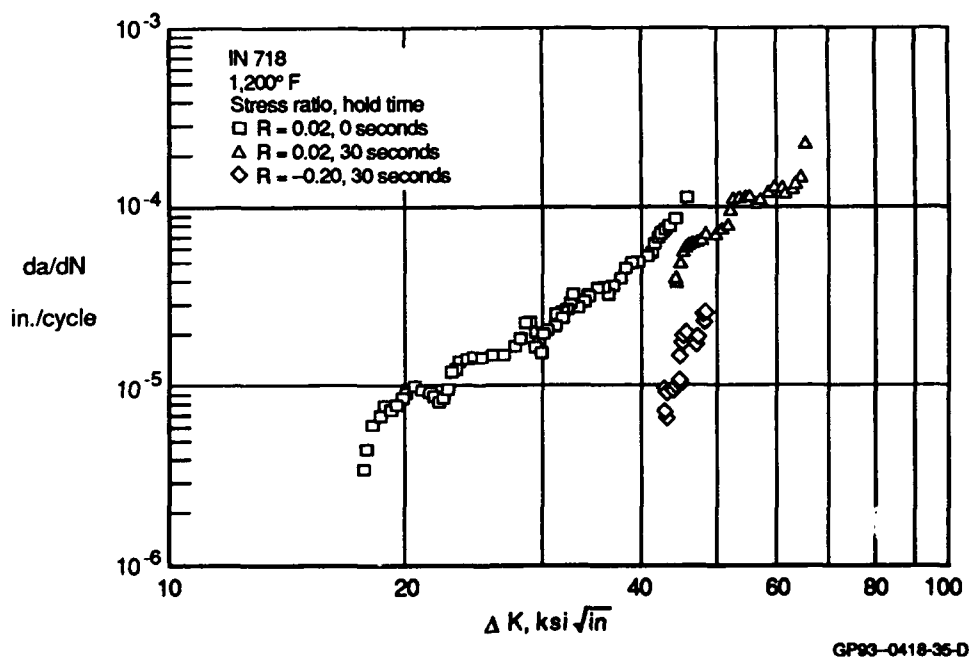
Figure 43. Hold Time Effects on Crack Growth Rate of IN 718 at 1,200°F

51
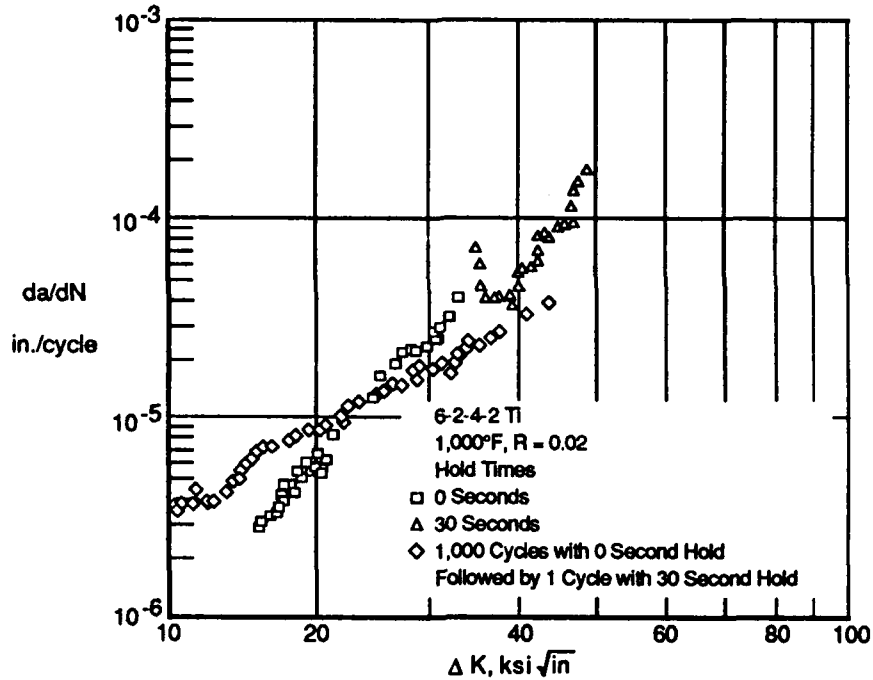
Figure 44. Non-Repeating Hold Time Effects on Crack Growth Rate of 6-2-4-2 Ti
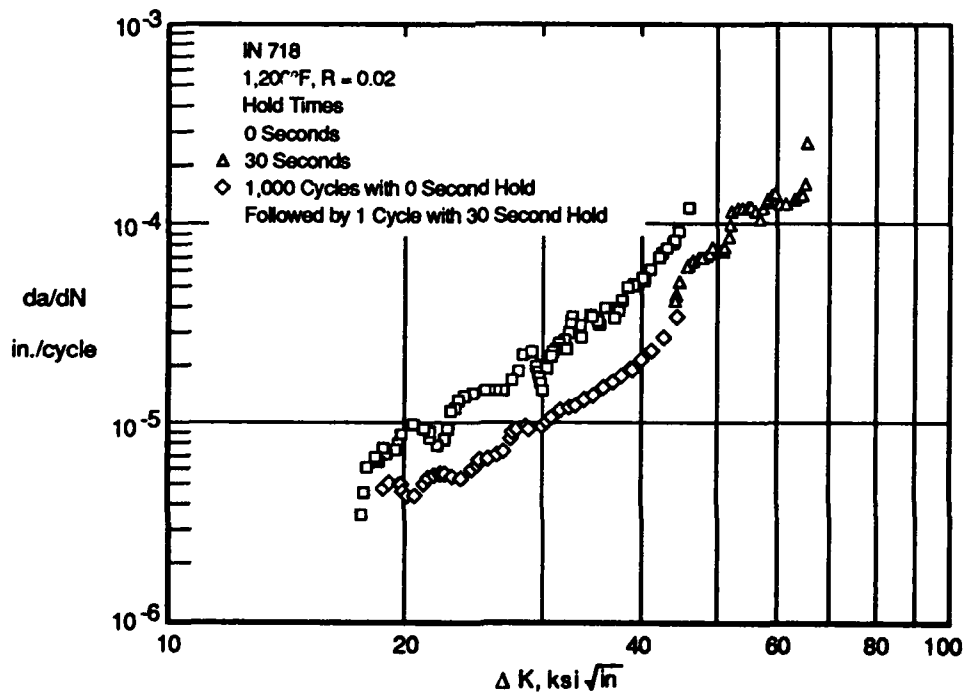
Figure 45. Non-Repeating Hold Time Effects on Crack Growth Rate of IN 718

52

The room temperature vacuum tests indicate that 6-2-4-2 Ti is more sensitive to its environment than IN 718. The vacuum 6-2-4-2 Ti data is shown in Figure 46 along with data from a test performed in lab air. The lab air accelerates crack growth rate compared to the vacuum data. Conversely, the IN 718 data (Figure 47) indicates that there is no effect on crack growth rate when tested in lab air as opposed to a vacuum. This reinforces the observation that our IN 718 material is insensitive to its chemical environment.

Crack growth rates of 6-2-4-2 Ti at 1000°F also display environmental sensitivity compared to tests conducted in a vacuum (Figure 48). However, vacuum tests with hold times applied at peak load have a minimal influence on the crack growth rate. This is consistent with lab air data (Figure 37).

Vacuum fatigue tests of IN 718 at 1200°F yielded highly questionable data (Figure 49). This data indicates that IN 718 is extremely sensitive to the environment. This is inconsistent with lab air data (Figure 39). The high frequency crack growth rate data is much slower than the lab air data. In addition, the replotted hold time data in Figure 49 shows substantial crack growth acceleration. Lab air hold time fatigue data displayed the opposite trend - crack growth retardation. If the material were environmentally sensitive, sustained load crack growth acceleration would be more prominent in lab air compared to a vacuum.

The vacuum fatigue hold time data was replotted because the original hold time data, provided by Georgia Tech, had stress intensities well above the fracture toughness of IN 718. This data was replotted assuming the crack lengths were incorrectly measured from the specimen edge and not from the center of the CT specimen loading holes. This assumption was based on the recorded crack lengths. The initial crack length machined into the CT specimen was 0.50 inch, but the first recorded crack length was 0.9 inch. In addition, the final crack length recorded was greater than the specimen width.

f. <u>Overload Fatigue Tests</u> - Georgia Tech performed a series of constant amplitude fatigue tests which were intermixed with single overload cycles. The purpose of these tests was to determine the retardation effects caused by

53
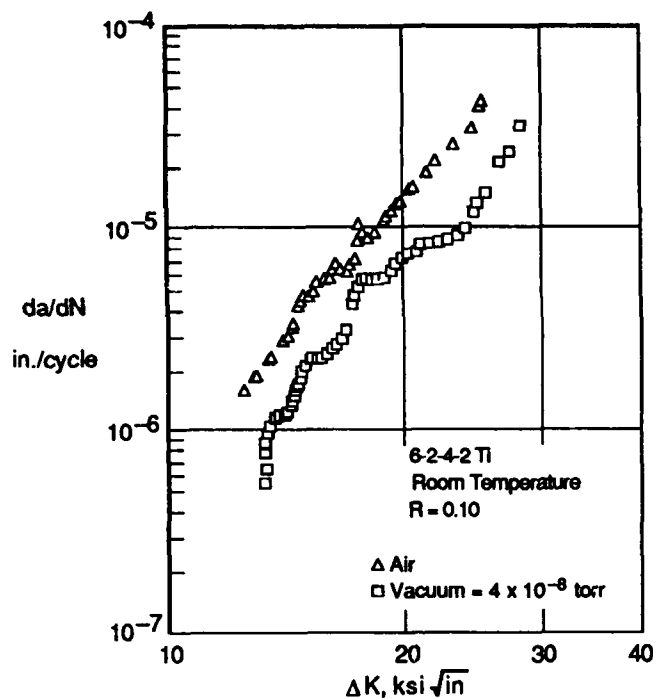
Figure 46. Environmental Effects on Crack Growth Rate
of 6-2-4-2 Ti at Room Temperature
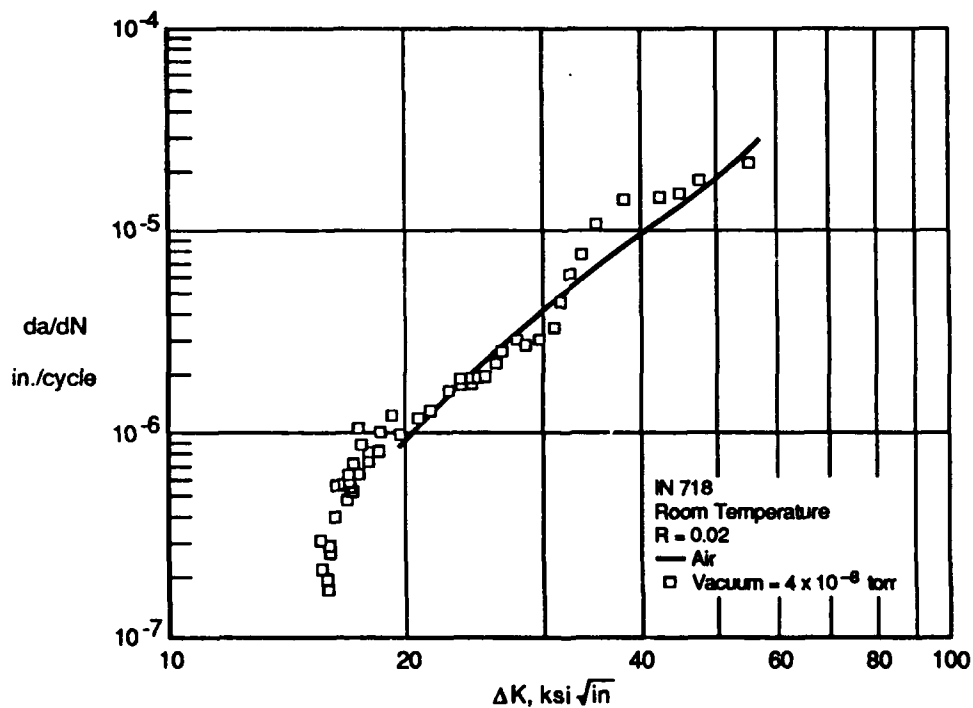
Figure 47. Environmental Effects on Crack Growth Rate of IN 718
at Room Temperature
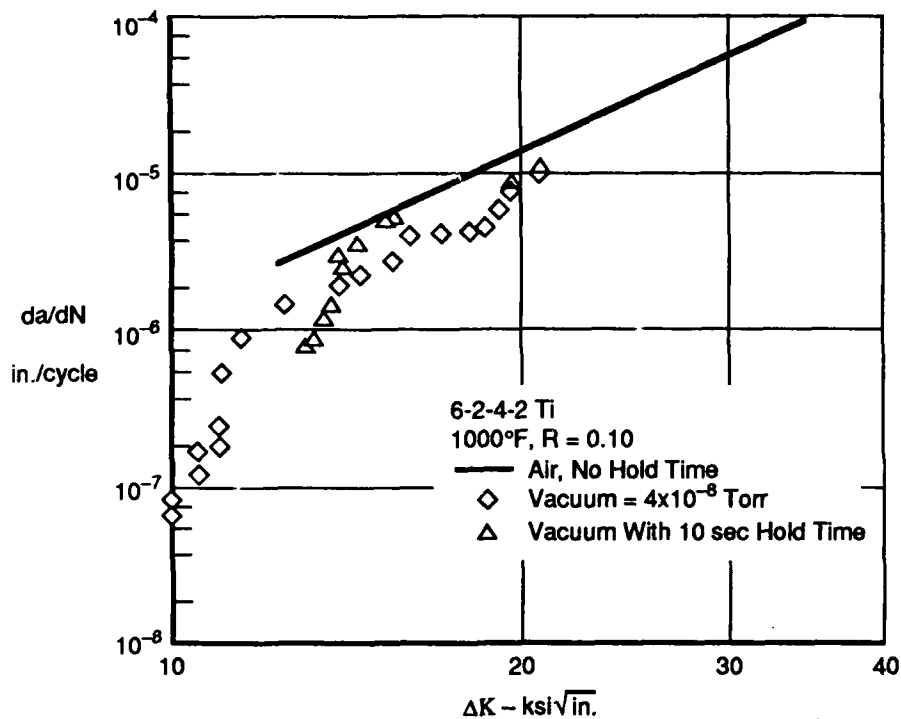
Figure 48. Environmental Effects on Crack Growth Rate of 6-2-4-2 Ti at 1000°F
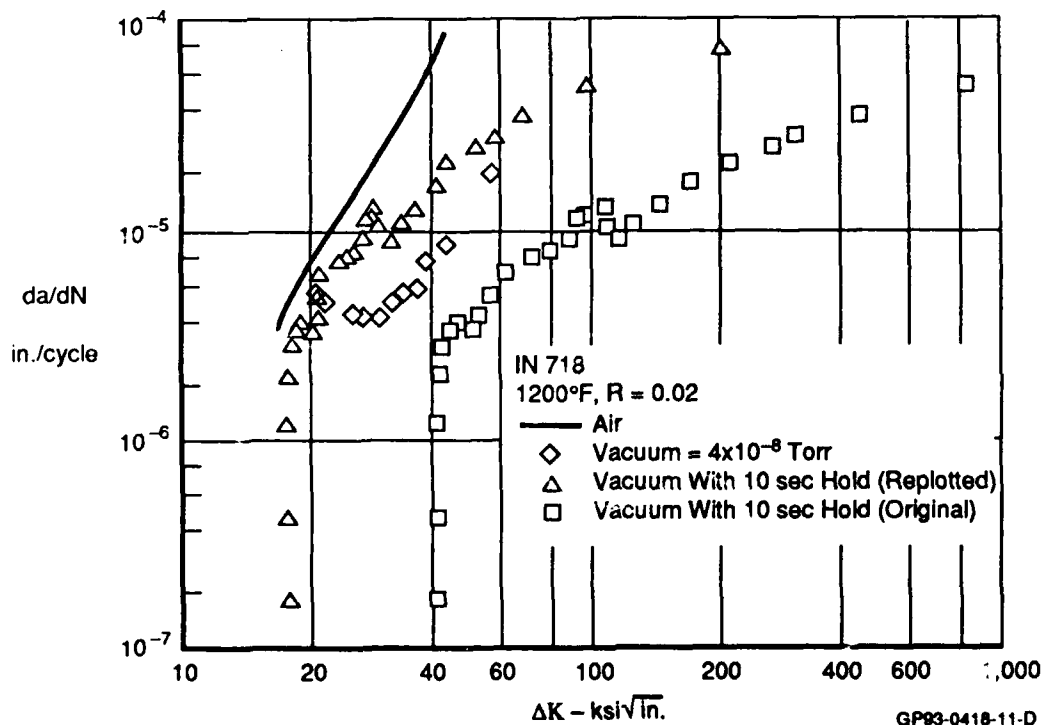
Figure 49. Vacuum Fatigue Test Results of IN 718 at 1200°F

55

the overloads on 6-2-4-2 Ti and IN 718 at elevated temperatures. A second set of tests with 30 second hold times during peak load was performed. The overload ratio was 1.8 for 6-2-4-2 Ti and 1.5 for IN 718. A smaller overload ratio was required for the IN 718 specimens to keep the overload under the 20,000 lb. capacity of the MTS testing machine. The stress ratio was 0.02 for all of the tests.

As discussed in an earlier section, crack growth data for hold time tests was difficult to obtain because of the length of time required to run a test. In these tests, the initial stress and crack length were selected to provide continuous crack growth curves. This meant, however, that a complete curve could not be obtained.

Local retardation after application of the overload is evident in the plots of crack growth rate vs. ΔK in 6-2-4-2 Ti (Figures 50 and 51). An overload yields additional material in front of the crack tip, which subsequently reduces the crack growth rate. Once the crack grew beyond the plastic zone created by the overload, the crack growth rate increased.

The additional plasticity caused by hold times at peak load and at elevated temperatures in creep sensitive materials has the effect of an overload. The plastic zone size increases and therefore, the crack growth rate decreases. The hold times applied in the overload tests increase retardation in the 6-2-4-2 Ti material.

Perhaps the most intriguing aspect of the 6-2-4-2 Ti elevated temperature overload data was that the retardation effects were more dominant at 700°F than at 1000°F in 6-2-4-2 Ti. The number of cycles required to recover from the retardation effect after the overload (known as delay cycles) is plotted against stress intensity in Figure 52 for both temperatures. Material property degradation and environmental sensitivity could possibly account for the decreased retardation effect seen at 1000°F. This would be consistent with the high frequency (Figure 33) and hold time (Figure 44) fatigue data discussed earlier.
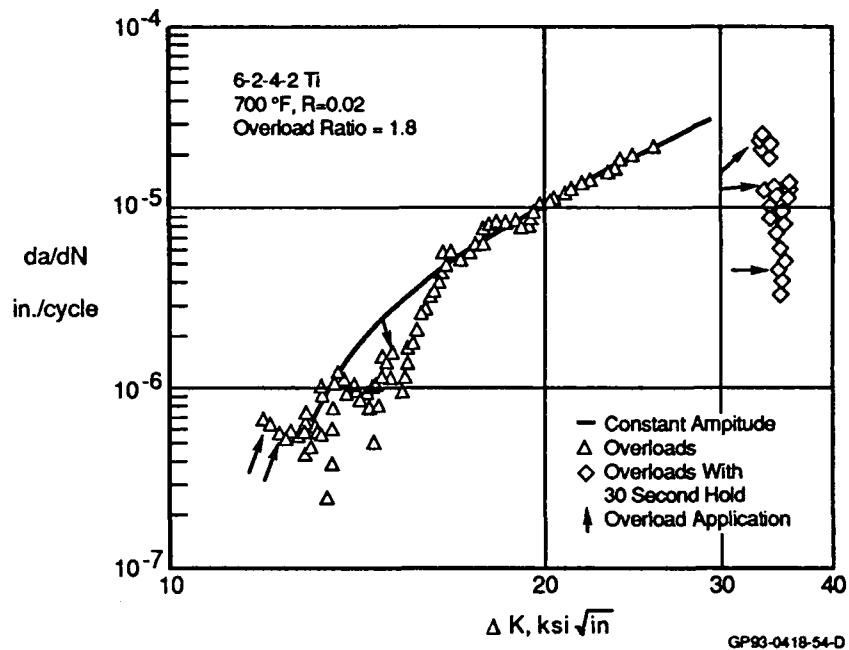
Figure 50. Crack Growth Retardation Due to Overloads in 6-2-4-2 Ti at 700°
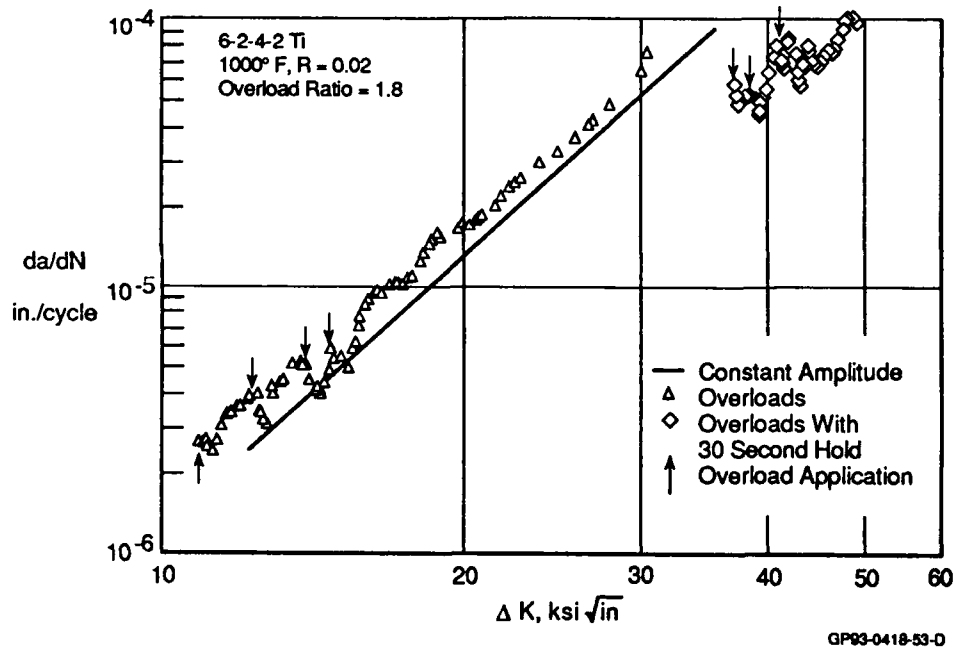
Figure 51. Crack Growth Retardation Due to Overloads in 6-2-4-2 Ti at 1000° F

57
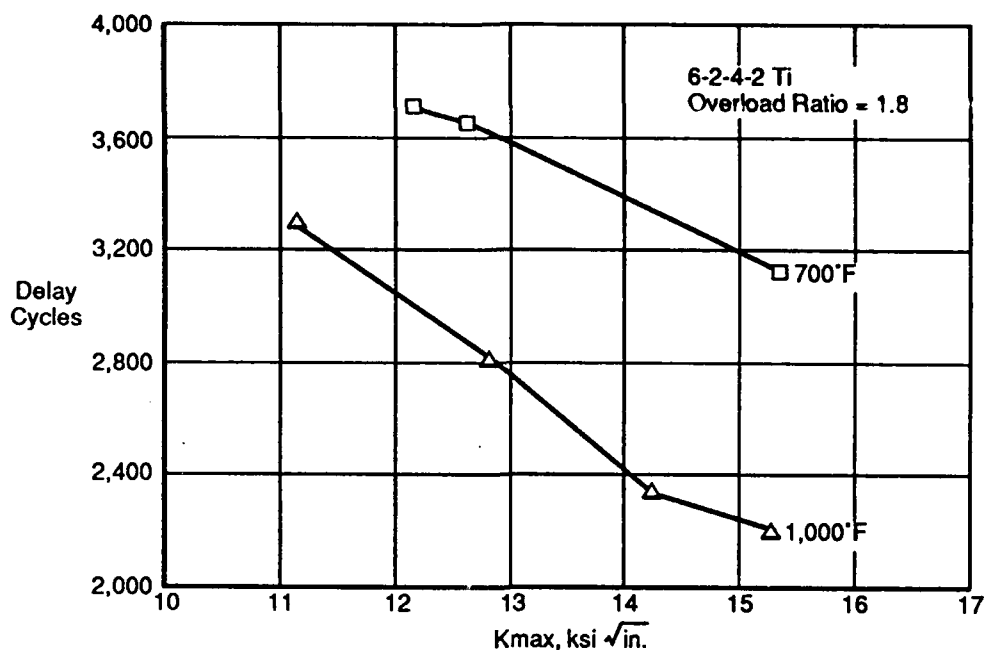
Figure 52. Delay Cycles at K_{max} for 6-2-4-2 Ti

The effects of overloads on crack growth retardation in IN 718 were the same as those for 6-2-4-2 Ti (Figures 53 and 54). Retardation developed in the vicinity of the overload. Hold times at peak load made the retardation more pronounced. At 700°F, the overload crack growth data coincided with the constant amplitude fatigue data.

In general, retardation was more pronounced in IN 718 at 1200°F than at 700°F. The initial overload cycle retarded crack growth by a factor of 3 as compared to the constant amplitude fatigue data at 1200°F (Figure 54). As ΔK increased and two additional overload cycles were applied, the retardation was less pronounced. A final overload was applied once the crack growth rate equaled that of the constant amplitude fatigue test. This overload produced a larger retardation effect than the two previous overloads.

g. _Overload/Underload Fatigue Tests_ - The final set of tests performed by Georgia Tech were overload/underload fatigue tests. In these tests, a compressive underload was applied directly after the tensile overload. The overload and underload ratios were 1.8 and -0.3 for 6-2-4-2 Ti, and 1.5 and -0.2 for IN 718. The constant amplitude stress ratio was 0.02 for all the tests.
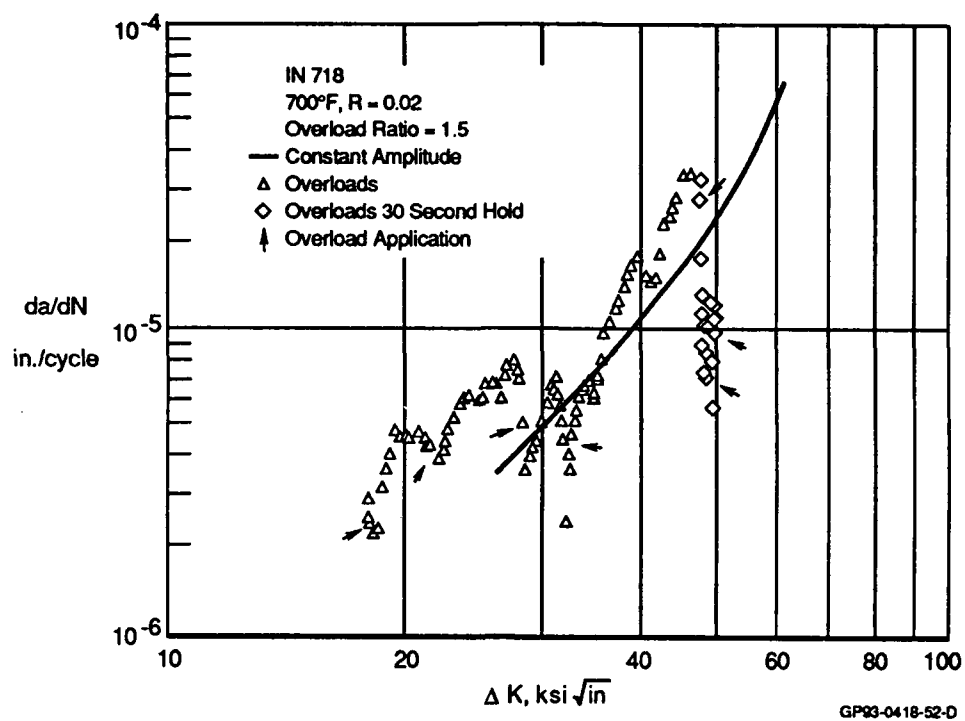
Figure 53. Crack Growth Retardation Due to Overloads in IN 718 at 700°F
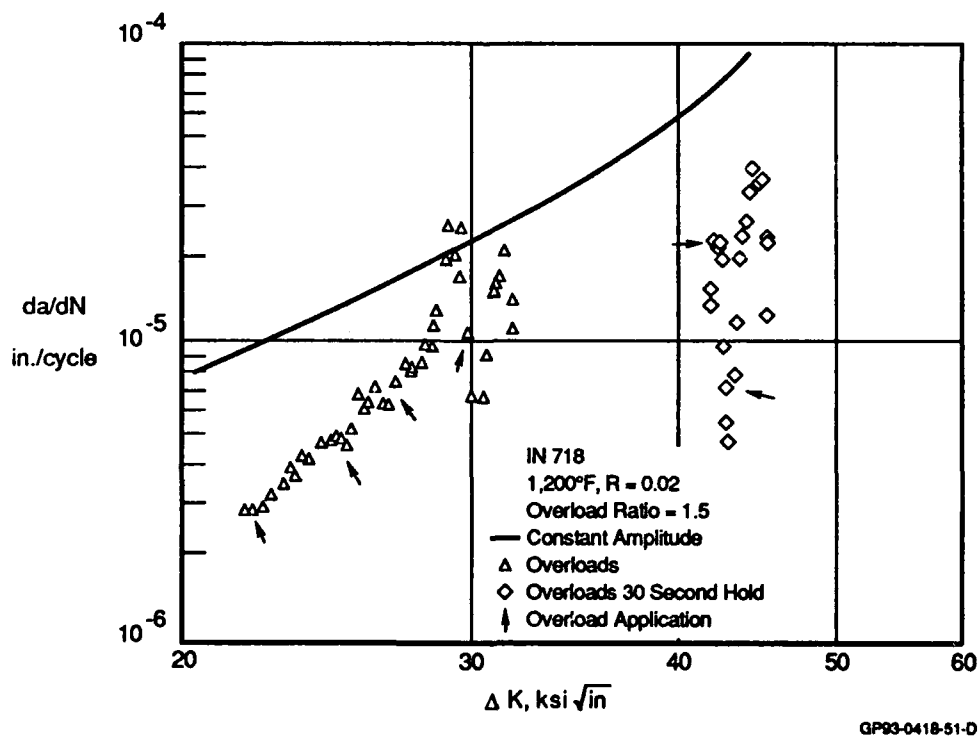
Figure 54. Crack Growth Retardation Due to Overloads in IN 718 at 1,200°F

59

The purpose of the overload/underload tests was to determine if crack growth retardation produced by a single overload could be reduced by the immediate application of a compressive underload. As discussed in the last section, the overload tends to increase the plastic zone in front of the crack tip. Conversely, an underload compresses the yielded material in the plastic zone, and thus reduces the effect of the plastic zone. Any crack growth retardation that may have resulted from the overload would, therefore, be reduced.

The high frequency overload/underload data at 700°F and 1000°F for 6-2-4-2 Ti display the same type of behavior as seen in the overload tests (Figures 55 and 56). Local retardation is more evident at 700°F than at 1000°F. In fact, all of the 700°F overload/underload data fall below the constant amplitude crack growth rate curve. Typically, 3 or 4 overload/underload cycles are applied, but in this particular test, a total of 18 overload/underload cycles were applied. This probably prevented the crack growth rate from fully recovering its constant amplitude value. Every time the crack growth rate would begin to recover, another overload/underload cycle was applied, thereby continually retarding crack growth.

The 1000°F, overload/underload crack growth rate data for 6-2-4-2 Ti directly coincides with the constant amplitude data (Figure 56). The minimal amount of retardation in this data makes the curve appear smooth. However, the hold time overload/underload crack growth rate data at this temperature show much more retardation. This data falls well below the constant amplitude data.

Very little retardation is noticeable in either the 700°F or the 1200°F high frequency crack growth rate data for IN 718 (Figures 57 and 58). As ΔK increased, local retardation effects increased at both temperatures. The largest retardation is evident at 1200°F when 30 second hold times are applied.

It is difficult to make any specific conclusions about this data. When only one test is run per test condition, it is impossible to distinguish bad data from good. More tests are needed to help define the effects of the

60
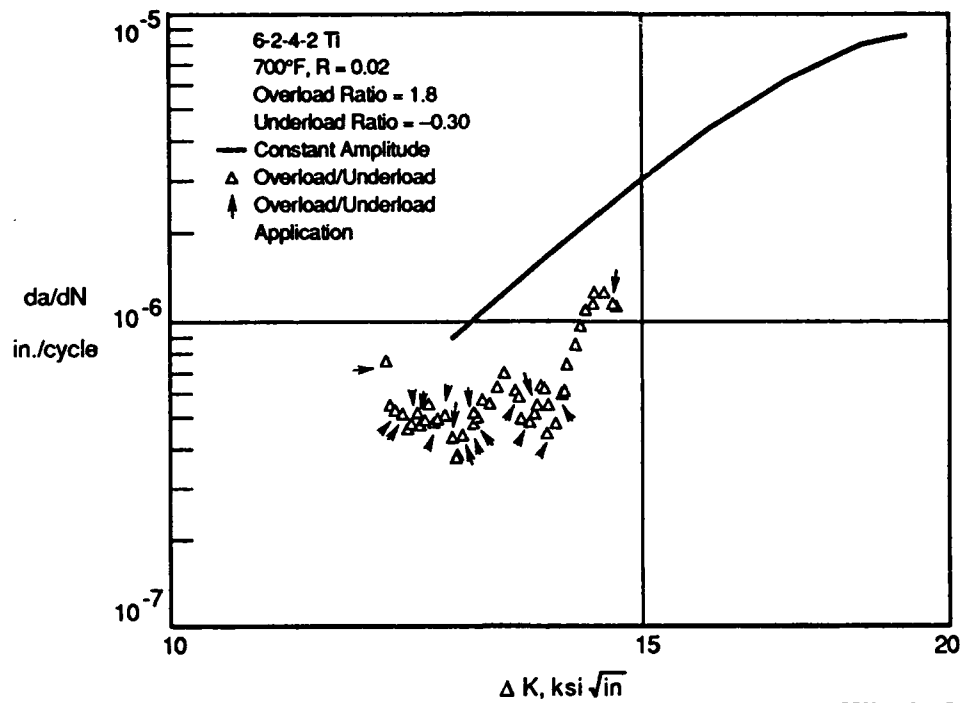
Figure 55. Crack Growth Retardation Due to Overload/Underload Cycles in 6-2-4-2 Ti at 700°F
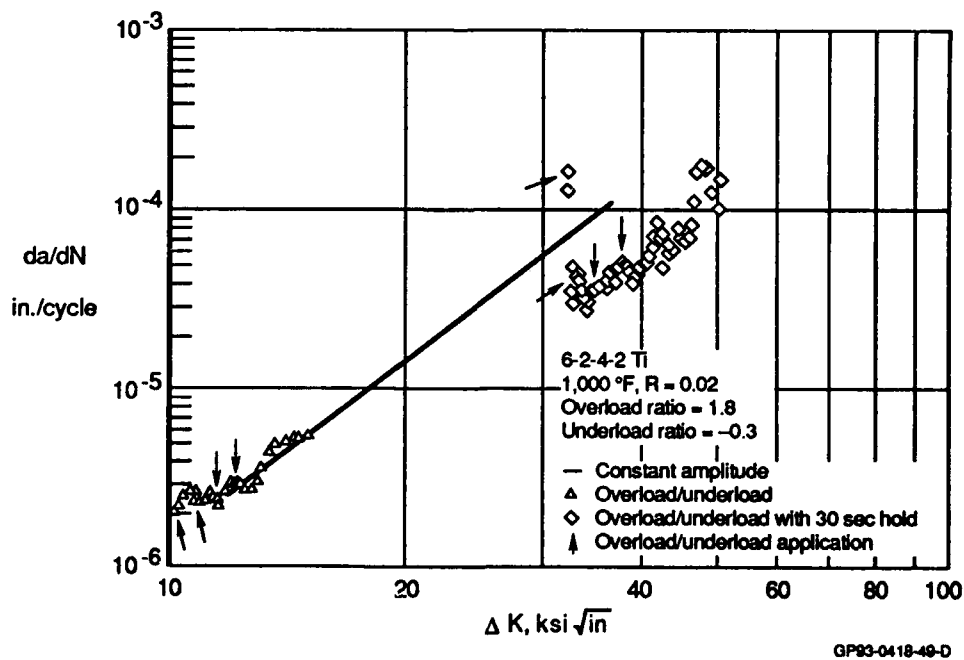
Figure 56. Crack Growth Retardation Due to Overload/Underload Cycles in 6-2-4-2 Ti at 1,000 °F

61
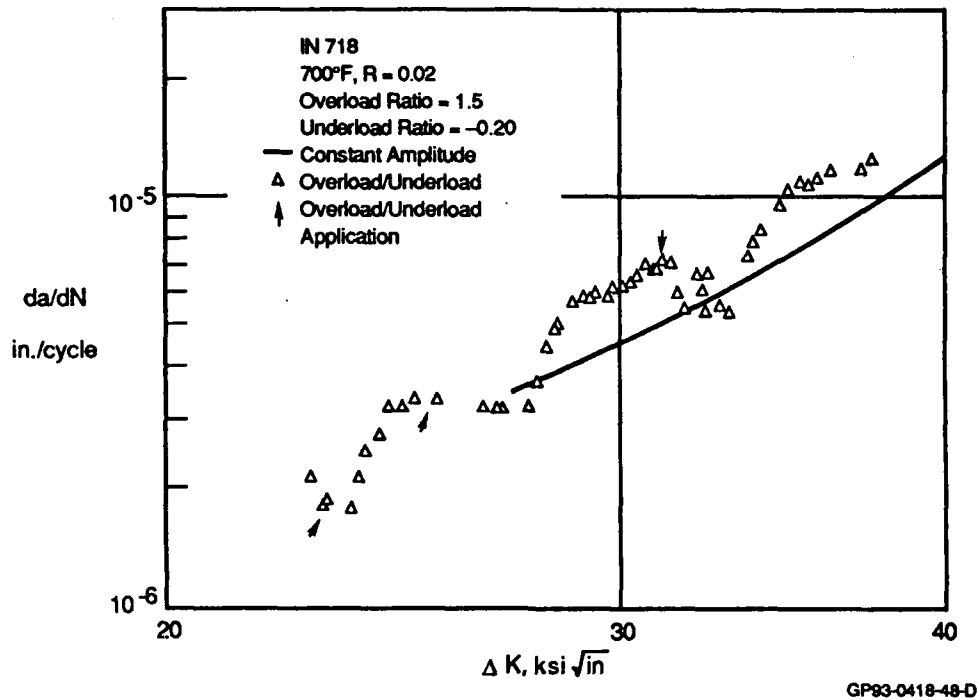
Figure 57. Effect of Overload/Underload Cycles on Crack
Growth Rate in IN 718 at 700°F
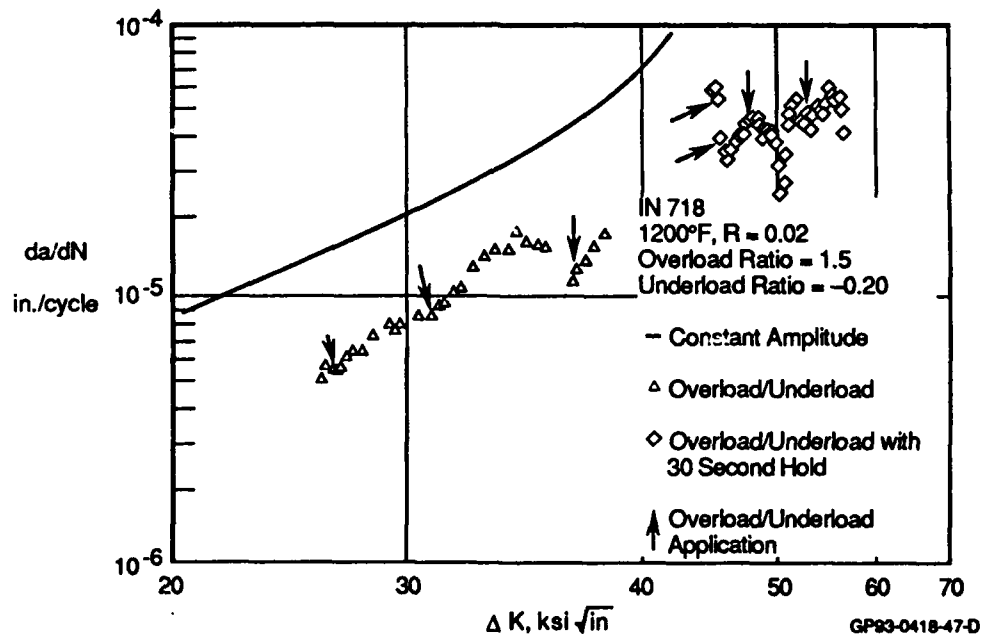
Figure 58. Crack Growth Retardation Due to Overload/Underload
Cycles in IN 718 at 1,200°F

overloads and the overload/underloads on crack growth. In addition, tests are needed which span the entire crack growth curve.

h. <u>Spectrum Load Fatigue Tests</u> - Spectrum load fatigue tests were performed at MCAIR. These tests were conducted at constant temperatures: room temperature for both 6-2-4-2 Ti and IN 718, 1000°F for 6-2-4-2 Ti, and 1200°F for IN 718. The tests were run with and without applying hold times at peak loads. The hold time lasted 30 seconds.

A load-time history typical of an aerospace vehicle was developed for these tests. The peaks in this spectrum range between 72.0 percent and 100.0 percent of the test load. The spectrum consists of 50 flight hours and 100 missions. A detailed explanation of the development of this spectrum is provided in Section VI-3b.

Plots of crack length vs. life for the room temperature tests are provided in Figures 59 and 60. Two stress levels were tested for each material. Plots also compared the crack growth behavior of constant amplitude tests vs. spectrum tests (Figures 61 and 62). These plots indicate that the crack growth behaviors of 6-2-4-2 Ti and IN 718 are similar for spectrum and constant amplitude loading. The curves separate in the advanced stages of life due to the different maximum stresses for each test. A higher maximum stress corresponds to a shorter critical crack length.

Elevated temperature tests produced shorter lives than the room temperature tests for both 6-2-4-2 Ti and IN 718 (Figures 63 and 64). In the case of 6-2-4-2 Ti, this was unexpected. Previously, 1000°F tests had yielded higher crack growth rates than room temperature tests. At higher ΔK values however, the crack growth rate decreased below that of room temperature tests (Figure 33). This indicated that creep dominates crack growth rates at high stress intensities. There is no indication of this effect, however, in the 1000°F spectrum test. High frequency, constant amplitude tests of IN 718 at 1200°F degrade crack growth rate (Figure 35). Therefore, it is not surprising that the 1200°F spectrum test had a shorter life.
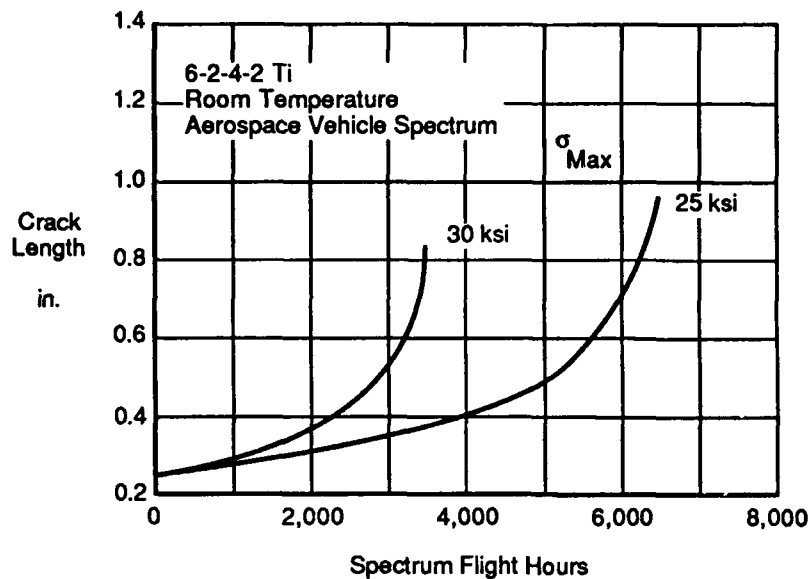
Figure 59. Room Temperature Spectrum Load Fatigue Tests in 6-2-4-2 Ti
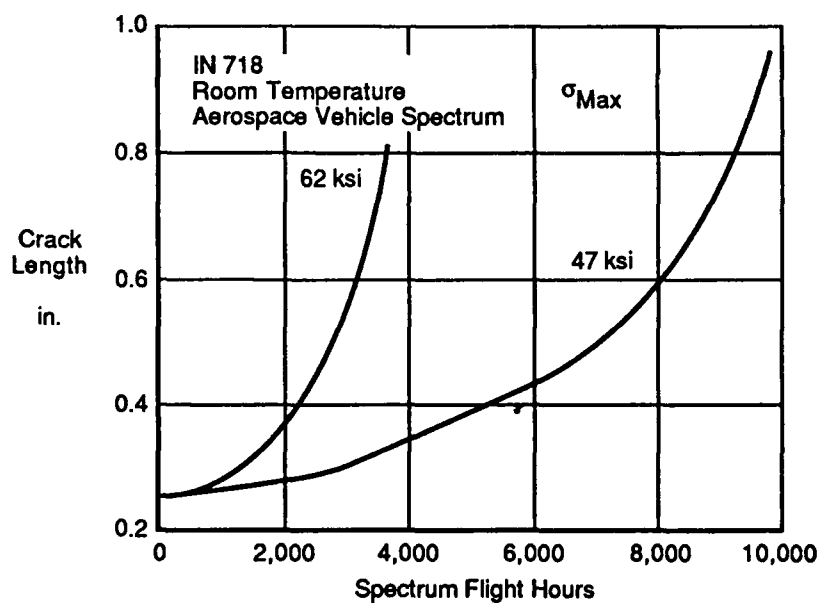
Figure 60. Room Temperature Spectrum Load Fatigue Tests in IN 718

64
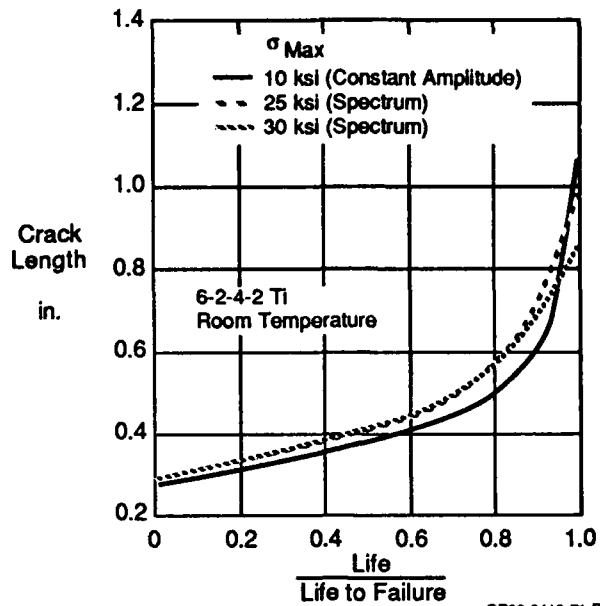
Figure 61. Spectrum and Constant Amplitude Crack Growth in 6-2-4-2 Ti
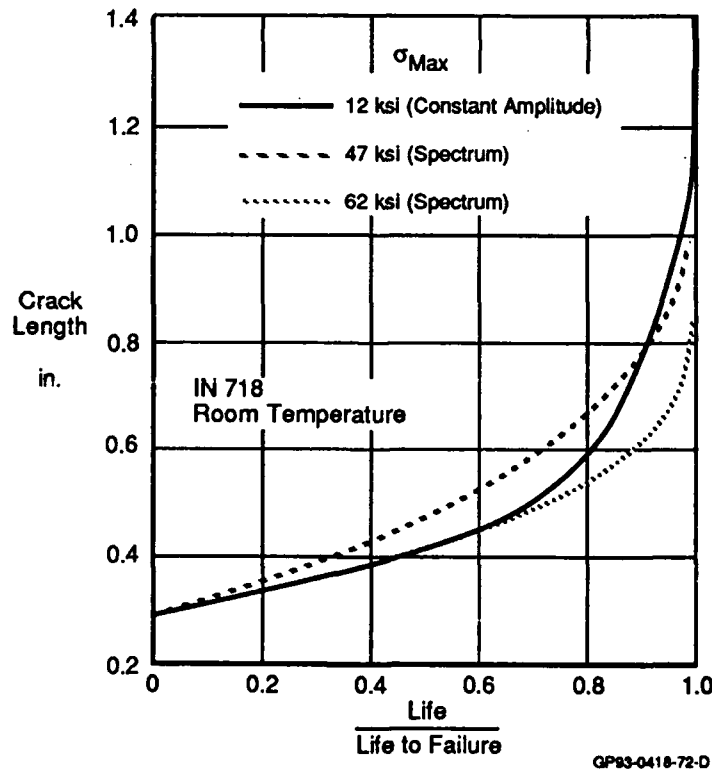
Figure 62. Spectrum and Constant Amplitude Crack Growth in IN 718

65

Hold times could not be applied continually throughout the tests due to time limitations. Instead, for each material 30 second hold times were applied for the first few hundred flight hours.

The hold time in the 6-2-4-2 Ti test was applied for the first 350 flight hours. The crack growth rate appeared to be slightly retarded during the hold time flight hours (Figure 63). After the hold times were stopped, the crack growth continued to trail behind that of the high frequency test, resulting in a longer life. This was consistent with the data obtained from the constant amplitude fatigue tests with hold times (Figure 37).
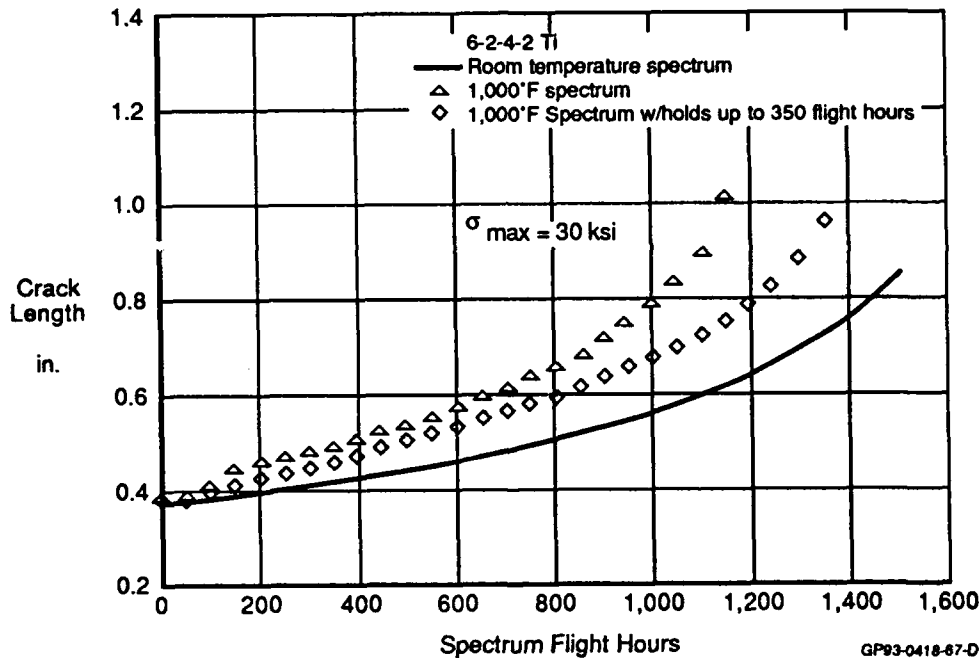
Figure 63. Isothermal Spectrum Fatigue Tests in 6-2-4-2 Ti

In the IN 718 test, the hold times were applied for the first 500 flight hours. During this time the crack growth rate accelerated (Figure 64). The crack growth decreased sharply when the hold time cycles were complete. This indicated that during sustained loads, IN 718 was susceptible to environmental attack. This was exactly the opposite behavior seen in the 1200°F hold time constant amplitude fatigue tests (Figure 39). In those tests, creep dominated more than did environmental sensitivity. Despite the conflicting behavior, it is still evident that the IN 718 material tested in this program was not as sensitive to environment as that tested by Larsen (Figure 41 and Reference 11).
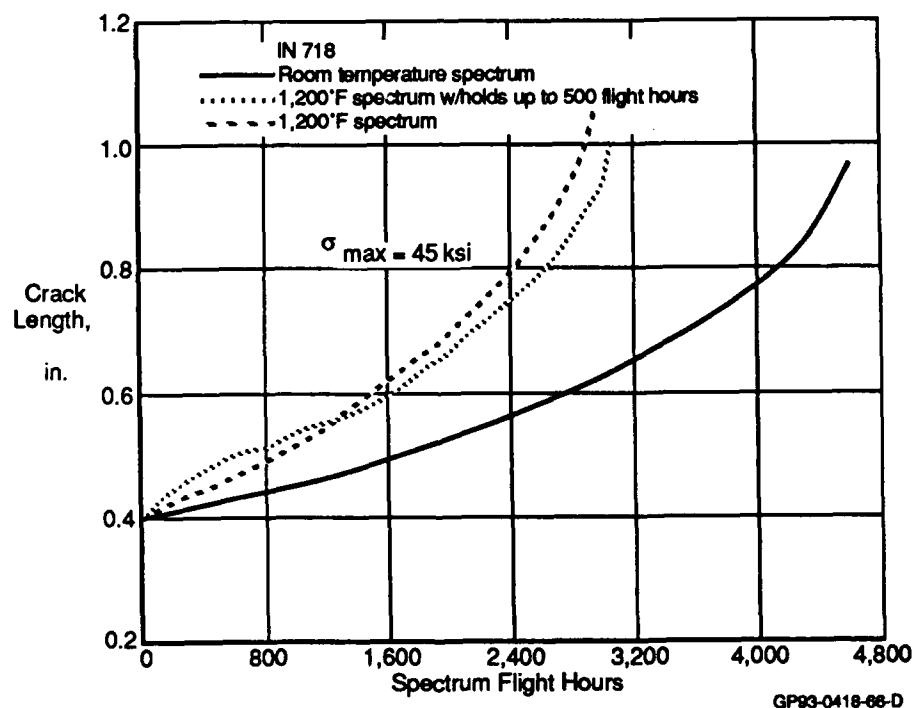
Figure 64. Isothermal Spectrum Fatigue Tests In IN 718

SECTION V

ANALYSIS DEVELOPMENT

1. <u>Analysis Summary</u> - A method has been developed for crack growth life prediction of metals subjected to combined mechanical and thermal loads. This analysis has been incorporated into a computer program called "<u>D</u>amage <u>A</u>nalysis of <u>M</u>etals subjected to <u>AG</u>gresive <u>E</u>nvironments" (DAMAGE). Volume II of this report is a user's manual for the program. DAMAGE is an extension of the computer program, CRKGRO, which was developed by Rockwell International for room temperature, spectrum fatigue analysis.

The DAMAGE program includes the following capabilities for elevated temperature analysis: 1) a temperature dependent Walker equation for fitting crack growth data; 2) a Wei-Landes method for sustained load crack growth; 3) Larson-Miller data to determine the effective yield strength based on time at temperature; 4) a method which accounts for a reduction in yield strength with temperature; 5) a method for predicting the effects of temperature on fracture toughness; and 6) a temperature dependent overload shut-off ratio for calculating retardation effects caused by overloads. DAMAGE will analyze crack growth in specimens with part-through or through cracks emanating from open holes or slots. Specimens may be subjected to axial loads and/or out-of-plane bending moments.

Theoretically, it is possible for the effects of sustained load cracking and creep due to hold time at temperature to compensate for each other and produce no net effect on crack growth rates. The model formulated under this contract would predict that an environmentally sensitive material which also creeps at elevated temperatures might demonstrate the behavior shown in Figure 65. During sustained loads, the crack growth is accelerated by environmental attack. But as cyclic loading is resumed, growth is retarded because of the additional plastic deformation caused by the hold time. This additional plasticity makes the sustained load behave like an overload.

The scope of this contract included using relatively simple methods to analyze elevated temperature crack growth, and to determine the accuracy of

these methods. The methods described in this section have been used by various investigators to model specific characteristics of crack growth behavior. In this contract, we attempted to consolidate these methods into one crack growth analysis.
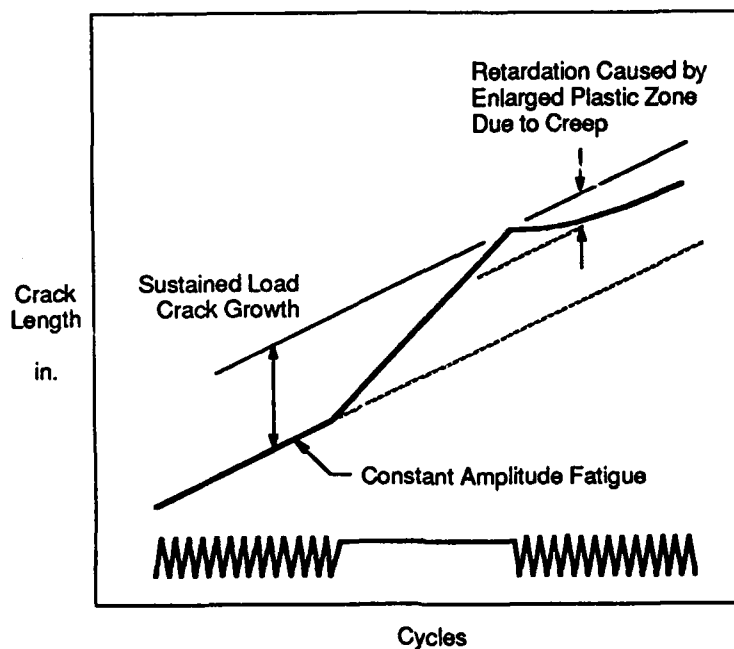
Figure 65. Offsetting Effects of Sustained Loads and
Creep on Crack Growth

2. **High Frequency, Elevated Temperature Crack Growth** - A number of schemes are available to model crack growth rate data. The engine community has been directly responsible for the development of two of the more popular methods: the Modified Sigmoidal Equation (MSE) Method developed by General Electric (Reference 11), and the Hyperbolic Sine Method developed by Pratt & Whitney (Reference 12). These two methods attempt to fit crack growth rate data in terms of four test variables: stress ratio, frequency, temperature, and hold time at peak load. These methods have been shown to produce some very good curve fits (Figure 66). However, as with any curve fit routine, the accuracy of the curve fit is directly dependent on the amount of data available.

70
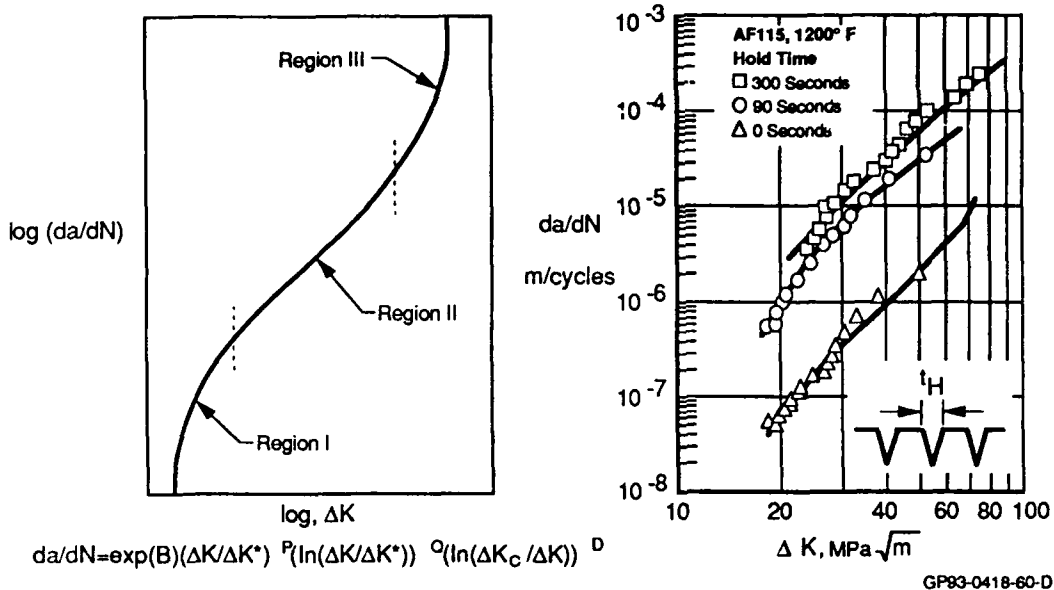
**Figure 66. Fitting Crack Growth Rate Data With the Modified
Sigmoidal Equation Model**

We have developed a method to account for elevated temperature effects on
high frequency crack growth rate. This method is based on the Modified Walker
equation and the Chang equation used in CRKGRO. The Modified Walker equation
is used to define positive stress ratio crack growth in a material for a given
temperature. Negative stress ratio crack growth is defined by the Chang
equation. This method models the dc/dN vs. ΔK curve for a variety of stress
ratios. The baseline crack growth equation is:

$$dc/dN = C \, [(1-R)^M K_{max}]^N \quad \text{for } R \geq 0$$

and

$$dc/dN = C \, [(1+R^2)^Q K_{max}]^N \quad \text{for } R < 0$$

C, M, N, and Q are constants which are calculated within the DAMAGE program.
When dc/dN is plotted against $(1-R)^M K_{max}$ (for positive stress ratios) and
$(1+R^2)^Q K_{max}$ (for negative stress ratios) on a logarithmic scale, the log(C)
represents the intercept of the curve with the log(dc/dN) axis, and N
represents the slope of the line. M and Q are the values which best collapse
the crack growth data for different stress ratios onto one line.

71

The constants C and N are determined from the R=0 test data. When R=0, the above equations reduce to:

$$dc/dN = C \, K_{max}{}^N$$

The equation for a line is found when the log of both sides is calculated:

$$\log(dc/dN) = \log(C) + N \log(K_{max})$$

A least squares fit is then used to determine the values of C and N.

Data for positive stress ratios, R>0, determines the value of M. An expression for M is found by the ratio of the dc/dN equation for R>0 and the dc/dN equation for R=0.

$$\frac{dc/dN_{R>0}}{dc/dN_{R=0}} = \zeta = \frac{C \, [(1.0-R)^M \, K_{max}]^N}{C \, K_{max}{}^N} = (1.0-R)^{M \, N}$$

The equation for M is determined by taking the log of both sides of the above equation.

$$M = \sum_{i=1}^{npt} \log(\zeta_i)/[N \, \log(1.0-R)]$$

where npt = number of dc/dN vs. ΔK data points for R>0 curves.

A similar equation for Q is determined using the same procedure. In this case, however, only data from negative stress ratio (R<0) tests are used. The expression for Q is:

$$Q = \sum_{i=1}^{npt} \log(\dot{c}_i)/[N \log(1.0+R^2)]$$

The Modified Walker equation and the Chang equation, as described above, allow for only linear curve fits of crack growth rate data. However, if the dc/dN vs. ΔK data is partitioned, theoretically it is possible to obtain a multi-linear curve fit. DAMAGE is limited to producing linear and bi-linear curve fits.

To account for elevated temperatures, crack growth data is required at room temperature and at either one or two elevated temperatures. Each set of data is fit using the Modified Walker and Chang equations, such that values of C, M, N, and Q are determined at each temperature. Given a value of ΔK, the crack growth rate, dc/dN, is calculated for each temperature. If data for only two temperatures is provided, the actual dc/dN for a specified temperature is interpolated from between the room and maximum temperature logarithmic dc/dN values. If data for three temperatures is provided, a quadratic curve is fit to the logarithmic dc/dN data.

The Modified Walker and Chang equations were used to curve fit the crack growth rate data from the constant amplitude fatigue tests performed in the test program. The curve fits for 6-2-4-2 Ti and IN 718 are plotted along with room and elevated temperature data in Figures 67 and 68. The Modified Walker and Chang coefficients for 6-2-4-2 Ti and IN 718 are listed in Figure 69.

The Modified Walker and Chang equations correctly determine a crack growth rate within the data provided. However, this method does not extrapolate accurately. The data provided for 6-2-4-2 Ti at room temperature includes stress ratio values of 0.02, 0.50, and -0.3. The Modified Walker and Chang coefficients (C, N, M, and Q) based on this data calculates extremely conservative dc/dN values for stress ratios smaller than -0.3. Therefore, when using the Modified Walker and Chang equations, upper and lower bounds for the stress ratio should be defined.

73
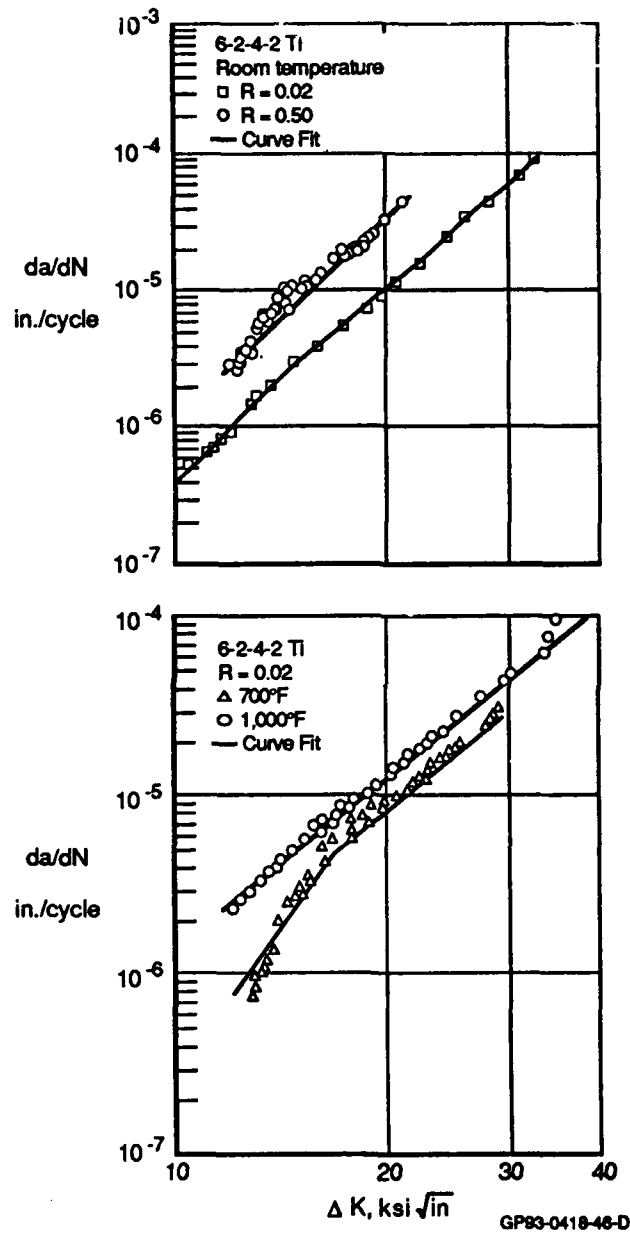
Figure 67. Fitting High Frequency (10Hz)
Crack Growth Rate Data with the
Modified Walker Equation(6-2-4-2 Ti)

74
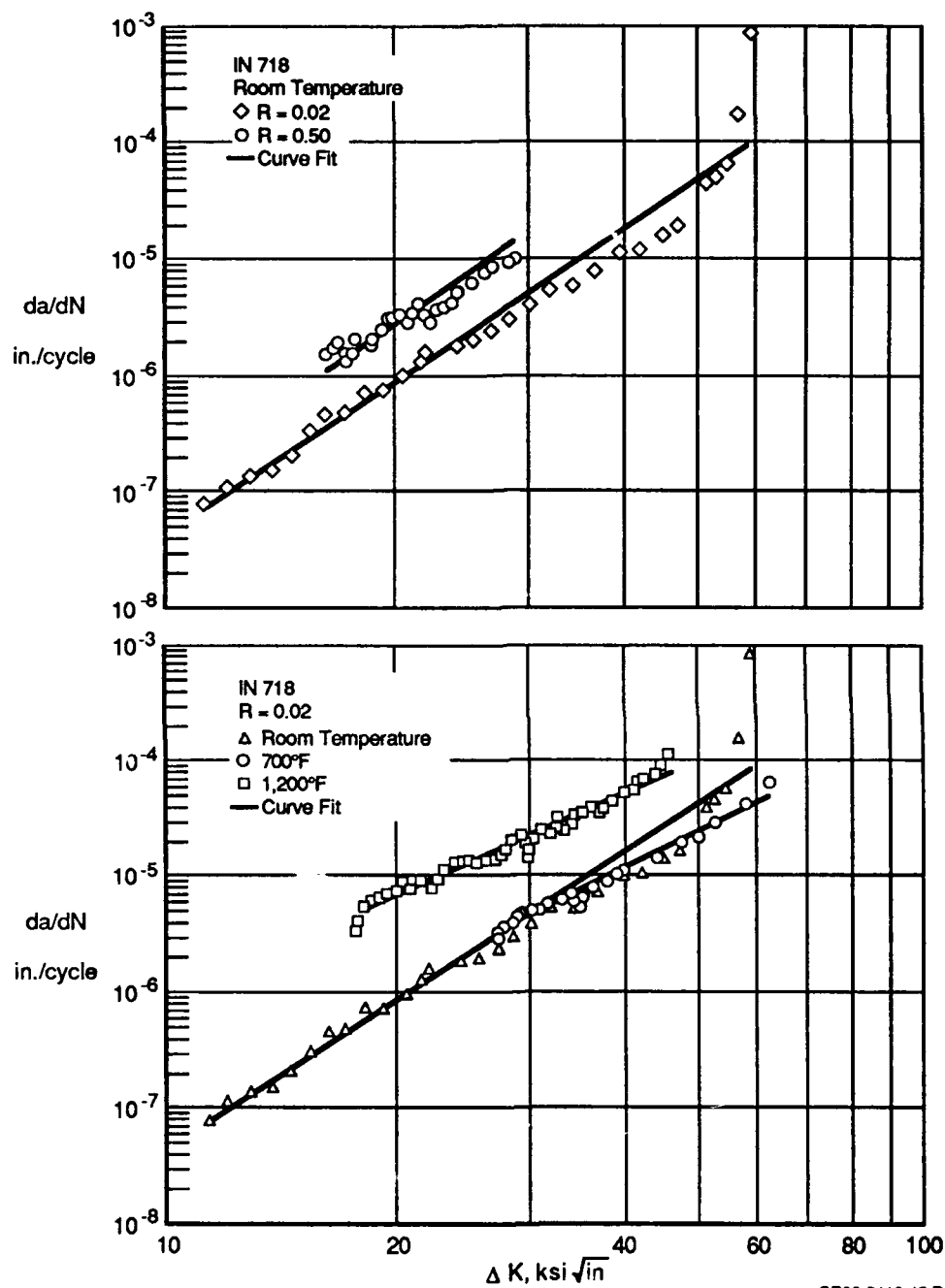
Figure 68. Fitting High Frequency (10Hz) Crack Growth
Rate Data with the Modified Walker Equation (IN 718)

	6-2-4-2 Ti		IN 718	
	Region I	Region II	Region I	Region II
Room Temperature				
C	1.149 E-12	1.059 E-11	—	2.256 E-12
N	5.566	4.689	—	4.280
M	0.529	0.618	—	0.596
Q	1.000	1.982	—	1.009
700°F				
C	8.729 E-12	1.494 E-10	—	6.857 E-11
N	4.616	3.641	—	3.269
M	1.000	1.000	—	1.000
Q	1.000	1.000	—	1.000
1,000°F				
C	—	4.974 E-10	—	—
N	—	3.409	—	—
M	—	0.771	—	—
Q	—	1.000	—	—
1,200°F				
C	—	—	—	1.406 E-9
N	—	—	—	2.855
M	—	—	—	0.941
Q	—	—	—	1.000

$$\frac{dc}{dN} \quad C[(1-R)^M K_{max}]^N \text{ for } R \geq 0$$

$$\frac{dc}{dN} \quad C[(1+R^2)^Q K_{max}]^N \text{ for } R < 0$$

**Figure 69. Modified Walker and Chang Equation Coefficients for
6-2-4-2 Ti and IN 718**

Some of the constant amplitude model development test data has been compared to life predictions obtained with the DAMAGE analysis program. Room and elevated temperature fatigue data are listed in Figure 70 along with the DAMAGE predictions. The predictions agree very well with the data.

3. <u>Crack Growth Acceleration Due to Environmental Effects</u> - The Wei-Landes approach for environmental acceleration of crack growth was incorporated into DAMAGE. This method is used to account for the effect of time at load upon crack growth. This approach uses the crack growth rate data for R=0 tests at high and low frequencies to determine dc/dt for a given temperature.

The Wei-Landes method as applied to elevated temperature crack growth separates the crack growth due to mechanical load cycling from that due to sustained loads. It is assumed that the total crack growth is the sum of these two terms. Mechanical load crack growth is measured in terms of crack

length per cycle, dc/dN. Sustained load crack growth is measured in terms of crack length per time, dc/dt.

Material	R	Cycle Time (sec)	Temperature (°F)	Stress (ksi)	Initial Crack Length (in.)	DAMAGE Life (cycles)	Test Data Life (cycles)
Ti	0.02	0.100	R.T.	10.000	0.27	415,891	404,807
Ti	0.02	0.111	R.T.	11.884	0.35	96,149	126,100
Ti	0.50	0.111	R.T.	20.901	0.37	41,573	43,760
Ti	−0.30	0.111	R.T.	11.207	0.37	47,242	43,090
Ti	0.02	0.167	700	11.205	0.39	157,400	154,100
Ti	0.02	0.167	1,000	10.144	0.41	97,228	98,600
Ti	0.50	0.125	1,000	25.362	0.36	31,099	30,830
Ti	0.02	0.167	1,000	11.782	0.38	66,898	80,300
In	0.02	0.100	R.T.	12.000	0.28	2,070,076	1,976,864
In	0.02	0.250	R.T.	15.841	0.41	290,410	302,700
In	0.50	0.100	R.T.	28.829	0.36	165,447	163,360
In	−0.20	0.100	R.T.	14.414	0.40	377,255	382,300
In	0.02	0.167	700	23.041	0.40	75,168	76,300
In	0.02	1.000	1,200	18.290	0.28	50,175	50,170
In	0.50	0.125	1,200	29.144	0.35	60,651	62,070

GP93-0418-4-T

Figure 70. DAMAGE Predictions and Isothermal Fatigue Test Results
(Constant Amplitude)

To use the Wei-Landes method, two crack growth curves must be supplied: one obtained from a high frequency test and one from a low frequency test. An optimum curve for the low frequency data would be one which had the same loading speed as the high frequency data, but had a hold time at peak load.

Figure 71 demonstrates how the Wei-Landes model is used to determine dc/dt from the differences between high and low frequency crack growth rate data. In this figure, 10 Hz is the high frequency and 0.10 Hz is the low frequency. First, it is assumed that hold time has little or no effect on crack growth rate at the 10 Hz frequency. Thus the difference between crack growth rates for cycles having the 10 second hold times (0.10 Hz) and those having no hold times (10 Hz) is used to determine dc/dt for each test temperature. The dc/dt versus K_{max} curves for each temperature are integrated as a function of stress intensity factor to determine the cracking due to sustained loads during (1) loading, (2) hold at maximum load, and (3) unloading.

77
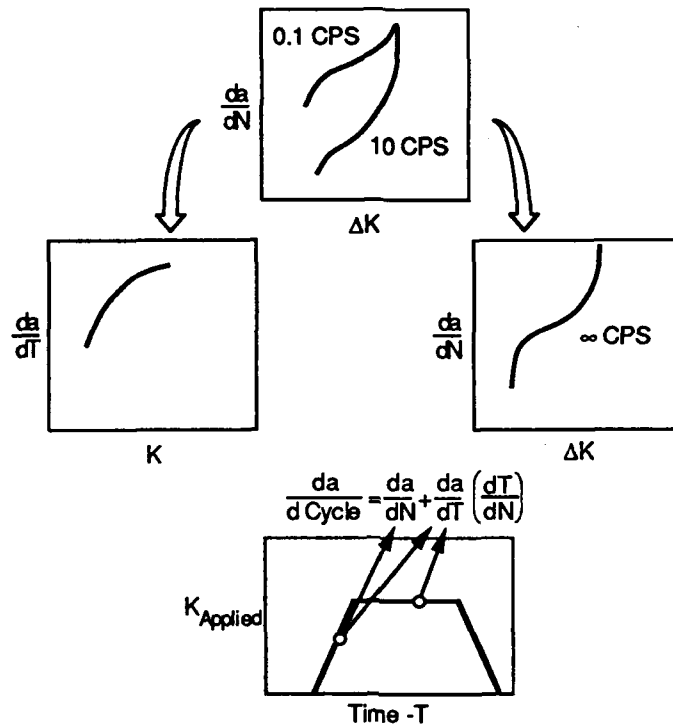
Figure 71. Wei - Landes Method

$$\frac{dc}{dN}\bigg|_s = \int_{Ts}^{Tf} \frac{dc}{dt}(K) \ dt = \int_{Ts}^{T1} \frac{dc}{dt}(K) \ dt + \frac{dc}{dt}(K_{max}) \ast (T2-T1) + \int_{T2}^{Tf} \frac{dc}{dt}(K) \ dt$$

The stress intensity, K, is a function of time, t, and Ts and Tf are the cycle start and finish times (Figure 72). In DAMAGE, the loading and unloading portions of the applied load curve are assumed to be in the form of a sine wave such that:

$$K(t) = K_{min} + (K_{max}-K_{min}) \ sin(\pi t) = K_{max} \ [R + (1.0-R)sin(\pi t)]$$

where R is the stress ratio.

$$\frac{da}{dN}_{Sustained} = \int_{T_s}^{T_1} \frac{da}{dt}(K)dt + \frac{da}{dt}(K_{max}) \times (T_2 - T_1) + \int_{T_2}^{T_f} \frac{da}{dt}(K)dt$$
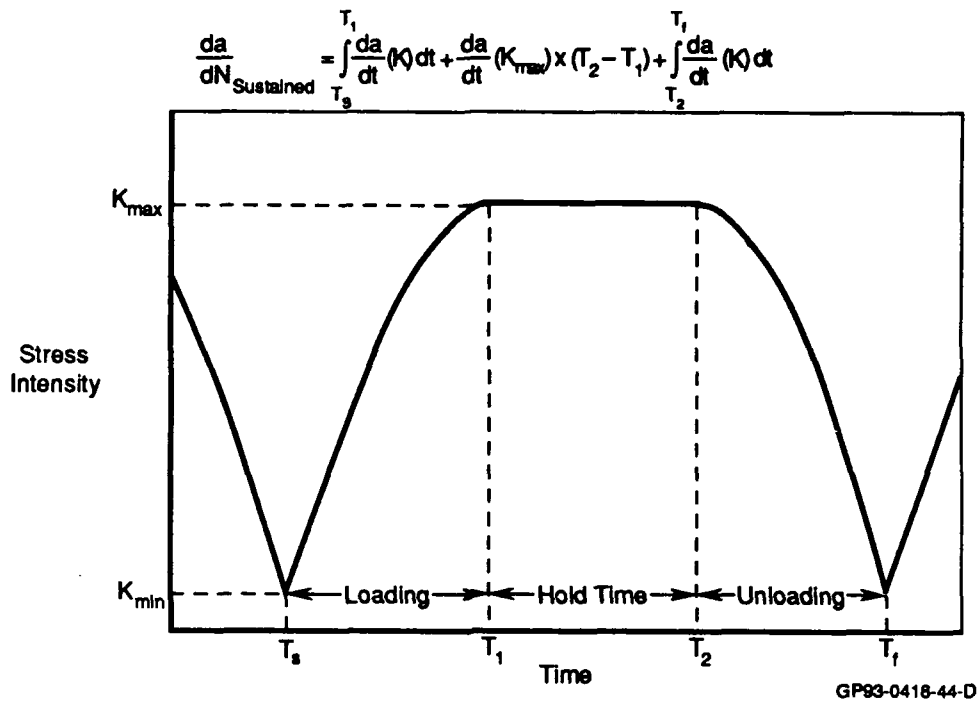
Figure 72. Stress Intensity as a Function of Time

It was found in Reference 13 that the unloading portion of the load history could be ignored once loads were below 80 percent of the peak load. The same effect was noted by Larsen (Reference 11) in his tests of IN 718.

The total crack growth rate is found by summing the cyclic crack growth rate, dc/dN_c, and the sustained crack growth rate, dc/dN_s.

$$dc/dN = dc/dN_c + dc/dN_s$$

The cyclic crack growth rate is determined using the Modified Walker equation, as discussed in the previous section. This equation will account for stress ratio and temperature effects.

The Wei-Landes method has been included in DAMAGE. It was previously used to predict the effect of load frequency on crack growth rates of 300M steel in salt water (Figure 73). It has also been used to predict crack growth behavior of AF115 engine alloy at 1200°F with 90 second hold times at peak load (Figure 74). In each case, the high and low frequency crack growth

79

curves were used to calculate the creep rate of the material. The Wei-Landes model can be used to curve fit crack growth acceleration due to hold times at temperature as shown in Figure 74, since acceleration at temperature is a product of the chemical environment.
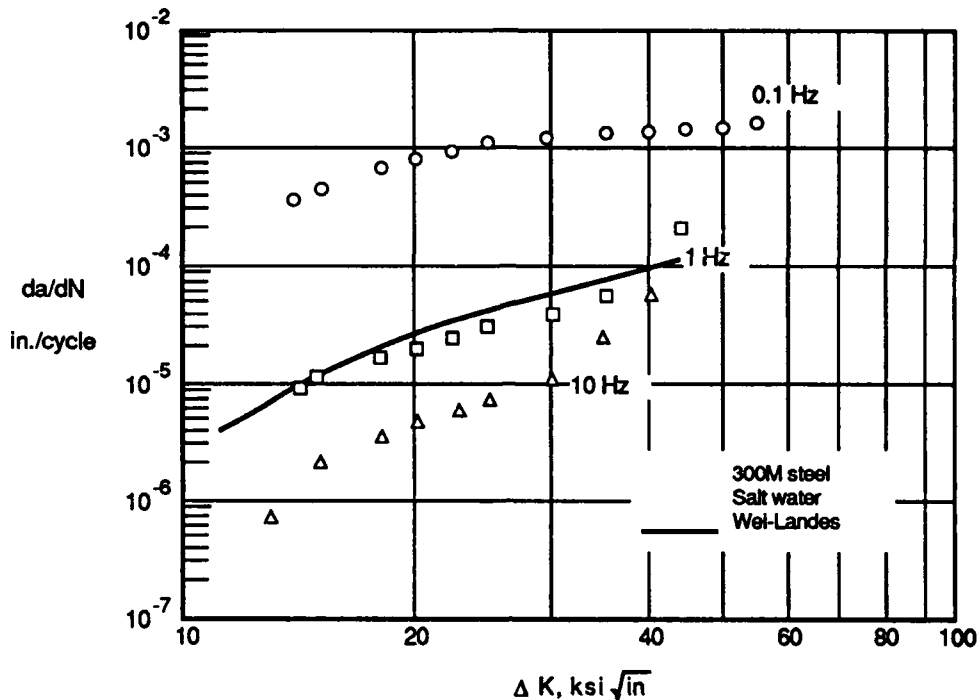
GP93-0418-62-D

Figure 73. Predicted and Actual Crack Growth Data for 300M Steel in Salt Water
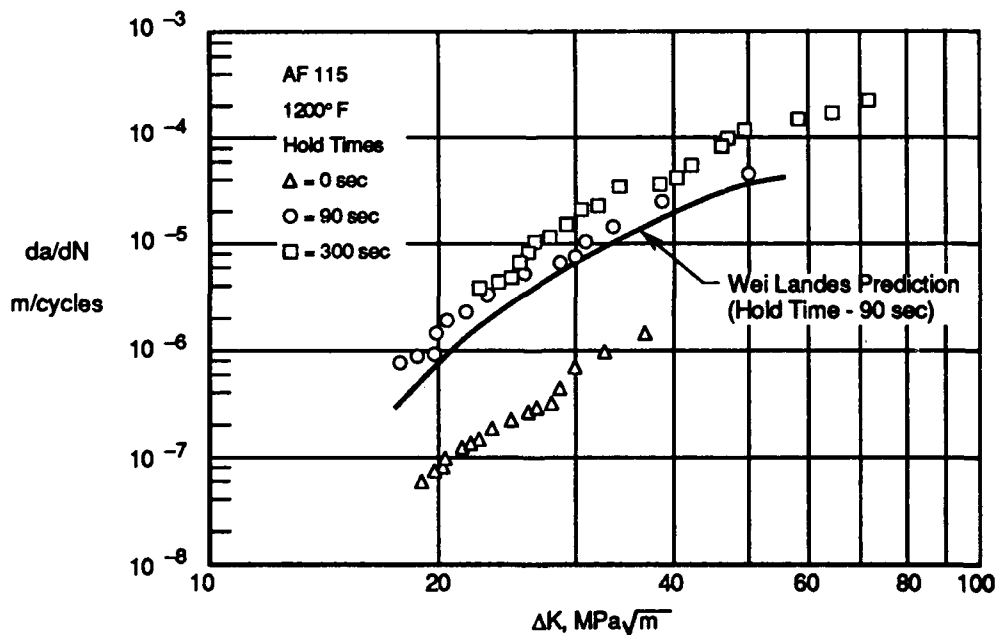
GP93-0418-80-D

Figure 74. Predicted and Actual Crack Growth Data for AF115 at 1200° F Subject to Sustained Loads

80

Larsen has shown (Reference 11) that as hold time at load increases in IN 718 at 1200°F, the sustained load crack growth dominates the cyclic crack growth (Figure 41). For small cycle times with essentially no sustained loads, the crack growth rate is determined by mechanical loads. Testing with different stress ratios but the same K_{max} produce different crack growth rates. But as the cycle time increases, the crack growth rate data for the two stress ratios fall on the same line. The dominance of the sustained load crack growth can be predicted with the Wei-Landes method.

IN 718 was chosen for model development testing because of its environmental sensitivity. Previous testing, as described in Reference 11, demonstrated that when subjected to sustained loads at high temperatures (1200°F), the crack growth rate increased substantially. The material tested in this program did not show this behavior. In fact, just the opposite behavior was found. Crack growth decelerated during elevated temperature hold times at peak load (Figure 39). The reason for this difference in behavior is unclear. Metallurgical examinations were conducted to determine if the aging process performed on the as-received material adversely affected the material. These tests proved inconclusive. Although the grain structure changed during the aging cycle, this should not have affected the environmental sensitivity of the material.

4. <u>Crack Growth Retardation Due to Creep Effects</u> - A major influence on elevated temperature crack growth in metals is creep. Creep will blunt the crack tip, and thereby reduce the crack growth rate. This behavior has been seen in both the 6-2-4-2 Ti (Figure 37) and the IN 718 (Figure 39).

The crack growth model incorporated into DAMAGE models the plastic zone in front of the crack tip as shown in Figure 75. The plastic zone increases due to reduced yield strength at high temperatures. This zone is also affected by increased plasticity with hold time at temperature (creep). The Willenborg model calculates the plastic zone size as follows:

$$\rho = \gamma/(2\pi) \ (K_{max}/F_{ty})^2$$

where

$$\gamma = 1 - \text{plane stress}$$

$$\gamma = 1/3 - \text{plane strain}$$

$$\text{and } F_{ty} = \text{material yield strength.}$$

The plastic zone size is inversely proportional to the material yield strength.

GP93-0418-59-D
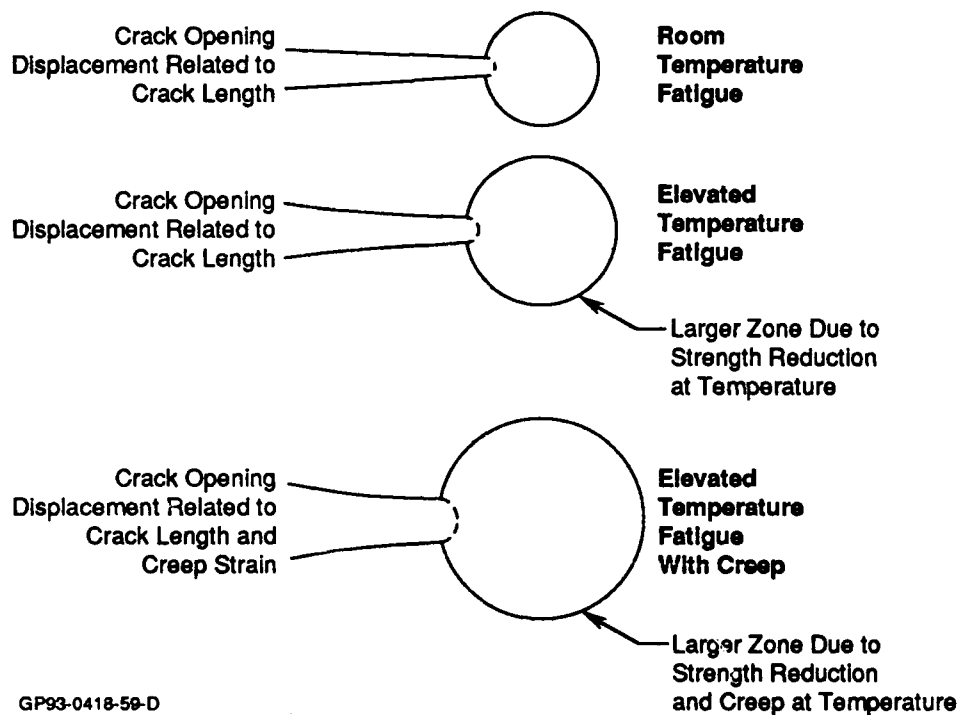
Figure 75. Effect of Temperature and Sustained Loads on Plastic Zone Size

Creep is introduced into this model through the effective yield strength, F_{ef-ty}. The effective yield strength is defined as the stress level required to produce 0.2 percent strain in a material at a given temperature and hold time. The effective yield strength is calculated at each load cycle and is used to determine the plastic zone size. As the temperature and hold time increase, the effective yield strength decreases and the plastic zone size increases. Crack growth is retarded as long as the crack is within the plastic zone.

82

Data are available which define the effective yield stress for various materials. These data are in the form of Larson-Miller graphs which plot the effective yield strength vs. a temperature and hold time parameter, P.

$$P = (460 + T)(P_{lm} + \log(t_h)) \; 10^{-3}$$

where T is the temperature in degrees Fahrenheit, t_h is the hold time in hours, and P_{lm} is a material constant. The value of P_{lm} is 20 for 6-2-4-2 Ti and 25 for IN 718.

DAMAGE has been modified to allow the use of Larson-Miller data to determine the effective yield strength of the material given a temperature and hold time. Larson-Miller plots are provided in Figures 76 and 77 for 6-2-4-2 Ti and IN 718, respectively. These plots compare the Larson-Miller curves with data from MCAIR tests and from the Aerospace Structural Metals Handbook (Reference 10).

5. <u>Effects of Temperature on Material Properties</u> - Material properties will change with temperature. DAMAGE will account for changes in three different properties: 1) yield strength, 2) fracture toughness, and 3) overload shut-off ratio. In each case, DAMAGE accepts input files which contain temperature vs. percent reduction of the material property.

a. <u>Yield Strength</u> - The reduction in the yield strength due to elevated temperature in 6-2-4-2 Ti and IN 718 was shown in Figures 19 and 20. A larger plastic zone in front of the crack tip is the result of a reduction in the yield strength. The crack growth rate is reduced as long as the crack length does not exceed the plastic zone. Therefore, if the plastic zone size increases, the crack growth rate is reduced for a longer period of time. This behavior is similar to that described in the previous section on creep effects.

b. <u>Fracture Toughness</u> - The fracture toughness of a material will also change with increased temperature. The net effect is an increase in the critical crack length. However, when the crack is in the vicinity of the critical crack size, the crack growth rate is high. As a result, it will not
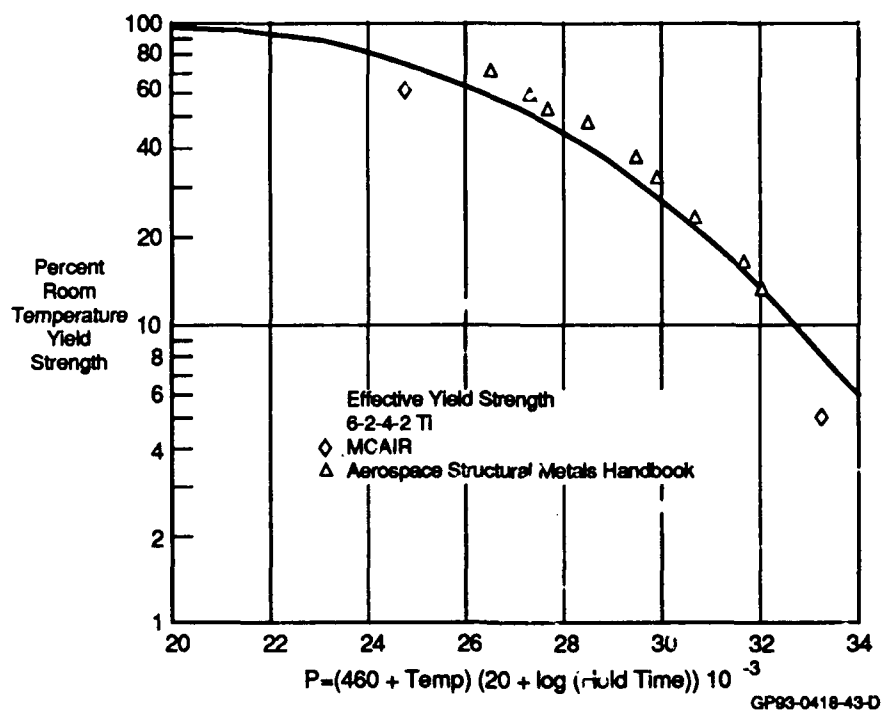
Figure 76. Larson – Miller Plot for 6-2-4-2 Ti
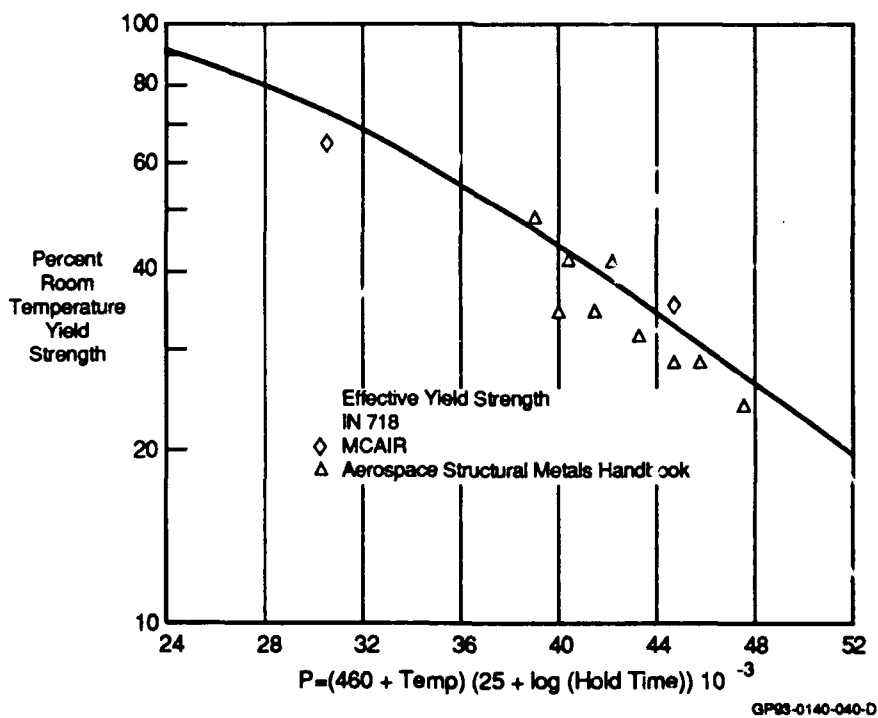
Figure 77. Larson – Miller Plot for IN 718

84

take many cycles for the crack to grow to the point where the critical crack length and the fracture toughness are exceeded. Therefore, the change in fracture toughness should have a minimal effect on life predictions.

Temperature vs. fracture toughness, K_c, data are plotted in Figure 78 for 6-2-4-2 Ti and IN 718. These data were obtained from the model development tests.
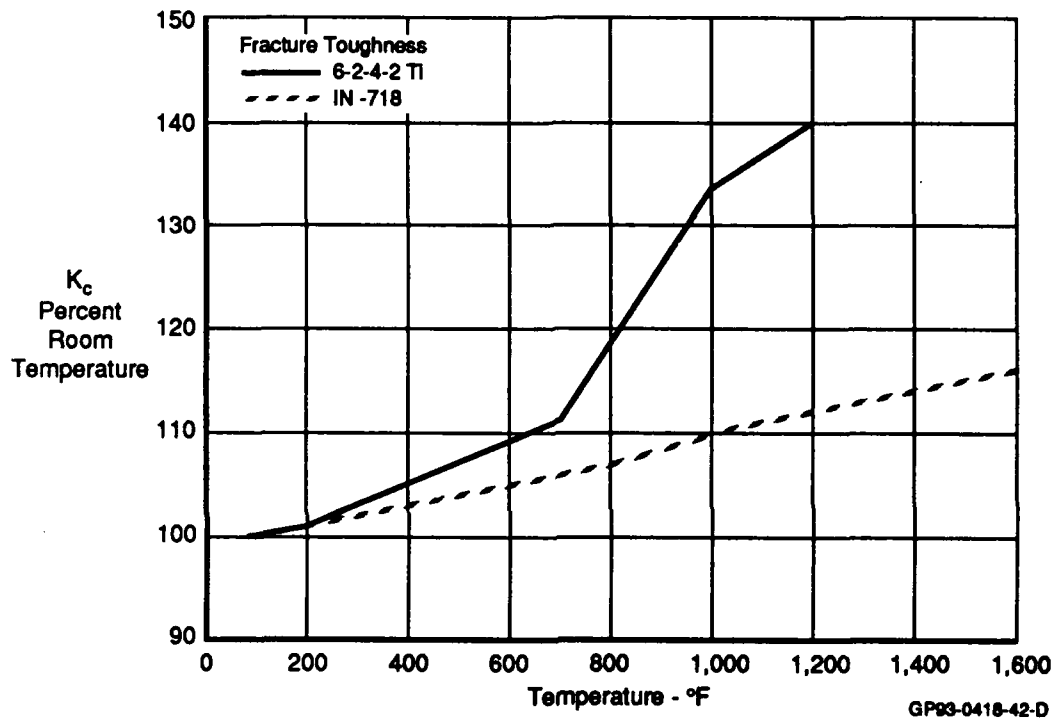
Figure 78. Fracture Toughness vs Temperature

c. <u>Overload Shut-Off Ratio</u> - The load interaction model in CRKGRO is the generalized Willenborg model for tensile overloads, with a reduction in overload zone size proposed by Chang for compressive overloads. This same model is used in DAMAGE.

Retardation in the generalized Willenborg model can be expressed:

$$K_{eff-max} = K_{\infty max} - \phi [K_{ol-max} (1-\Delta c/\rho_{ol})^{1/2} - K_{\infty max}]$$

$$K_{eff-min} = K_{\infty min} - \phi [K_{ol-max} (1-\Delta c/\rho_{ol})^{1/2} - K_{\infty max}]$$

where

$$\phi = (1 - K_{th-max}/K_{\infty max})/(R_{SO} - 1)$$

where $K_{\infty max}$ is the stress intensity factor corresponding to the maximum remotely applied stress, K_{ol-max} is the stress intensity factor corresponding to the maximum stress of the overload, K_{th-max} is the maximum threshold stress intensity, "Δc" is the incremental growth following the overload, and ρ_{ol} is the plastic zone size. R_{SO} is the overload shutoff ratio, which is defined as:

$$R_{SO} = K_{ol-max}/K_{\infty max}$$

The generalized Willenborg model accounts for the ability of high spectrum loads to retard the crack growth produced by subsequent low load cycles. This retardation is accounted for by using the overload shut-off ratio, R_{SO}. This ratio determines the magnitude of the overload required to shut-off crack growth completely. A high R_{SO} value indicates that the material is insensitive to overloads. Conversely, decreasing R_{SO} increases the predicted crack growth retardation after an overload and results in a longer predicted life.

To select the overload shut-off ratio, R_{SO}, values were correlated with results from isothermal spectrum load fatigue tests performed on center cracked specimens. The R_{SO} values for 6-2-4-2 Ti and IN 718 at room and elevated temperatures are listed in Figure 79. The value of R_{SO} for a material changes with temperature. Figures 80 through 83 compare crack length vs. life data to data predicted using the values of R_{SO} listed in Figure 79.

Temperature (°F)	6-2-4-2 Ti	IN 718
R.T.	2.00	2.40
1,000	4.50	—
1,200	—	1.70

GP93-0140-38-T

Figure 79. Values of the Overload Shut-Off Ratio, R$_{so}$, for 6-2-4-2 Ti and IN 718 at Room and Elevated Temperatures

R_{SO} increases with temperature for 6-2-4-2 Ti (Figures 80 and 81). This implies that as the temperature increases, the material becomes less sensitive to overloads. This behavior was also found in the single overload tests performed at 700°F and 1000°F. The number of cycles required to overcome the retardation effects of an overload (known as delay cycles) decreased as the temperature increased (Figure 52).

Conversely, R_{SO} decreases with temperature for IN 718 (Figures 82 and 83). This implies that as the temperature increases, the material becomes more sensitive to overloads. This is consistent with the behavior found in the single overload tests performed at 700°F and 1200°F.

6. Geometry Library - One of the reasons CRKGRO was selected as a basis for model development in this program is that it contains an extensive library of stress intensity factor solutions for common flaw configurations in air-frame structures. DAMAGE uses an updated library of solutions for the same flaw configurations (Figure 3). Equations have also been included which account for out-of-plane bending, as well as axial tension.

a. Stress Intensity Solutions - DAMAGE will analyze crack growth in plates with the following geometries:

Part-Through Flaws

1) Center Surface Crack;

2) One Corner Crack from Center Open Hole;

3) Two Corner Cracks from Center Open Hole;

4) One Corner Edge Crack;

Through Flaws

1) Center Crack;

2) One Crack from Centered Open Hole;

3) Two Cracks from Centered open Hole;

4) One Edge Crack;

5) Two Edge Crack;

6) Compact Tension Specimen.

These plates may be subject to axial tension loads or out-of-plane bending moments.
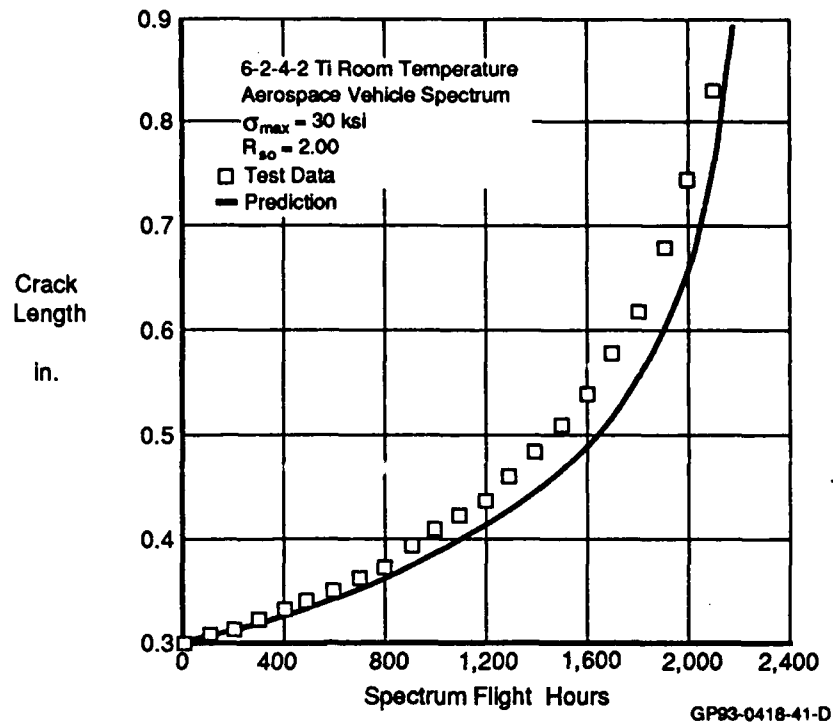
Figure 80. Fatigue Test to Determine R_{so} For 6-2-4-2 Ti (Room Temperature)
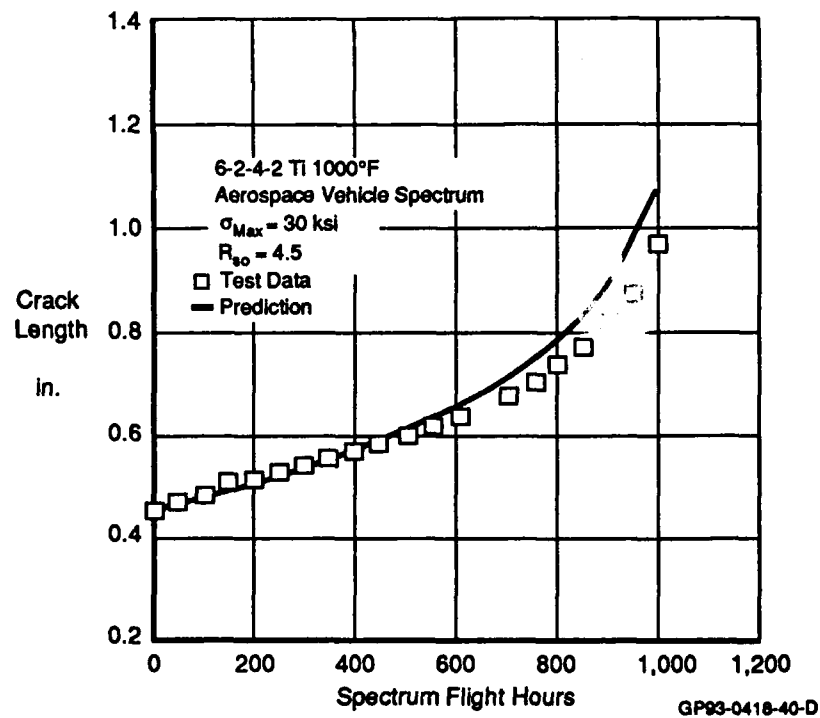
Figure 81. Fatigue Test to Determine R_{so} for 6-2-4-2 Ti (1,000°F)

88
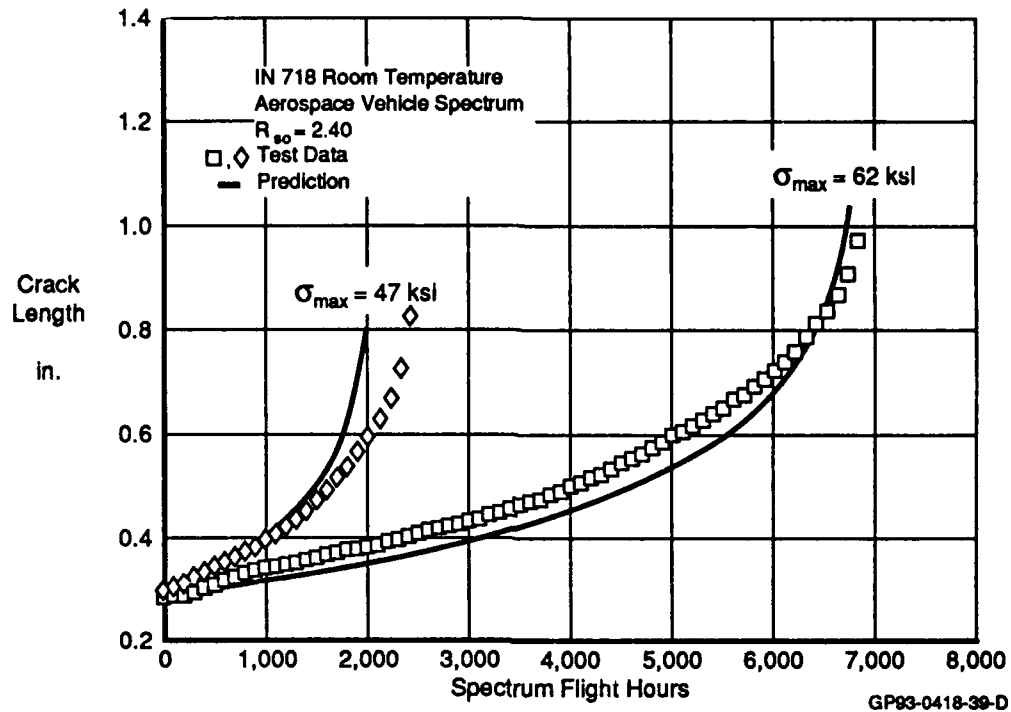
Figure 82. Fatigue Tests to Determine R_{so} for IN 718 (Room Temperature)
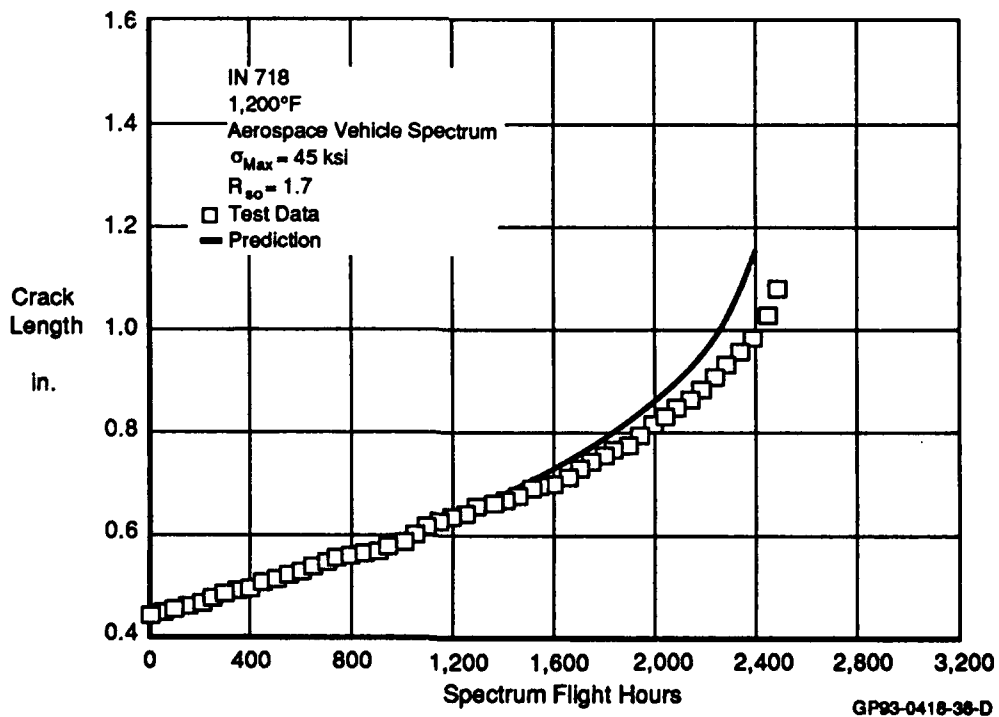
Figure 83. Fatigue Test to Determine R_{so} for IN 718 (1,200°F)

89

Stress intensity solutions were obtained from three sources: 1) Newman and Raju; 2) Tada, Paris and Irwin; and 3) Rooke and Cartwright (References 14 through 17). In these solutions, stress intensity factors are determined separately for tension and bending. The total stress intensity is then the sum of the two solutions.

$$K = (\sigma_t \beta_t + \sigma_b \beta_b) (\pi c)^{1/2}$$

where "c" is the crack length, σ_t and σ_b are the tension and bending stresses at the surface of the part, and β_t and β_b are the tension and bending geometry factors. The bending stress, σ_b, is determined from the out-of-plane bending moment, M.

$$\sigma_b = M \, a_0/I$$

I is the moment of inertia, and for a rectangular cross-section of width, W, and thickness, t, is equal to $Wt^3/12$. The term "a_0" is the distance between the mid-plane of the plate and the location where the bending stress is calculated. At the specimen surface, $a_0 = t/2$ and the bending stress is

$$\sigma_b = 6 M / (W t^2)$$

Newman and Raju have determined axial tension and bending stress intensity solutions for all of the part-through flaw configurations used in DAMAGE (Reference 14). These solutions have been incorporated into DAMAGE, updating those originally programmed in CRKGRO.

Stress intensity solutions for plates with through thickness flaws subjected to axial tension loads were obtained from Newman and Tada (References 15 and 16). Newman provided solutions for center cracked panels and open hole panels with one or two cracks. Tada supplied solutions for panels with edge cracks.

Stress intensity solutions for plates with a center crack subjected to out-of-plane bending moments were obtained from Rooke and Cartwright (Reference 17). Rooke also had solutions for an infinite width panel with one

or two cracks growing from a center open hole. Finite width effects were incorporated into this solution by multiplying the infinite width solution by the ratio of finite width to infinite width correction factors for a panel subjected to axial tension.

$$\beta = \beta_2 \, (\beta_1/\beta_3)$$

where

β_1 = finite width axial tension solution (Newman),

β_2 = infinite width bending solution (Rooke),

β_3 = infinite width axial tension solution (Newman).

Solutions for finite width panels with one or two through edge cracks subjected to bending moments could not be found in any of the references described above. A solution was derived for a single edge crack in a finite width panel by multiplying the infinite width solution by the ratio of finite width to infinite width solutions for a center cracked panel.

$$\beta = \beta_2 \, (\beta_1/\beta_3)$$

where

β_1 = finite width solution for center cracked panel
    = $(\sec(\pi c/W))^{1/2}$,

β_2 = infinite width solution for single edge crack
    = 1.12,

β_3 = infinite width solution for center cracked panel
    = 1.00.

The solution for a finite width panel with two edge cracks subjected to bending loads is calculated by multiplying the axial tension solution for the same geometry by the ratio of the bending to tension solutions for a single edge crack panel.

$$\beta = \beta_2 \, (\beta_1/\beta_3)$$

where

β_1 = bending solution for a single edge crack (derived above),

β_2 = tension solution for two edge cracks (Tada),

β_3 = tension solution for a single edge crack (Tada).

The stress intensity library in DAMAGE will analyze stress intensities of arbitrary flaw geometries and loading conditions. However, for those cases which do not have a regular flaw shape or stress distribution, a user-defined solution routine is available in DAMAGE which will allow for the input of a table of crack length vs. stress intensity factors to describe the flaw. A table look-up procedure will then interpolate a solution.

b. <u>Incorporation of Out-of-Plane Bending</u> - DAMAGE will calculate crack growth for panels with part through or through cracks subjected to axial tension loads and out-of-plane bending moments. The incorporation of bending moments into DAMAGE required that the load interaction module be modified.

The crack growth analysis of panels subjected to bending moments is limited by the following assumptions:

1) Moments are out-of-plane;

2) Moments are applied at the same frequency as the axial tension loads; and

3) Moments are applied as constant amplitude with a moment ratio, R_m = minimum moment/maximum moment = -1.0.

The bending stress, σ_b, is calculated from the bending moment, M, at the crack tip for part through and through cracks.

$$\sigma_b = 12 \, M \, a_0 / \, (W \, t^3)$$

where

a_0 = (a-t/2) for a crack depth, "a", through the thickness and

a_0 = t/2 for a surface crack.

92

The major modification of the crack growth analysis is the addition of bending terms in the stress intensity factor solutions. The total stress intensity is the sum of the bending and tension terms:

$$K = (\sigma_t\, \beta_t + \sigma_b\, \beta_b)\, (\pi c)^{1/2}$$

where "c" is the crack length, and β_t and β_b are the tension and bending geometry factors. The stress intensity solutions provided in DAMAGE were discussed in the previous section.

The load interaction module in DAMAGE also required modification to accept bending stresses. The generalized Willenborg model in DAMAGE is discussed in detail in Section III-3b.

In the generalized Willenborg model, effective stresses are calculated to account for crack growth retardation due to the application of an overload. To incorporate bending into the analysis, it was assumed that the ratio of the overload to applied tension stress should be equal to the ratio of the overload to applied bending moment. Therefore, in addition to determining effective tension stresses, effective bending stresses must also be calculated. These effective stresses are used to calculate the effective stress intensity and the effective stress ratio.

$$K_{eff\text{-}max} = (\sigma_{t,eff\text{-}max}\, \beta_t + \sigma_{b,eff\text{-}max}\, \beta_b)\, (\pi c)^{1/2}$$

$$K_{eff\text{-}min} = (\sigma_{t,eff\text{-}min}\, \beta_t + \sigma_{b,eff\text{-}min}\, \beta_b)\, (\pi c)^{1/2}$$

$$\Delta K_{eff} = K_{eff\text{-}max} - K_{eff\text{-}min}$$

$$R_{eff} = K_{eff\text{-}min}/K_{eff\text{-}max}$$

The development of the effective bending stress equations parallels the rationale used in developing the effective tension stress equations described in Section III-3b. The effective bending stresses are calculated as:

$$\sigma_{b,eff\text{-}max} = \sigma_{b,max} - \sigma_{b,red}$$

$$\sigma_{b,eff-min} = \sigma_{b,min} - \sigma_{b,red}$$

σ_{red} is the additional stress required to extend the instantaneous interaction zone to that created by the overload. $\sigma_{b,red}$ is the bending portion of σ_{red}.

Using the same approach as in the generalized Willenborg model, the expression for $\sigma_{b,red}$ is

$$\sigma_{b,red} = (\sigma_{b,req} - \sigma_{b,max})\, \phi$$

$\sigma_{b,req}$ is the total bending stress required for a particular cycle to stop crack growth retardation. This expression is found by rearranging the equation for the interaction zone, z, required to stop retardation.

$$z_{ol} = c_{ol} + \rho_{ol} = c_i + \rho_{req} = z_{req}$$

By substituting the expression for the plastic zone, ρ, the following is obtained:

$$z_{ol} - c_i = \rho_{req} = [\gamma/(2\pi)]\, (K_{req}/F_{ty})^2$$

where

$$\gamma = 1 - \text{plane stress}$$
$$\gamma = 1/3 - \text{plane strain}$$

In this expression, K_{req} is defined as:

$$K_{req} = (\sigma_{t,req}\, \beta_t + \sigma_{b,req}\, \beta_b)\, (\pi c)^{1/2}$$

DAMAGE defines the ratio of the bending to tension required stresses to be equal to the ratio of bending to tension applied stresses.

$$R_{b-t} = \sigma_{b,max}/\sigma_{t,max} = \sigma_{b,req}/\sigma_{t,req}$$

Therefore, the expression for K_{req} now becomes:

$$K_{req} = \sigma_{t,req} (\beta_t + R_{b-t} \beta_b) (\pi c)^{1/2}$$

By substituting this expression into the equation for the interaction zone and rearranging terms, the following expressions for the required stresses are found:

$$\sigma_{t,req} = [F_{ty}/(\beta_t + R_{b-t} \beta_b)] [2 (\rho_{ol} - \Delta c)/c_i/\gamma]^{1/2}$$

$$\sigma_{b,req} = R_{b-t} \sigma_{t,req}$$

With these modifications, the generalized Willenborg model will determine the effects of overloads due to axial tension loads and/or out-of-plane bending moments on crack growth rate retardation.

SECTION VI

VERIFICATION

1. __Testing Summary__ - The verification test matrix outlined in Figure 84 rigorously and economically tested the predictive methodology. The test plan was based on the selection of materials and specimens that included geometries representing typical structural details. The thermal environment and load spectra represent the expected usage of two types of aircraft. One spectrum was typical of an aerospace vehicle, and the other, a significantly different spectrum, was typical of an advanced fighter.

Test Description	Materials	
	6Al-2Sn-4Zr-2Mo Titanium	IN 718
__Center Cracked Specimen__		
Advanced Fighter Spectrum	3	3
Aerospace Vehicle Spectrum	3	3
__Open Hole Specimen__		
Advanced Fighter Spectrum	3	3
Aerospace Vehicle Spectrum	3	3
Totals	12	12

GP93-0140-89-T

Figure 84. Verification Test Matrix

The goal of the verification task was to test the model's predictive accuracy at realistic limits of geometry, environment, and load and temperature spectra. All of the testing was performed at MCAIR under the supervision of Mr. Russell Bill.

2. __Material Selection__ - The materials chosen for testing were the same as those tested in the model development test program: 6Al-2Sn-4Zr-2Mo Ti (6-2-4-2 Ti) and Inconel 718 (IN 718). These materials were chosen because they exhibit a wide range of responses to temperature, hold time, and environment.

Typically, 6-2-4-2 Ti is susceptible to crack growth retardation caused by creep blunting the crack tip. This was consistent with the model development data. Constant amplitude fatigue tests with 30 second hold times

97

at peak load were conducted. Crack growth retardation was evident when this data was compared to the high frequency data (Figure 37).

The model development data also indicated that 6-2-4-2 Ti is sensitive to the environment. Vacuum tests were compared to lab air tests in Figure 46. The lab air tests consistently displayed a higher crack growth rate.

The IN 718 material was also sensitive to creep. Tests conducted at 1200°F with 30 second hold times showed substantial crack growth deceleration compared to high frequency tests (Figure 39). This material was also less sensitive to the environment than initially expected (Figure 47). There was no difference in the room temperature crack growth rate when tested in lab air or vacuum. This was surprising since, for IN 718, many researchers have documented the crack growth rate's strong dependence on the environment (Reference 11). As discussed in Section III, the IN 718 material was aged in-house in an attempt to make it more sensitive to the environment. It is apparent from the test data, however, that this process failed.

3. Load and Temperature Spectrum Development - The methodology developed in Section V was used to predict the crack growth of center cracked and open hole specimens subject to variable load-time and temperature-time histories. Two load/temperature profiles were developed for testing.

The first spectrum represents an advanced fighter mission with a peak temperature of 800°F. The load spectrum is characterized by high temperatures and moderate loads during supersonic cruise and dash. The large, infrequent overloads typical of combat fighter aircraft were assumed to occur at much lower temperatures in the subsonic and transonic regimes.

The second spectrum represents two aerospace vehicle missions. The highest temperature in this spectrum depends on the maximum temperature capability of the material being tested. IN 718 specimens were subjected to 1200°F. and 6-2-4-2 Ti specimens were subjected to 1000°F. The aerospace vehicle spectrum is characterized by high temperatures during atmospheric exit and re-entry, long load durations representing synergetic turns, and frequent but moderate overloads typical of transport aircraft.

a. Advanced Fighter Spectrum - This section describes the development of a load and temperature spectrum for an advanced fighter. This spectrum was used for half of the verification tests.

The verification test program required an advanced fighter temperature spectrum with a peak temperature in the 600°F-800°F range. To develop this spectrum, a mission profile was created for a Mach 3.0-3.5 fighter. This profile was divided into seven mission segments which include take-off/climb, initial cruise, track/intercept, weapon delivery, maximum acceleration/dash, return cruise, and approach/landing (Figure 85).

Mission Segment	Time (min)	Mach	Altitude (1,000 ft)	Angle-of-Attack (Degree)
Take-Off/Climb	5	0 - 3.1	0 - 50	0 - 10
Cruise	20	3.1	50 - 80	0 - 5
Track/Intercept	4.5	3.5	80 - 50	0 - 25
Weapon Delivery	1	2.2	50	0 - 35
Max. Acceleration Dash	4.5	3.5	50 - 80	0 - 10
Cruise	20	3.1	80 - 50	0 - 5
Approach/Land	5	0 - 0.7	50 - 0	0 - 15

GP93-0418-81-D
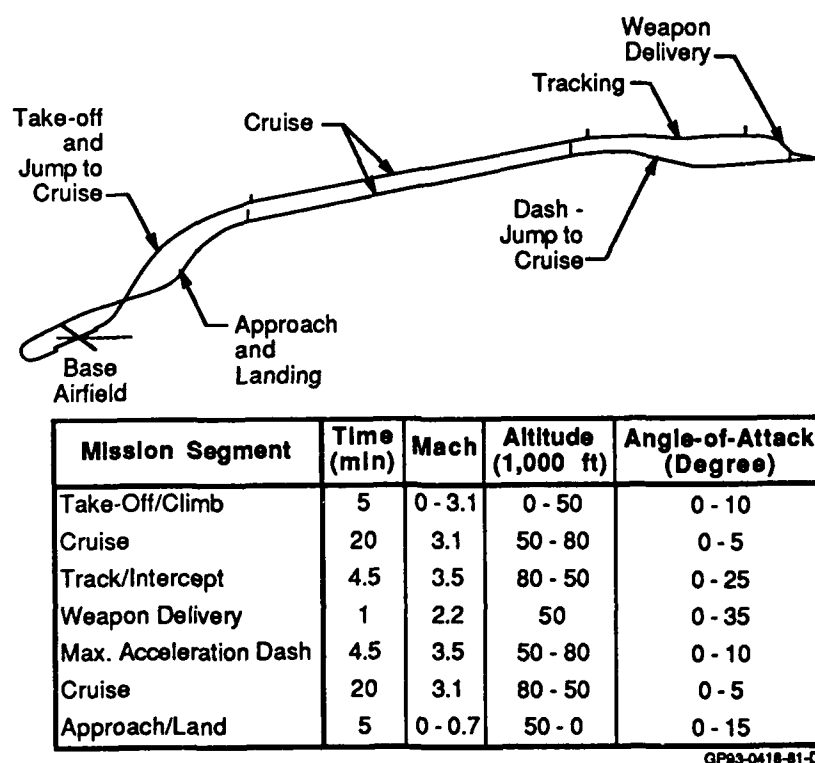
Figure 85. Advanced Fighter Profile

For each segment in the advanced fighter profile, a maximum execution time was specified along with the Mach range, altitude, and angle of attack. To create the thermal spectrum, it was also necessary to identify the aircraft configuration and materials to be examined. The forward portion of a wing box, consisting of an IN 718 leading edge and a 6-2-4-2 Ti skin, was selected (Figure 86). The time-temperature history shown in Figure 87 was then created using an aerodynamic heating routine.

99

- 3 Spar-Highly Swept Wings
- No Active Cooling
- Inconel Leading Edge
- Titanium Lower Skin
- Titanium Ribs and Spars

GP93-0418-82-D
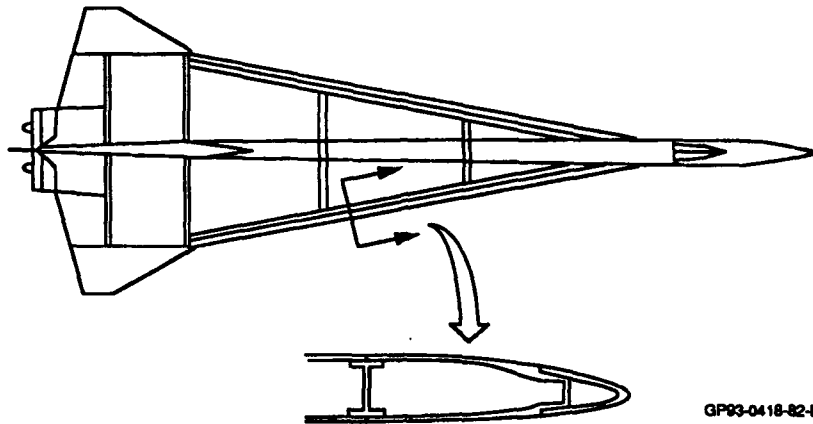
Figure 86. Advanced Fighter Aircraft Configuration
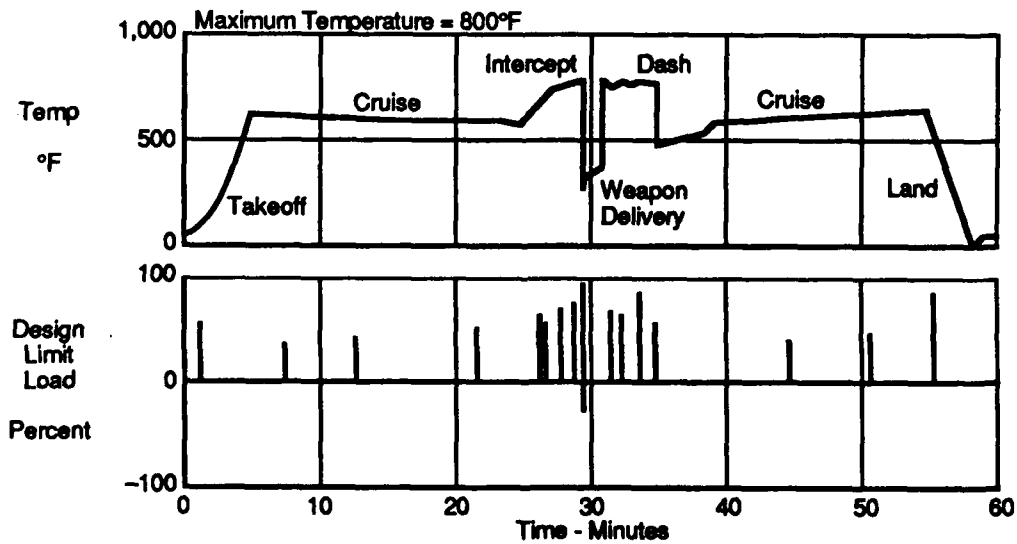
Figure 87. Load –Temperature –Time Profile for an Advanced Fighter

100

The load history was developed from usage data of a current fighter. This data is presented in the form of an exceedance curve in Figure 88. An advanced fighter exceedance curve which encompasses this data was selected.

Peak and valley loads were distributed among the seven mission segments to resemble the chosen exceedance curve. The exceedance curve has 16,000 load cycles per 1000 flight hours. The mission length is one hour. Therefore, each mission has 16 load cycles. These 16 cycles were divided among the mission segments. Load ranges for both the peak and valley loads were then assigned to these segments (Figure 85). One thousand missions were defined. Each mission identifies actual peak and valley loads for each mission segment by randomly assigning loads within each defined range. The number of loads in each mission segment were counted to tailor the load-time profile to meet the exceedance curve. This method resulted in a slightly sequenced load history in which all of the loads above 100 percent applied load occur in the first 400 missions. The load-time history for one mission is shown in Figure 87. The loads and temperatures for the first mission are listed in Figure 89.

b. Aerospace Vehicle Spectrum - The aerospace vehicle load and temperature spectrum was developed using a procedure similar to that used in developing the advanced fighter spectrum. The load-time history for the aerospace vehicle was used under constant temperature in the model development tests. The combined load and temperature profiles were used in the verification tests.

The aerospace vehicle spectrum consists of two 30 minute missions per flight hour. The load spectrum for each mission contains only the portion of the mission within the atmosphere. One thermal cycle is applied for each exit or entry of the atmosphere.

The first mission contains an orbital plane change, known as a synergetic turn (Figure 90) in which the vehicle leaves and re-enters the atmosphere twice during the mission. The second mission represents a cruise mission with high altitude maneuvers. The vehicle does not leave the atmosphere in this mission. The combination of these two missions provided a rigorous load-temperature-time profile for testing.
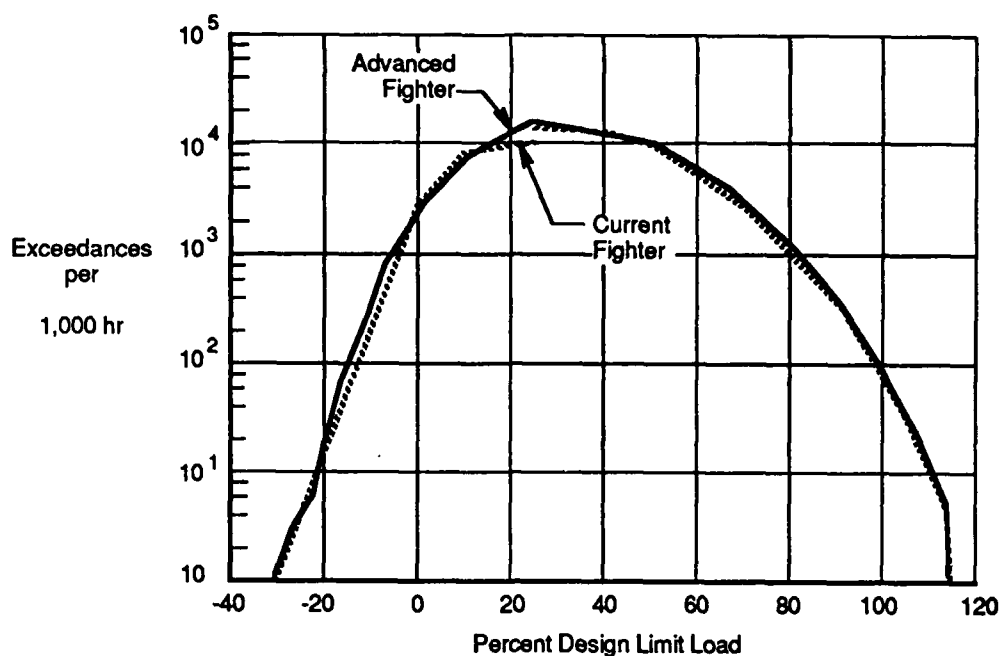
GP93-0418-83-D

**Figure 88. Exceedance Curves for Advanced
Fighter and Current Fighter**

1 Mission – 60 min (16 Load Cycles)

	Peak (percent)	Valley (percent)	No. of Cycles	Temperature (°F)	Cycle Time (sec)	Cumulative Time (sec)
Mission 1 Step No.						
1	54.1	2.8	1	78.0	300.00	300.00
2	36.5	13.5	1	610.0	400.00	700.00
3	40.3	14.3	1	600.0	400.00	1,100.00
4	48.3	3.4	1	590.0	400.00	1,500.00
5	58.3	13.7	1	650.0	67.50	1,567.50
6	56.3	16.1	1	700.0	67.50	1,635.00
7	68.9	7.2	1	750.0	67.50	1,702.50
8	72.1	11.0	1	800.0	67.50	1,770.00
9	84.8	−21.0	1	300.0	60.00	1,830.00
10	65.2	4.0	1	780.0	67.50	1,897.50
11	59.6	7.9	1	750.0	67.50	1,965.00
12	79.7	3.2	1	780.0	67.50	2,032.50
13	51.8	14.8	1	750.0	67.50	2,100.00
14	34.1	7.1	1	590.0	600.00	2,700.00
15	38.7	19.7	1	610.0	600.00	3,300.00
16	76.6	0.4	1	78.0	300.00	3,600.00

GP93-0140-90-T

Figure 89. Table of Loads and Temperatures for 1 Mission of the Advanced Fighter

102

Entry Trajectory

① , ② Maximum Heat Rates – Selects Surface Materials

③ , ④ Maximum Heat Loads – Sizes Insulation Thickness

⑤ Long Term Severe Heating – Adds Active Cooling Requirements for Primary Structure at Junctions With Thermal Protection Attachments

GP93-0418-85-D
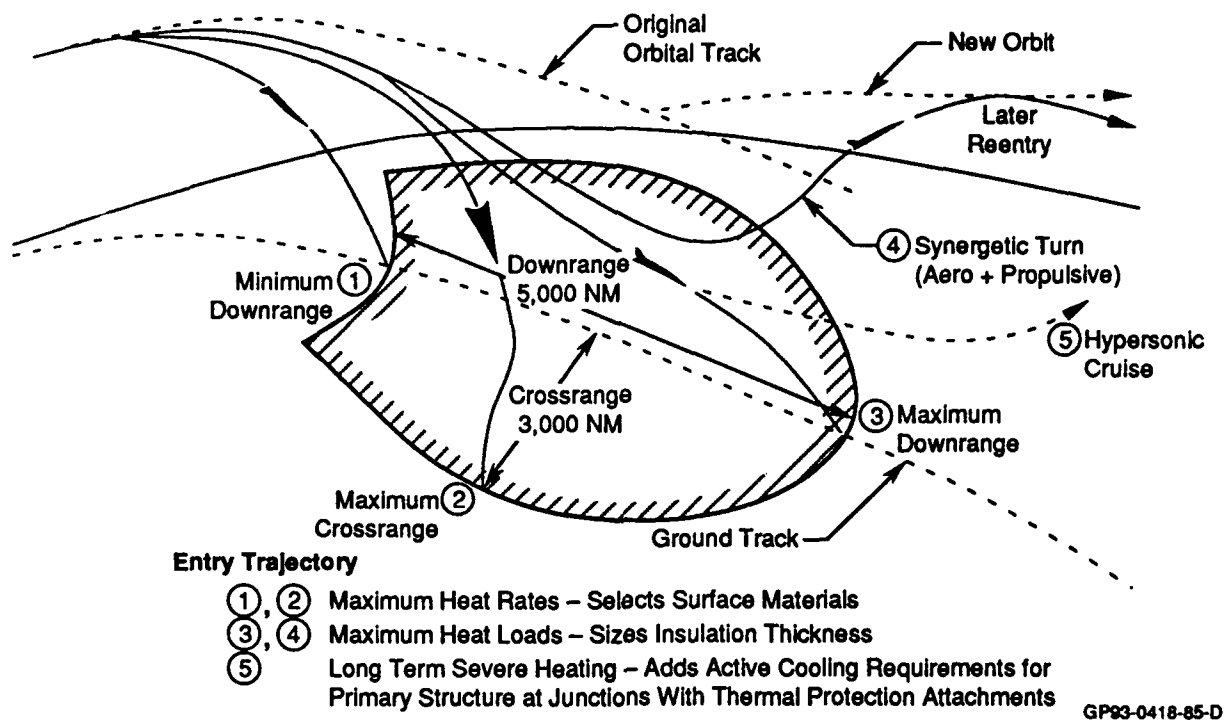
Figure 90. Possible Trajectories of an Aerospace Vehicle

The load spectrum was designed such that its exceedance curve matched the exceedance curve of a transport vehicle (Figure 91). The transport exceedance curve was presented in the final report for the contract "Effect of Transport/Bomber Loads Spectrum on Crack Growth" (Reference 18). The load-time history presented in Figure 92 represents 1 flight hour. The test spectrum block consisted of 50 flight hours (100 missions). Each hour is identical to the one shown in Figure 92, except the maximum loads differ in each mission. These maximum loads vary between 72.0 percent and 100.0 percent of the applied load. There are a total of 319 load cycles per flight hour.

It was necessary to scale down the number of flight hours for the transport vehicle to obtain the same number of load cycles as in the aerospace vehicle load profile. The exceedance curve presented in Figure 91 represents 50 flight hours for the aerospace vehicle and 250 flight hours for the transport vehicle.
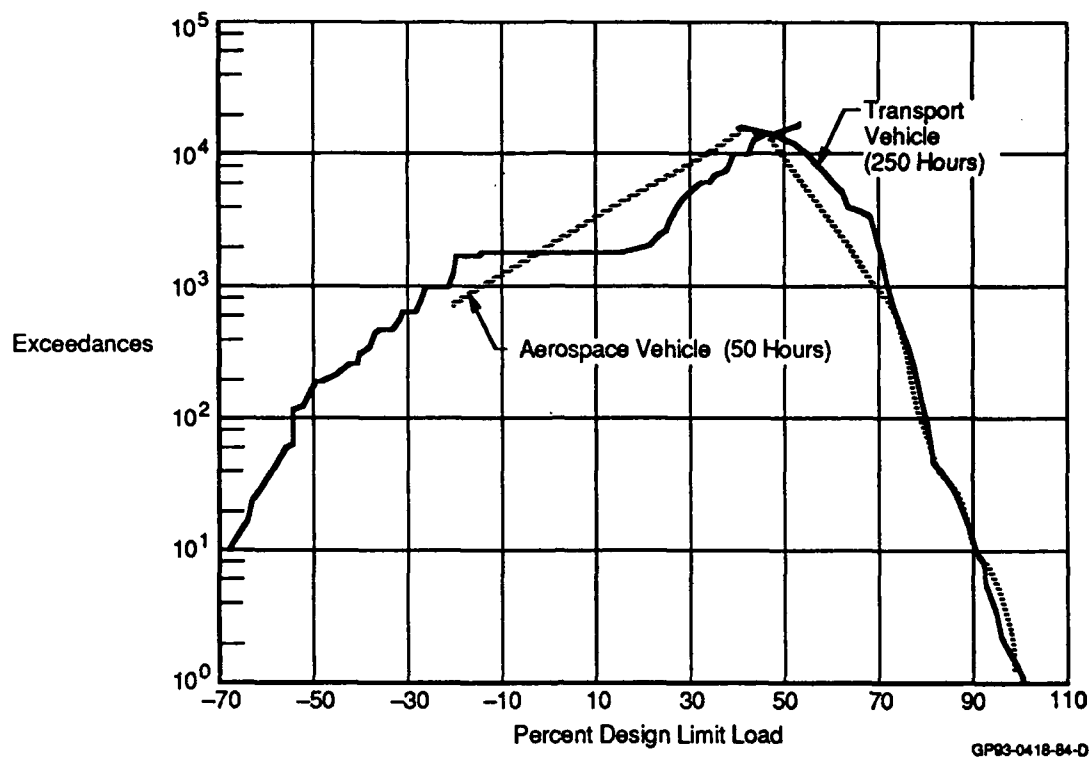
Figure 91. Exceedance Curves for Aerospace Vehicle and Transport Vehicle
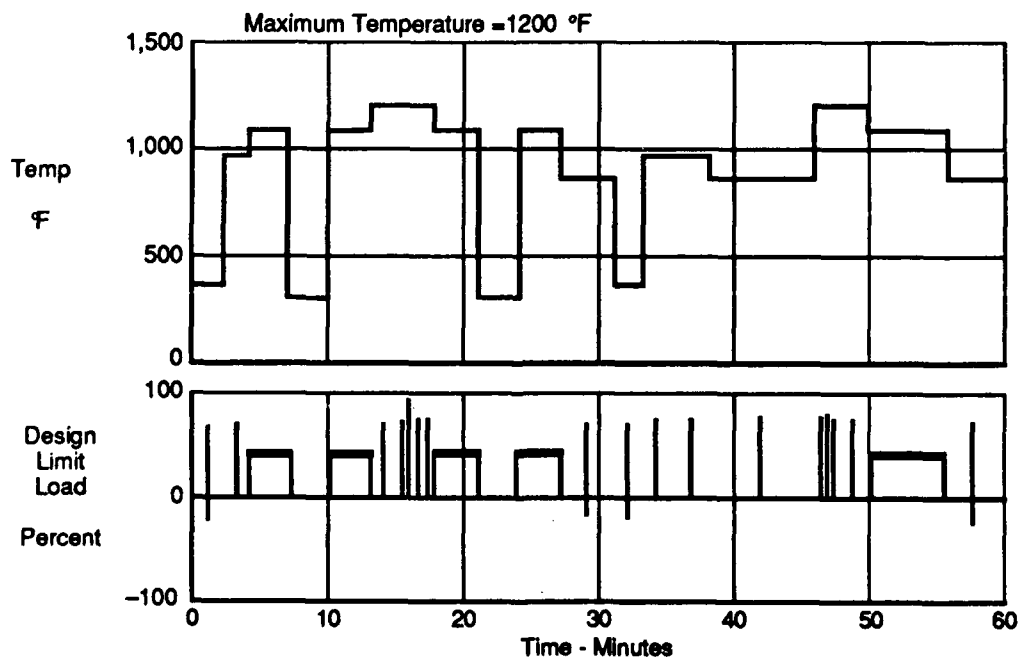
Figure 92. Load –Temperature –Time Profile for an Aerospace Vehicle

104

The temperature spectrum maintains a relatively high temperature throughout the entire two missions. The hottest portion of the spectrum is the orbital plane change. The coolest temperature in the spectrum is 300°F. It occurs between atmospheric exit and re-entry when the aerospace vehicle is in orbit (Figure 92). This was the lowest temperature the specimen would reach during the time provided.

The exit and re-entry portions of the load spectrum consists of a group of 50 high stress ratio (R=0.9) load cycles conducted at constant temperature. As an aerospace vehicle leaves and re-enters the atmosphere, the temperature will rise. However, once an orbit is achieved, the vehicle temperature will decrease. Thus, a severe thermal cycle occurs between exit and re-entry of the earth's atmosphere.

Members of the NASP team at MCAIR reviewed the aerospace vehicle spectrum (Figure 92) before it was used in the verification testing. It was agreed that this generic spectrum provided a good representation of typical aerospace vehicle missions. The loads and temperatures for the first two missions are provided in Figure 93.

4. Specimen Configuration - Two specimen types were selected for verification testing. The center cracked tension specimen (Figure 11) was chosen because it was used in all model development testing and is the simplest specimen for data interpretation.

The second verification specimen selected was an open hole specimen containing one or two through thickness radial cracks (Figure 94). This specimen provided a simple but realistic structural detail that had a large stress gradient and developed significant local plasticity.

Pre-crack sizes were selected to be in the range expected in aircraft service, yet large enough to be accurately monitored. Pre-cracks were started on both sides of the open hole specimens. In some cases, however, cracks only initiated out of one side. This was not a major concern because the predictive methodology is designed to predict crack growth from open holes with either one or two cracks.

105

2 Missions – 60 min (319 Load Cycles)

	Peak (percent)	Valley (percent)	No. of Cycles	IN 718 Temperature (°F)	6-2-4-2 Ti Temperature (°F)	Cycle Time (sec)	Cumulative Time (sec)
Mission 1 Step No.							
1	71.8	−20.0	1	360.0	300.0	120.00	120.00
2	74.1	50.0	1	960.0	800.0	120.00	240.00
3	45.2	40.0	50	1,080.0	900.0	3.60	420.00
4	0	0	1	300.0	250.0	180.00	600.00
5	45.2	40.0	50	1,080.0	900.0	3.60	780.00
6	72.3	46.0	1	1,200.0	1,000.0	120.00	900.00
7	74.1	50.0	1	1,200.0	1,000.0	36.00	936.00
8	92.0	50.0	1	1,200.0	1,000.0	36.00	972.00
9	74.1	50.0	1	1,200.0	1,000.0	36.00	1,008.00
10	72.3	46.0	1	1,200.0	1,000.0	60.00	1,068.00
11	45.2	40.0	50	1,080.0	900.0	3.84	1,260.00
12	0	0	1	300.0	250.0	180.00	1,440.00
13	45.2	40.0	50	1,080.0	900.0	3.84	1,632.00
14	72.3	−20.0	1	840.0	700.0	240.00	1,872.00
Mission 2 Step No.							
15	71.8	−20.0	1	360.0	300.0	120.00	1,992.00
16	74.1	50.0	2	960.0	800.0	150.00	2,292.00
17	72.3	46.0	1	840.0	700.0	480.00	2,772.00
18	74.1	50.0	1	1,200.0	1,000.0	36.00	2,808.00
19	78.9	50.0	1	1,200.0	1,000.0	36.00	2,844.00
20	74.1	50.0	1	1,200.0	1,000.0	36.00	2,880.00
21	72.3	46.0	1	1,200.0	1,000.0	120.00	3,000.00
22	45.2	40.0	100	1,080.0	900.0	3.60	3,360.00
23	72.3	−20.0	1	840.0	700.0	240.00	3,600.00

GP93-0140-91-T

Figure 93. Table of Loads and Temperatures for 2 Missions of the Aerospace Vehicle
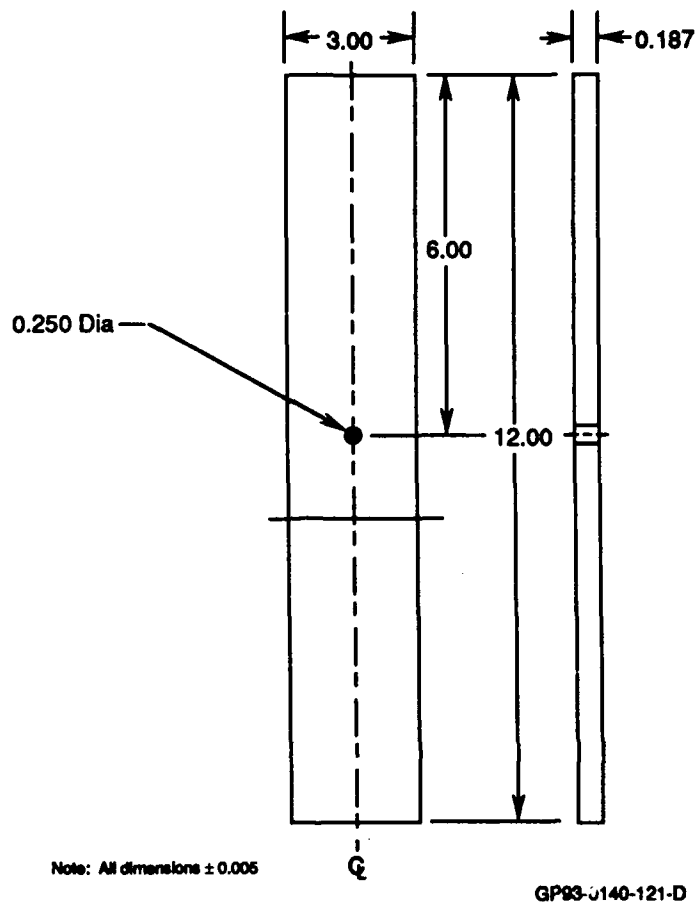
Figure 94. Open Hole Tension Specimen (OHT)

5. <u>Verification Test Program</u> - The verification test program was designed to identify limitations with the elevated temperature crack growth analysis model (DAMAGE). The model predicts life while accounting for: 1) the effects of temperature on material properties and crack growth rate, 2) the effects of the chemical and thermal environment on crack growth acceleration, and 3) the effects of creep on crack growth deceleration or retardation.

Center cracked and open hole specimens made of IN 718 and 6-2-4-2 Ti were subject to combined load and temperature profiles. Crack growth measurements were taken until failure. Three replicates were conducted for each test condition (Figure 84).

107

Two load and temperature spectra were used for testing. One represented that of an advanced fighter with a peak temperature of 800°F and the other represented that of an aerospace vehicle with a peak temperature of 1000°F for 6-2-4-2 Ti and 1200°F for IN 718. In the model development testing, it was determined that at 1200°F, the 6-2-4-2 Ti could not carry substantial load. Therefore, the maximum test temperature for this material was changed to 1000°F. Similarly, in the model verification testing, the thermal profile for the aerospace vehicle was scaled down such that its maximum temperature for the 6-2-4-2 Ti tests was 1000°F. The maximum temperature in the aerospace vehicle spectrum for the IN 718 material remained 1200°F.

To run the verification tests in an efficient and timely manner, the load profiles for both the advanced fighter and the aerospace vehicle spectra were time compressed as discussed below. Two versions of each spectrum were tested. This further tested the crack growth model.

Prior to testing, it was required to make life predictions for all of the verification tests. These predictions were sent to the contract monitor before testing and are discussed in Section VI-5c.

a. <u>Spectrum Time Compression</u> - Each mission in the advanced fighter load spectrum had only 16 load cycles per hour. Conducting a real-time test with this spectrum would not have been practical due to time limitations. A time compressed load spectrum was created which combined loads from multiple missions into each hour of the thermal history. The temperature spectrum was not modified. The compressed load spectrum allowed for the application of more than 16 load cycles per hour. Therefore, each test required less time to complete.

Life predictions were made with DAMAGE using both the time compressed load spectrum and the full load spectrum. The number of missions compressed into the 1 hour standard mission length was determined by limiting the difference between life predictions to 5 percent. Two versions of the advanced fighter load profile were created. One had 100 missions of loading compressed into each thermal spectrum hour and the other had 10 missions compressed into 1 hour. Figure 95 shows the time compressing study performed for both 6-2-4-2 Ti and IN 718.

No. of Missions Compressed Into 1 Hour	Load Cycles Per Hour	Predicted Life			Percent Difference
		Real Hours	Flight Hours	Cycles	
6-2-4-2 Ti **Applied Stress = 30 ksi Initial Crack Length = 0.25 in.**					
1	16	3,320	3,320	53,120	0
2	32	1,682	3,363	53,808	1.3
5	80	673	3,363	53,808	1.3
10	160	336	3,355	53,680	1.1
20	320	166	3,311	52,976	-0.3
50	800	65	3,225	51,600	-2.9
100	1,600	32	3,150	50,400	-5.1
200	3,200	16	3,100	49,600	-6.6
500	8,000	6	3,013	48,208	-9.2
IN 718 **Applied Stress = 45 ksi Initial Crack Length = 0.25 in.**					
1	16	8,002	8,002	128,032	0
2	32	4,014	8,027	128,432	0.3
5	80	1,612	8,058	128,928	0.7
10	160	811	8,105	129,680	1.3
20	320	406	8,110	129,760	1.3
50	800	162	8,075	129,200	0.9
100	1,600	81	8,050	128,800	0.6
200	3,200	38	7,606	121,696	-4.9
500	8,000	15	7,252	116,032	-9.4

GP93-0418-6-T

Figure 95. Study of Compressed Spectrum Load Profiles

The aerospace vehicle spectrum was also compressed. Each flight hour in this load spectrum contained two missions and had 319 load cycles. However, only 17 of those cycles had a stress ratio less than 0.9. Analyses showed that conducting real time tests with this spectrum and obtaining a reasonable amount of crack growth (minimum of 0.20 inch per 3 inch wide specimen) would have been impractical. Tests conducted with higher stress levels would have shortened the test life, but would have resulted in an unacceptably small amount of crack growth. This would not have verified the predictive methodology. Therefore, time compressed load spectra were created for the aerospace vehicle. The same time compression factors (10 and 100) used for the advanced fighter were chosen for the aerospace vehicle. Therefore, two versions of the aerospace vehicle load spectrum were created. One had 100 flight hours, or 200 missions, compressed into 1 hour. The other version had 10 flight hours, or 20 missions, compressed into 1 hour. The temperature spectrum was not modified.

The load profiles for both the aerospace vehicle and the advanced fighter were time compressed by the overlaying of missions. For example, if the time compression factor was 10, then the first load step from the first 10 missions would be applied at the same temperature and frequency as would the first load step if the missions were not compressed. Then the second load step from the first 10 missions would be applied and likewise for each step. Essentially, each load step in the time compressed profile would have 10 cycles instead of one. The temperature-time profile, however, would remain the same. The same procedure is used for a time compression factor of 100, except that the loads from the first 100 missions would be combined. The number of real hours required to run a test would be determined by dividing the flight hours by the time compression factor.

Unlike the advanced fighter profile, compressing 100 flight hours into 1 hour without modifying the thermal profile would have been impossible for the aerospace vehicle. The real-time spectrum has several groups of 50 and 100 load cycles with stress ratios, R, of 0.90. The allotted time in the thermal spectrum for these groups of load cycles are 180 and 360 seconds, respectively (Figure 93). In a spectrum test compressed 100 times, the number of R=0.90 load cycles increases to 5,000 and 10,000. Since the test frequency for the verification tests is 10 Hz, 500 seconds are required for the 5,000 R=0.90 load cycles and 1,000 seconds are required for the 10,000 R=0.90 load cycles. These are significantly larger times than allowed. Increasing the allotted time would have meant modifying the thermal spectrum. This was not an acceptable solution.

The R=0.90 load cycles were truncated from the aerospace vehicle load spectrum that had a time compression factor of 100. This permitted a full time compression of the load profile without modifying the thermal profile. The peak load in these cycles was less than 50.0 percent of the test load. The DAMAGE program analysis indicated that these cycles had very little effect on the crack growth and life of center cracked specimens (Figure 96).

b. Test Replication - The verification test matrix required that three tests be conducted for each test condition. The first two tests were conducted identically. If the first two test lives did not agree, then the

110

third test was conducted using the same procedure to discriminate between the two. If the first two test lives did agree, then the third test was used to explore other variables and their effect on life. Specifically, these tests were run as follows:

Tests 1 + 2 - Run with 100 hour compressed load spectrum and with same stress level and initial crack length.

Test 3 - If Tests 1 and 2 have similar lives, then run with the 10 hour compressed load spectrum. If Tests 1 and 2 have dissimilar lives, then run the same as Tests 1 and 2.

Material: 6-2-4-2 Ti
Load Spectrum: Aerospace Vehicle
Initial Crack Length: 0.25 in.
Stress Level: 40 ksi

Temperature (°F)	R = 0.90 Cycles Trucated?	Final Crack Length (In.)	Life (Flight Hours)
78	No	0.8647	366
	Yes	0.8630	366
1,000	No	1.0179	967
	Yes	0.8596	967

Material: IN 718
Load Spectrum: Aerospace Vehicle
Initial Crack Length: 0.25 in.
Stress Level: 80 ksi

Temperature (°F)	R = 0.90 Cycles Trucated?	Final Crack Length (In.)	Life (Flight Hours)
78	No	0.6312	667
	Yes	0.6312	667
1,200	No	0.7552	633
	Yes	0.7552	633

GP93-0418-7-T

Figure 96. Effect of R = 0.90 Load Cycles on Predicted Life

c. _Test Predictions_ - Life was predicted for all the verification tests (Figure 97). These predictions were made with the DAMAGE computer program.

The predictions made by DAMAGE were based on the model development tests that had been performed to date. At that time, the crack growth rate data for the tests with negative stress ratios (R<0) had not been received. Therefore, the Modified Walker coefficients (C, N, M, and Q) for fitting the crack growth rate curves, and the overload shut-off ratios, R_{SO}, used in accounting for overload effects, were based on data from only positive stress ratios (R≥0).

In Figure 97, two life predictions are given for each test. The first prediction was supplied to the Air Force. Failure was based on the computed crack length exceeding a previously computed critical crack length. The second prediction used the same crack growth analysis procedures, but based failure on fracture toughness instead of the critical crack length.

Spectrum	Specimen Type	Quantity	T_{max} (°F)	Stress (ksi)	C_{in} (in.)	Predicted*		Predicted**	
						C_f (in.)	Flight Hours	C_f (in.)	Flight Hours
6Al-2Sn-4Zr-2Mo Ti									
AF-C100	CCT	2	800	30	0.300	0.734	2,554.0	0.898	2,753.0
AF-C10	CCT	1	800	30	0.600	0.717	259.0	0.859	465.0
AF-C100	OHT	2	800	30	0.350	0.639	955.0	0.695	1,050.0
AF-C10	OHT	1	800	30	0.480	0.622	339.0	0.800	605.0
AV-C100	CCT	2	1,000	40	0.300	0.602	3,150.0	0.855	3,933.0
AV-C10	CCT	1	1,000	40	0.470	0.602	922.0	0.828	1,703.0
AV-C100	OHT	2	1,000	40	0.200	0.504	2,950.0	0.762	3,733.0
AV-C10	OHT	1	1,000	40	0.370	0.504	922.0	0.752	1,753.0
IN 718									
AF-C100	CCT	2	800	50	0.350	0.868	3,094.0	0.906	3,150.0
AF-C10	CCT	1	800	50	0.710	0.869	349.0	1.000	495.0
AF-C100	OHT	2	800	50	0.400	0.779	1,355.0	0.976	1,550.0
AF-C10	OHT	1	800	50	0.620	0.772	329.0	0.893	465.0
AV-C100	CCT	2	1,200	65	0.350	0.781	2,100.0	0.877	2,233.0
AV-C10	CCT	1	1,200	65	0.520	0.776	895.0	0.861	1,053.0
AV-C100	OHT	2	1,200	65	0.200	0.681	2,550.0	0.773	2,668.0
AV-C10	OHT	1	1,200	65	0.420	0.681	912.0	0.778	1,087.0

*Life prediction based on critical crack length
**Life prediction based on fracture toughness

AF   – Advanced Fighter Spectrum (1 mission per flight hour)
AF-C10   – Advanced Fighter Spectrum (10 missions per flight hour)
AF-C100 – Advanced Fighter Spectrum (100 missions per flight hour)
AV   – Aerospace Vehicle Spectrum (2 missions per flight hour)
AV-C10   – Aerospace Vehicle Spectrum (20 missions per flight hour)
AV-C100 – Aerospace Vehicle Spectrum (200 missions per flight hour,
                    R = 0.90 load cycles removed)

GP93-0418-8-T

Figure 97. Preliminary Verification Test Predictions

Life estimates should be based on the fracture toughness. Failures based on a previously computed critical crack length and the fracture toughness will provide identical life estimates for constant amplitude tests, but not for spectrum tests. The previously computed critical crack length is based on the material fracture toughness and the peak stress in the load profile. In a constant amplitude stress profile the peak stress occurs in every cycle. The peak stress in a spectrum stress profile occurs less frequently. Therefore, it is possible to exceed the critical crack length for the peak stress and not the fracture toughness in a spectrum crack growth test.

6. <u>Comparison of Test Results and Analysis</u> - A total of twenty-four verification tests were completed. The test results and the final DAMAGE predictions are listed in Figure 98. The test life and the predicted life represent the number of flight hours required to achieve the crack length specified in the column marked "c_f". They are not lives to failure. A comparison of life to failure can be misleading because it does not indicate the accuracy of the crack growth rate prediction.

In general, the methods used in DAMAGE predict the effects of temperature and environment on crack growth rate fairly accurately. Figure 99 summarizes the number of predicted crack growth lives that were within 20 percent of the test data.

It is obvious that the DAMAGE crack growth routine had the most difficulty predicting lives for tests which were run with the 10 hour compressed spectrum. These predictions are actually more accurate than the numbers indicate. These tests were conducted on the upper portion of the crack growth rate curve, which means the crack is growing at a faster rate. At high crack growth rates, the accuracy of the applied stress level and the initial crack length used in the analysis is very important. A small variation in either variable can have a significant effect on the predicted life.

It is also important to note that the 10 hour compressed spectrum tests typically ran twice as long as the 100 hour compressed spectrum tests. This means that these specimens were exposed to elevated temperatures twice as long. DAMAGE accounts for changes in material properties with temperature and

Specimen ID	Spectrum	Specimen Type	Stress (ksi)	C_{in} (in.)	C_f (in.)	Predicted Flight Hours	Test Flight Hours	Percent Difference
6Al-2Sn-4Zr-2Mo Titanium								
Ti-30	AF-C100	CCT	28.0	0.300	0.837	3,052.0	3,400.0	10.2
Ti-31	AF-C100	CCT	28.0	0.300	0.837	3,052.0	3,400.0	10.2
Ti-32	AF-C10	CCT	30.0	0.610	0.817	285.0	425.0	32.9
Ti-36	AF-C100	OHT	29.0	0.350	0.734	1,050.0	1,125.0	6.7
Ti-38	AF-C100	OHT	29.0	0.350	0.734	1,050.0	1,125.0	6.7
Ti-37	AF-C10	OHT	30.0	0.480	0.779	425.0	725.0	41.4
Ti-33	AV-C100	CCT	40.0	0.300	0.894	1,867.0	2,200.0	15.1
Ti-34	AV-C100	CCT	40.0	0.300	0.814	1,820.0	2,778.0	34.5
Ti-35	AV-C10	CCT	40.0	0.470	0.843	803.0	450.0	78.4
Ti-39	AV-C100	OHT	40.0	0.230	0.566	2,900.0	3,400.0	14.7
Ti-40	AV-C100	OHT	40.0	0.230	0.645	3,300.0	3,300.0	0
Ti-41	AV-C10	OHT	40.0	0.450	0.949	2,150.0	1,070.0	-100.9
IN 718								
In-30	AF-C100	CCT	50.0	0.350	0.885	3,053.0	3,400.0	10.2
In-31	AF-C100	CCT	55.0	0.350	0.815	2,055.0	2,125.0	3.3
In-32	AF-C100	CCT	55.0	0.350	0.815	2,055.0	1,750.0	-17.4
In-40	AF-C100	OHT	54.0	0.400	0.785	1,050.0	925.0	-13.5
In-41	AF-C100	OHT	54.0	0.400	0.785	1,050.0	1,025.0	-2.4
In-39	AF-C10	OHT	56.0	0.620	0.777	236.0	170.0	-38.8
In-33	AV-C100	CCT	65.0	0.350	0.873	2,233.0	3,550.0	37.1
In-34	AV-C100	CCT	65.0	0.350	0.873	2,233.0	4,000.0	44.2
In-35	AV-C10	CCT	65.0	0.520	0.871	1,053.0	1,025.0	2.7
In-36	AV-C100	OHT	65.0	0.200	0.800	2,733.0	3,000.0	8.9
In-37	AV-C100	OHT	65.0	0.200	0.800	2,733.0	3,350.0	18.4
In-38	AV-C10	OHT	65.0	0.420	0.697	930.0	840.0	10.7

AF   – Advanced Fighter Spectrum (1 mission per flight hour)   AV   – Aerospace Vehicle Spectrum (2 missions per flight hour)
AF-C10 – Advanced Fighter Spectrum (10 missions per flight hour)   AV-C10 – Aerospace Vehicle Spectrum (20 missions per flight hour)
AF-C100 – Advanced Fighter Spectrum (100 missions per flight hour)   AV-C100 – Aerospace Vehicle Spectrum (200 missions per flight hour. R = 0.90 load cycles removed)

GP93-0418-5-T

Figure 98. Verification Test Results and Final Predictions

Category	Number of Specimens	Number of Predictions Within 20% of Test Life	Percent
6-2-4-2 Ti	12	7	58.3
IN 718	12	9	75.0
CCT Specimen	12	7	58.3
OHT Specimen	12	9	75.0
Time Compression Factor = 100	17	14	82.3
Time Compression Factor = 10	7	2	28.5
Overall	24	16	66.7

GP93-0418-10-T

Figure 99. Predicted Lives Within 20% of Test Lives

114

for sustained loads at temperature, but not for time at temperature with no load. The additional exposure time at temperature could have caused a severe degradation in the material properties not fully accounted for in DAMAGE.

The final predictions listed in Figure 98 were based on all of the model development data and, therefore, do not match those provided to the Air Force. Negative stress ratio crack growth rate data were used to determine proper values for the Chang negative stress ratio coefficient, Q, and for the overload shut-off ratios. In addition, some of the initial conditions specified in the preliminary predictions (Figure 97) were not met in the actual tests. In certain cases, the proper stress level was not achieved, or pre-cracking went beyond the initial crack length. The final life estimates in Figure 98 represent the best predictions based on all of the model development data and on the actual initial test conditions.

In the following sections, each test will be discussed and predictions will be explained.

a. <u>Advanced Fighter Tests on Center Cracked Specimens</u> - Crack growth predictions using the 100 hour compressed spectrum show excellent correlation with the IN 718 and 6-2-4-2 Ti center cracked specimen data. Three IN 718 and two 6-2-4-2 Ti tests were run using the 100 hour compressed spectrum. One 6-2-4-2 Ti test was completed with the 10 hour compressed spectrum.

The results from three center cracked IN 718 tests are plotted in Figure 100. In the first test (IN-30), it was determined that the maximum spectrum loads were falling short of the prescribed values. In an attempt to rectify this, a higher initial load value was input into the load computer for the second and third tests. As a result, the maximum spectrum loads were matched, but the lower spectrum loads were exceeded. Higher average spectrum loads led to shorter test lives. When testing was complete, the average spectrum stress levels were approximately 50 Ksi for the first test, and 55 Ksi for the second and third tests. The stress level was determined from strip chart printouts of the peak and valley loads in the spectrum. The 10 hour compressed advanced

fighter spectrum was originally to be used with the third specimen, but due to the scatter in the first two specimens, the 100 hour compressed spectrum was used.
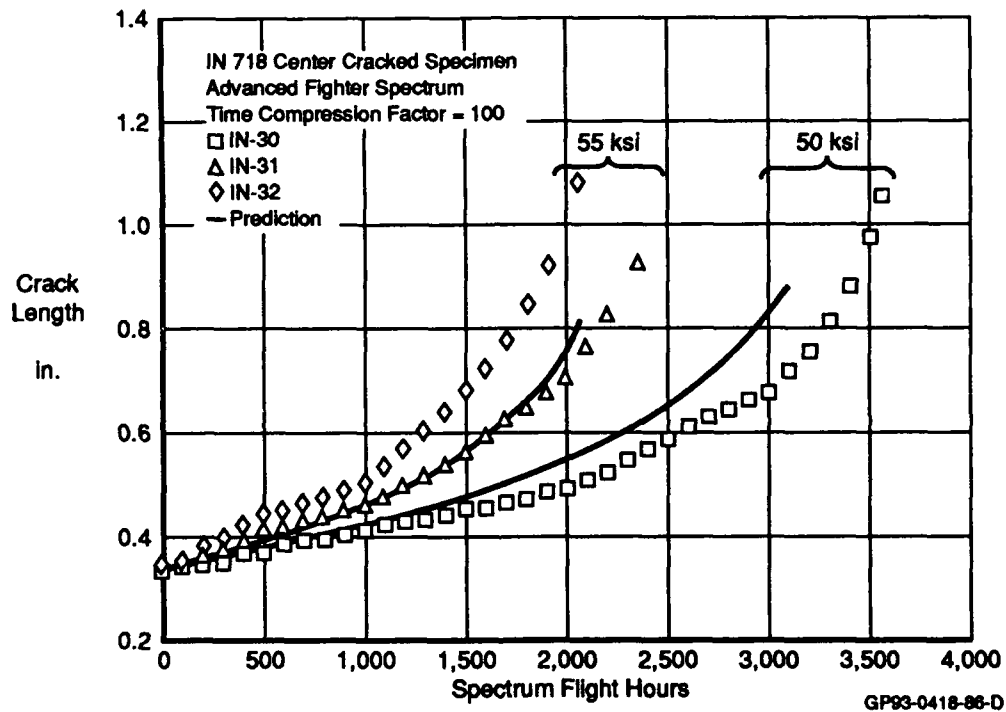
Figure 100. Verification Tests for IN 718 Center Cracked Specimens
(Advanced Fighter Spectrum, Time Compression Factor = 100)

Crack length vs. life data is plotted for two center cracked 6-2-4-2 Ti test specimens in Figure 101. The predicted crack growth curve falls directly on this data through 2500 flight hours.

116
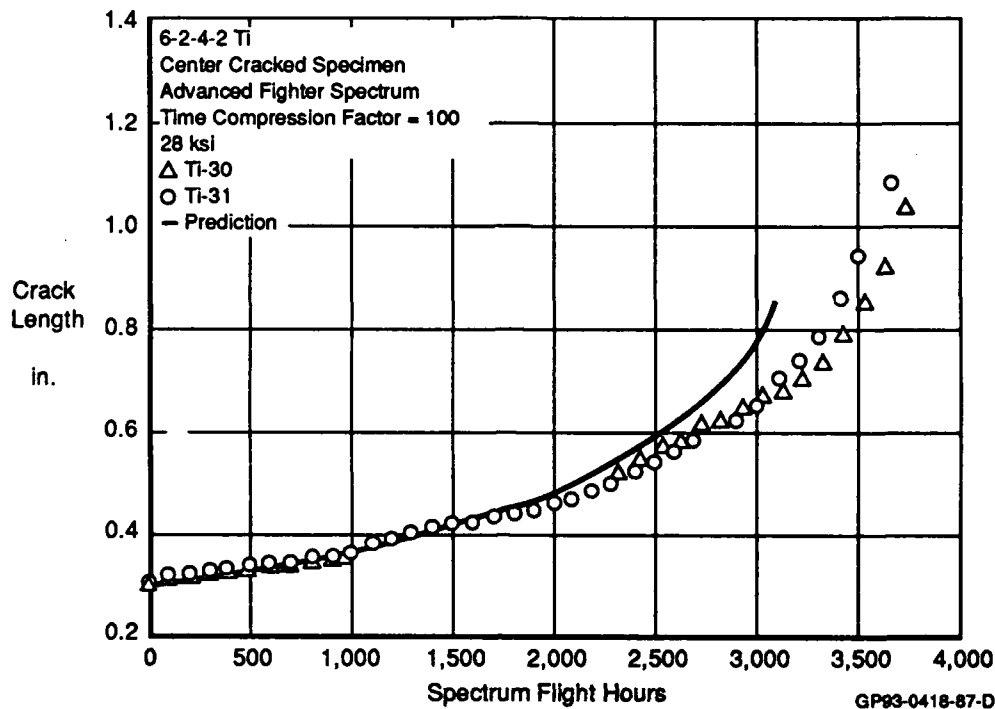
Figure 101. Verification Tests for 6-2-4-2 Ti Center Cracked Specimens (Advanced Fighter Spectrum, Time Compression Factor = 100)

The data for the first 6-2-4-2 Ti specimen (TI-30) is plotted in two groups. The first group of data had an initial crack length of 0.302 inch. The heat supplied by the quartz lamps was turned off due to a computer malfunction after the first 950 flight hours. At this point, the crack had grown to 0.35 inch. Once the problem was corrected, the test was restarted. The initial crack length for the second group of data was 0.53 inch. The initial life value for the second group of data was determined from the life of the second specimen (TI-31) when it was at the same crack length (0.53 inch). The stress level for these tests was supposed to be 30 Ksi. However, after the tests had been completed, it was determined that the actual stress level during the tests was approximately 28 Ksi.

DAMAGE is sensitive to stress level. The 30 Ksi 10 hour compressed spectrum prediction for the 6-2-4-2 Ti test is conservative (Figure 102). However, a second prediction at a slightly lower stress level (28 Ksi) shows a better correlation with the test data. A 6.7 percent decrease in stress produced a 66.7 percent greater life prediction.

The additional exposure time experienced by the 10 hour compressed spectrum test did not appear to affect the crack growth behavior. The 100 hour compressed spectrum data is also plotted in Figure 102. This data was plotted beginning with the same initial crack length as the 10 hour compressed spectrum. The 10 hour compressed spectrum test was exposed to temperature for 70 hours vs. 10 hours for the other two sets of data with the same amount of crack growth. The difference between the crack growth data is probably due to the stress levels of the three tests.

Figure 102. Verification Tests for 6-2-4-2 Ti Center Cracked Specimens
(Advanced Fighter Spectrum, Time Compression Factors = 10, 100)

118

All three of the 6-2-4-2 Ti tests had final crack lengths approximately 30 percent greater than were predicted. This implies that the fracture toughness is higher than predicted in DAMAGE. The fracture toughness data supplied to DAMAGE was obtained from the constant amplitude fatigue tests conducted at elevated temperature on center cracked specimens in the model development test matrix.

It is possible that time at temperature increases the fracture toughness. The time duration of the model development tests was much shorter than the verification tests. The model development data shows more of an instantaneous change in fracture toughness due to temperature.

b. Advanced Fighter Tests on Open Hole Specimens - The crack growth predictions for the open hole specimens follow the same pattern as the center cracked specimens. DAMAGE predicted the crack growth behavior better for the 100 hour compressed spectrum. Two 100 hour compressed spectrum tests and one 10 hour compressed spectrum test were completed on open hole specimens for each material, IN 718 and 6-2-4-2 Ti.

The 100 hour compressed spectrum predictions agree well with the test data. The IN 718 and 6-2-4-2 Ti test results are plotted in Figures 103 and 104. The gross stress levels for these tests were 54 Ksi for IN 718 and 29 Ksi for 6-2-4-2 Ti. In each case the predicted crack growth curve displays the same behavior as was seen in the tests.

The environment might adversely affect the crack growth rate in the IN 718 10 hour compressed spectrum test. The crack growth in this test is more accelerated than predicted, as shown in Figure 105. This plot also includes data from the two IN 718 tests run with the 100 hour compressed spectrum. The initial data point from these tests was chosen to correspond to the initial crack length from the 10 hour compressed spectrum test. The difference in crack growth between the different sets of data could simply be due to the test stress levels. However, it is also possible that the additional exposure time at temperature is causing the 10 hour compressed spectrum test to accelerate due to the chemical interaction with the environment. This test ran for 20 hours as opposed to 3 hours for the same crack growth in the two previous

119
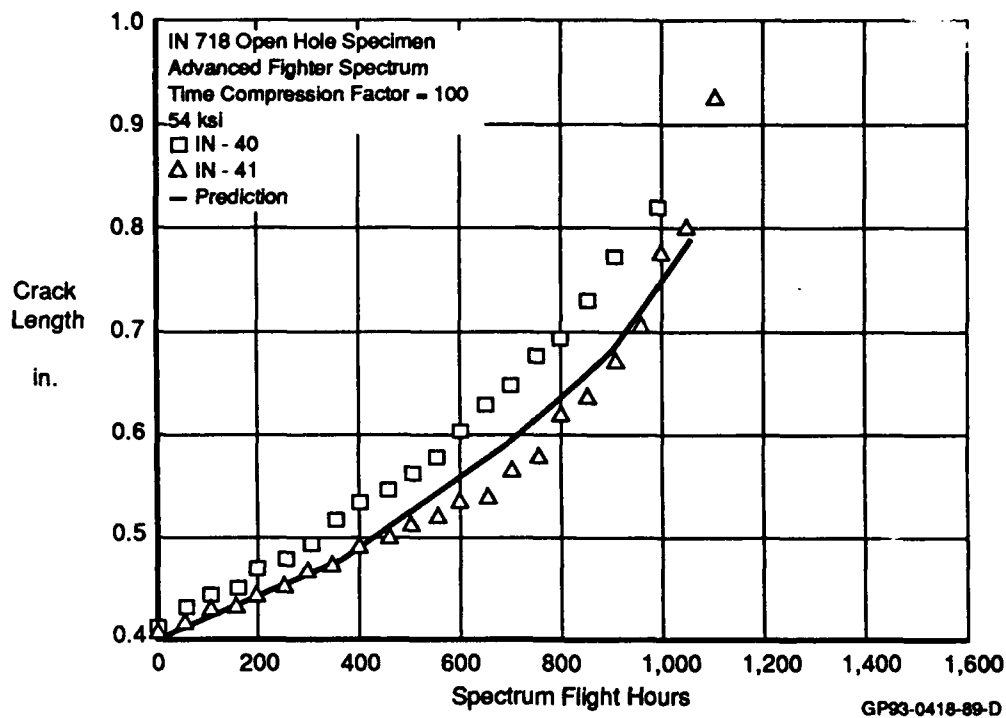
**Figure 103. Verification Tests for IN 718 Open Hole Specimens
(Advanced Fighter Spectrum, Time Compression Factor = 100)**
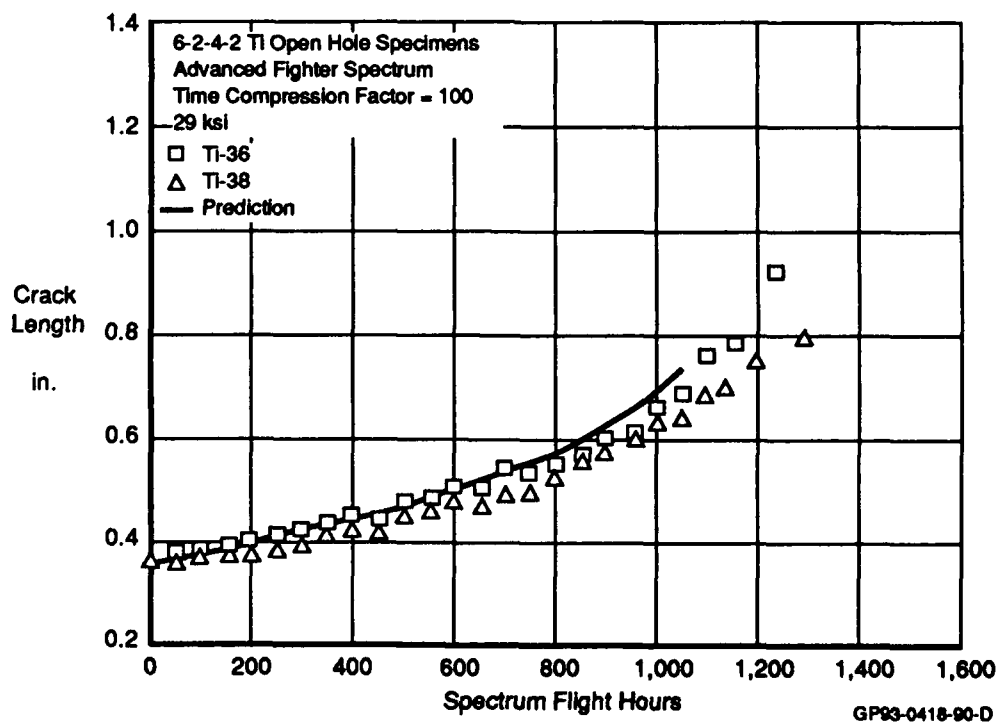
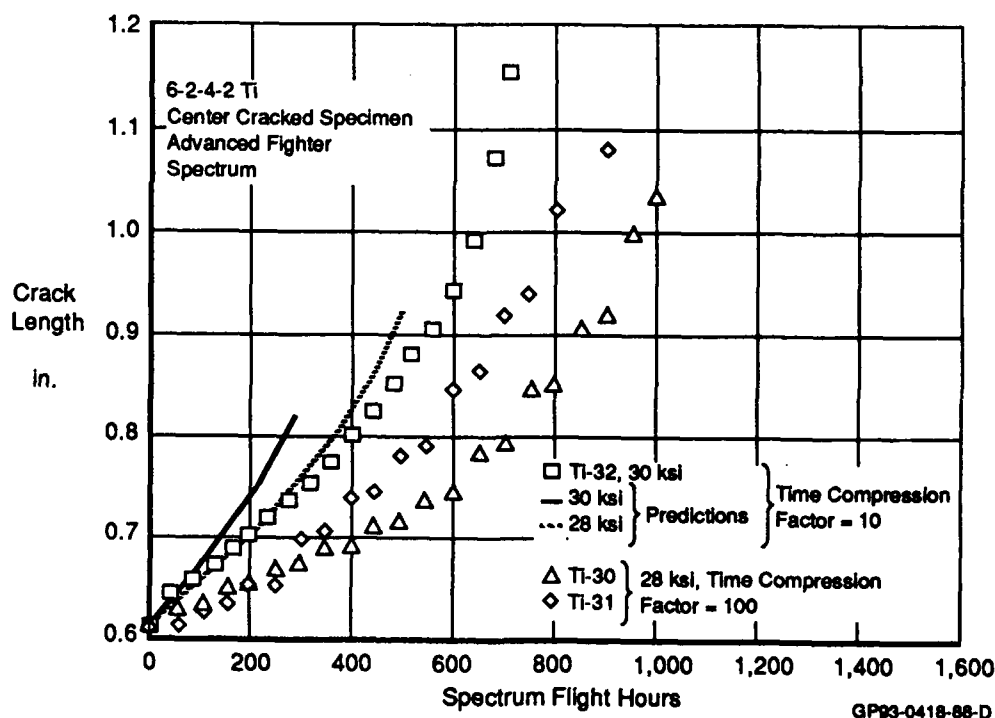

**Figure 104. Verification Tests for 6-2-4-2 Ti Open Hole Specimens
(Advanced Fighter Spectrum, Time Compression Factor = 100)**

120
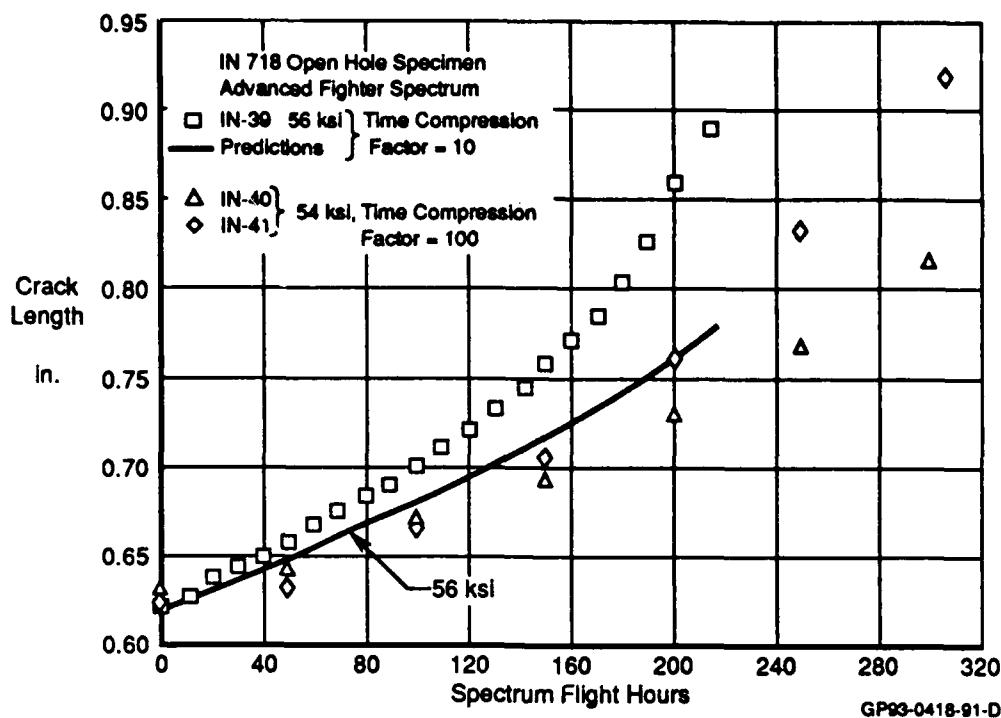
**Figure 105. Verification Tests for IN 718 Open Hole Specimens
(Advanced Fighter Spectrum, Time Compression Factors = 10, 100)**

IN 718 tests. The model development data showed little crack growth rate dependence on the environment. However, the majority of elevated temperature model development tests were performed at 1200°F. The maximum temperature for this test was 800°F. It is possible that the IN 718 material tested in this program is sensitive to the environment, but at 1200°F is overshadowed by retardation effects due to creep.

The crack growth data from the 10 hour compressed spectrum test for 6-2-4-2 Ti behaves the same as in the 100 hour compressed spectrum tests (Figure 106). The 30 Ksi stress level prediction for the 10 hour compressed spectrum test is slightly conservative. But, as was the case for the center cracked specimen, a second prediction at 27 Ksi improves the prediction considerably. A 10 percent decrease in stress level doubled the life prediction and correlated more favorably with the crack growth data curve.

The additional exposure time at 800°F in the 10 hour compressed spectrum does not appear to have affected crack growth behavior as compared to the 100

121

hour compressed spectrum in 6-2-4-2 Ti (Figure 106). The 10 hour compressed spectrum test lasted 90 hours. The 100 hour compressed spectrum tests lasted 7 hours for the same amount of crack growth.
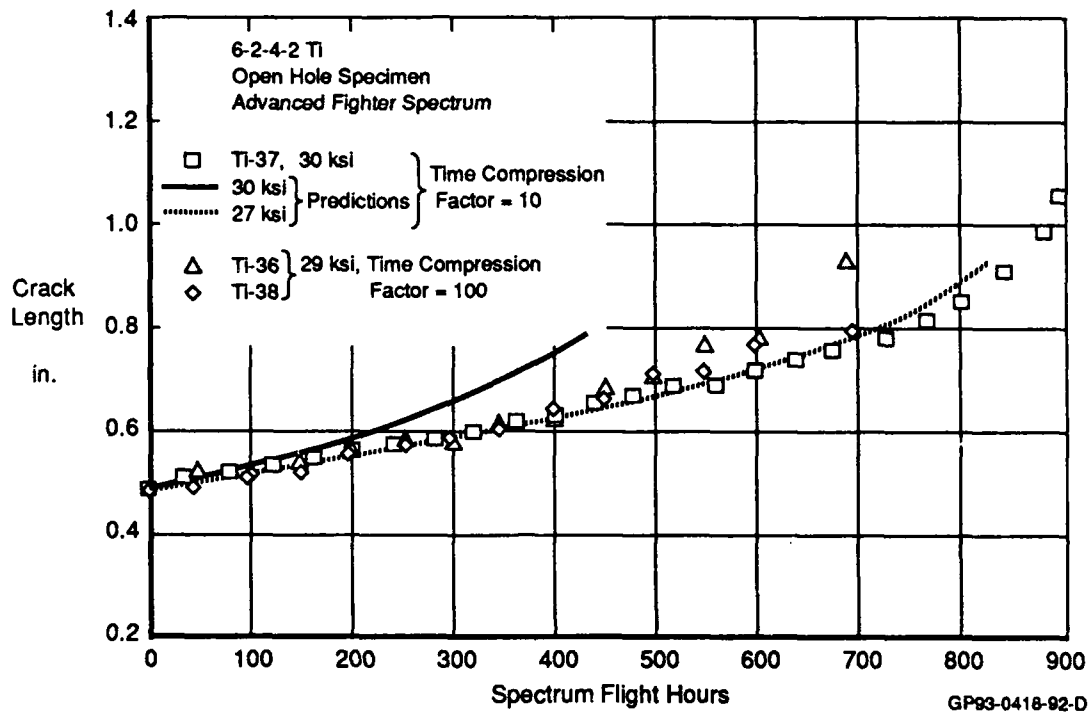
Figure 106. Verification Tests for 6-2-4-2 Ti Open Hole Specimens (Advanced Fighter Spectrum, Time Compression Factors = 10, 100)

The difference in the predicted vs. actual life to failure is magnified in the analysis of the 10 hour compressed spectrum tests. Typically, these tests last 10 times longer than the 100 hour compressed spectrum tests because there are one tenth as many load cycles per hour. To run the tests in a reasonable amount of time, these tests began with larger initial crack lengths, which correspond directly to a larger initial stress intensity. The entire test is, therefore, conducted on the upper portion of the crack growth rate curve. This is where the crack is growing the fastest. This explains why the life predictions for the 10 hour compressed spectrum tests have shown such sensitivity to stress level and fracture toughness. If either value is off by even a small amount, it could exaggerate the effect on the life estimate.

122

c. Aerospace Vehicle Tests on Center Cracked Specimens - The aerospace
vehicle spectrum had a maximum temperature of 1200°F for IN 718 and 1000°F for
6-2-4-2 Ti. These extreme temperatures had different effects on the crack
growth behavior than those described in the advanced fighter spectrum tests.

The IN 718 crack growth predictions match the test results better for the
10 hour compressed spectrum than for the 100 hour compressed spectrum. Two
tests were conducted with the 100 hour compressed spectrum. These tests were
run at a stress level of 65 Ksi, and appear to have experienced more crack
growth retardation than the model predicted (Figure 107). The model life
prediction is approximately 40 percent conservative for these tests. Unlike
previous results, this prediction is not extremely sensitive to stress level.
A stress level of 55 Ksi is required to produce a more accurate prediction.
This represents a 15 percent decrease in stress level to obtain a 80 percent
increase in life.
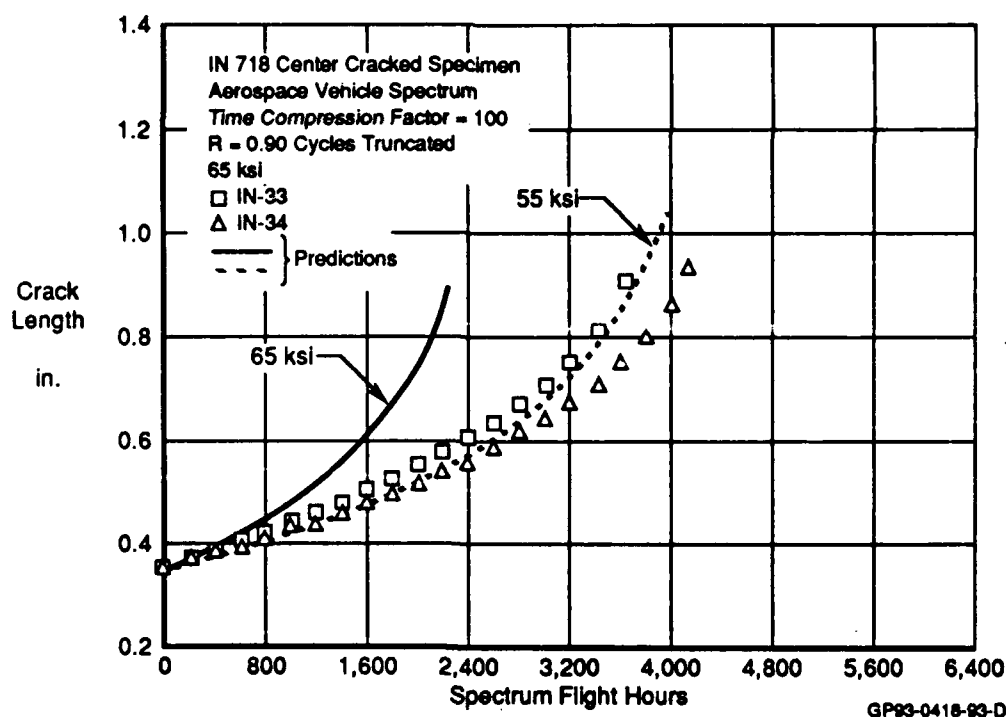
**Figure 107. Verification Tests for IN 718 Center Cracked Specimens
(Aerospace Vehicle Spectrum, Time Compression Factor = 100)**

The crack growth prediction for the 10 hour compressed spectrum test is
similar to the test result (Figure 108). This indicates that the model is

properly accounting for crack growth retardation. However, the 100 hour condensed spectrum test predictions were conservative. In addition, crack growth retardation would be more pronounced in a test which is exposed to elevated temperatures for a longer period of time. The 10 hour compressed spectrum test was exposed to temperature for 100 hours, while the 100 hour compressed spectrum tests were exposed to temperature for only 40 hours. Therefore, if retardation is being accounted for properly in the model (as is indicated by the 10 hour compressed spectrum test), we would have expected a more accurate prediction for the 100 hour compressed spectrum test.

There is a difference in the crack growth behavior of the 10 hour and 100 hour compressed spectrum tests (Figure 108). The 10 hour compressed spectrum data show accelerated growth compared to the 100 hour compressed spectrum data, which were run at the same stress level. Although the 10 hour compressed spectrum test was exposed to elevated temperatures for a longer period of time, environmental interaction causing accelerated crack growth does not adequately explain this behavior. The crack growth prediction, which agrees with the test data, was made assuming that IN 718 was not sensitive to the environment. The prediction was based on the high frequency crack growth rate curves for room temperature, 700°F and 1200°F obtained in the model development testing.

Since environmental sensitivity and creep cannot adequately explain the difference in the crack growth data seen in Figure 108, it must be related to the two load profiles used in this testing. As described in Section VI-5a, it was necessary to eliminate all of the R=0.90 load cycles in the 100 hour compressed spectrum so that the thermal profile would not have to be changed. The truncation of these cycles created a second exceedance curve for the aerospace vehicle spectrum (Figure 109). At 1000°F, these load cycles must have accelerated crack growth in the 10 hour compressed spectrum tests. In this spectrum there would be 3000 of these load cycles in each hour. The peak stress in this cycle is less than 50 percent of the test limit stress. A truncation study was performed with DAMAGE before testing began (Figure 96). Crack growth predicted by DAMAGE was identical regardless of whether or not the R=0.90 load cycles were eliminated. It appears, however, that these cycles do provide more damage than the model predicts.

124

Figure 108. Verification Tests for IN 718 Center Cracked Specimens (Aerospace Vehicle Spectrum, Time Compression Factors = 10, 100)
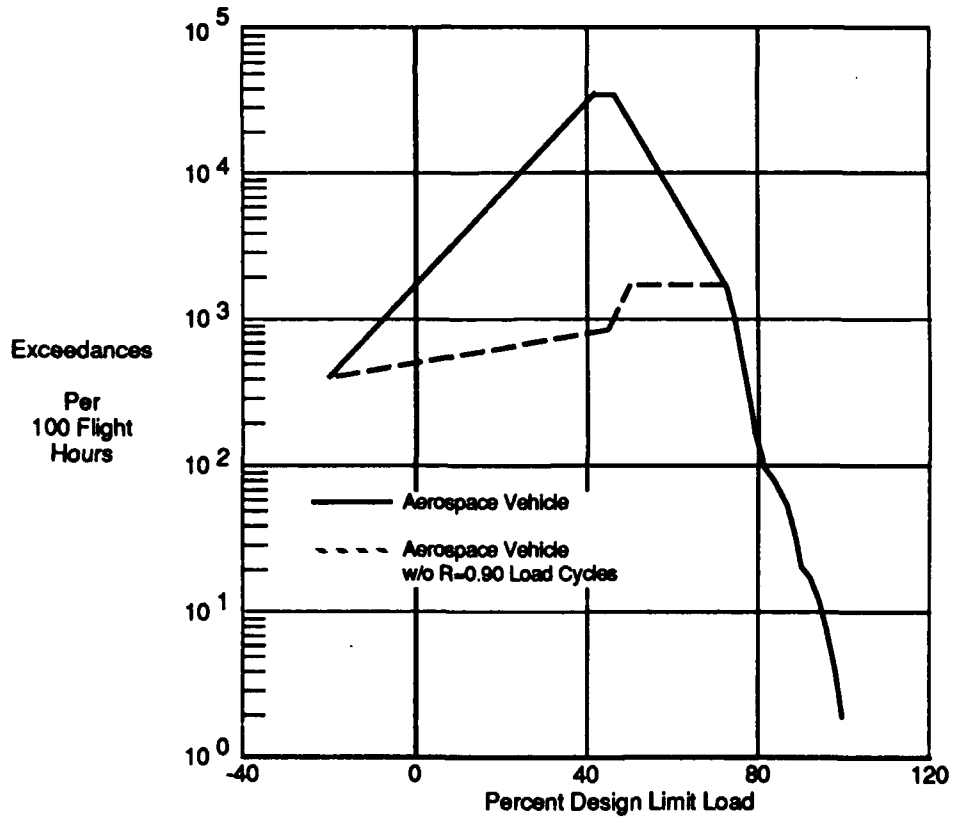
Figure 109. Aerospace Vehicle Exceedance Curve When R=0.90 Load Cycles are Eliminated

125

The 6-2-4-2 Ti 100 hour compressed spectrum prediction is conservative as compared to the test data, and is within acceptable range (Figure 110). The model predicts the crack growth behavior very well. The test was conducted at a stress level of 40 Ksi.

The 6-2-4-2 Ti 10 hour compressed spectrum prediction is unconservative as compared to the test data (Figure 111). This data also displays much different crack growth behavior than the two 100 hour compressed spectrum tests which were run at the same stress level (40 Ksi). The 10 hour compressed spectrum test is subject to a greatly increased crack growth rate. This behavior can be explained by one or any combination of the three reasons provided below:

1) The 3000 R=0.90 load cycles in the 10 hour compressed spectrum test accelerated crack growth even though DAMAGE predicted that these cycles would not affect crack growth (Figure 96).

2) Model development tests indicated that this material is sensitive to its environment (Figure 46). Long exposure times at elevated temperatures would accelerate crack growth in lab air.

3) This material was subject to a thermal profile with a maximum temperature of 1000°F, which is close to maximum temperature capability. The test lasted nearly twice as long as the two 100 hour compressed spectrum tests (45 hours vs. 25 hours). This added exposure time at elevated temperatures probably severely degraded material and crack growth properties, which is not accounted for properly in the crack growth model (DAMAGE).

Comparison of the 10 hour and 100 hour compressed spectra tests indicates that the R=0.90 cycles provide significantly more crack growth than predicted by DAMAGE. Whether this error is due to the high stress ratio of these cycles (a condition not tested during model development) or environmental acceleration enhanced by such cycles (a very real possibility given the high mean stress applied during these cycles) remains to be determined. Certainly, other investigators have shown that crack growth is accelerated by high stress ratio testing, but rarely so in the presence of significantly higher spectrum

126

Figure 110. Verification Tests for 6-2-4-2 Ti Center Cracked Specimens (Aerospace Vehicle Spectrum, Time Compression Factor = 100)

GP93-0418-96-D

Figure 111. Verification Tests for 6-2-4-2 Ti Center Cracked Specimens (Aerospace Vehicle Spectrum, Time Compression Factors = 10, 100)

GP93-0418-97-D

127

loads. This behavior requires more study and testing (See Conclusions and Recommendations).

   d. **Aerospace Vehicle Tests on Open Hole Specimens** - The open hole specimens displayed behavior similar to the center cracked specimens' for both the 100 hour and 10 hour compressed aerospace vehicle spectra. For each material two tests were conducted using the 100 hour compressed spectrum, and one using the 10 hour compressed spectrum.

   The crack growth behavior in each of the three IN 718 tests agrees with the prediction. The prediction is slightly conservative for the 100 hour compressed spectrum tests (Figure 112), and slightly unconservative for the 10 hour compressed spectrum test (Figure 113). The data from the 100 hour compressed spectrum tests is also plotted in Figure 113. The 10 hour compressed spectrum data again shows a faster crack growth rate. This was the same behavior discussed for the center cracked data. However, the difference for the open hole specimens is not as great. This disparity is best explained by the elimination of the R=0.90 load cycles in the 100 hour compressed load spectrum.

Figure 112. Verification Tests for IN 718 Open Hole Specimens
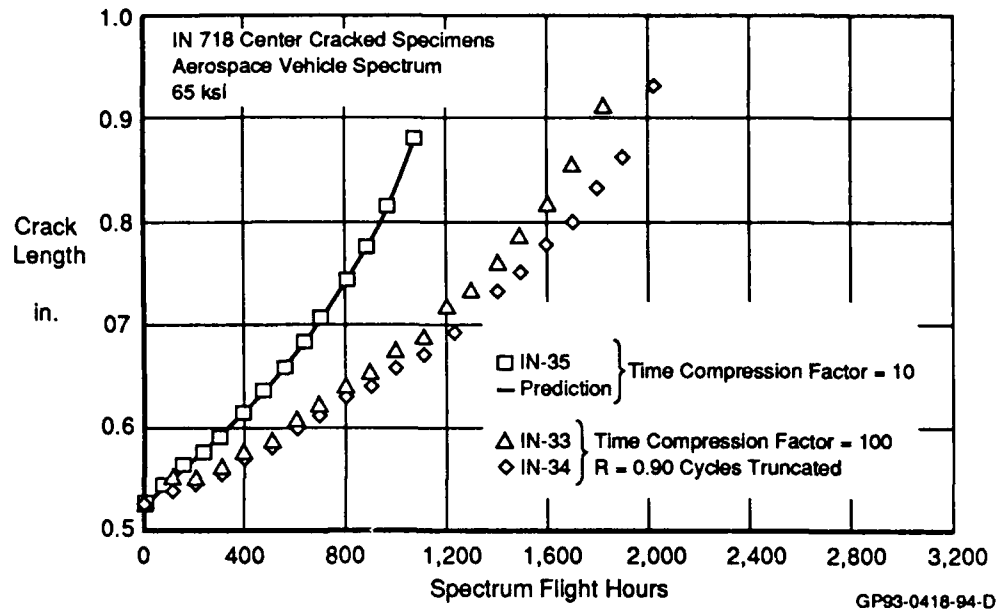**(Aerospace Vehicle Spectrum, Time Compression Factor = 100)**

128
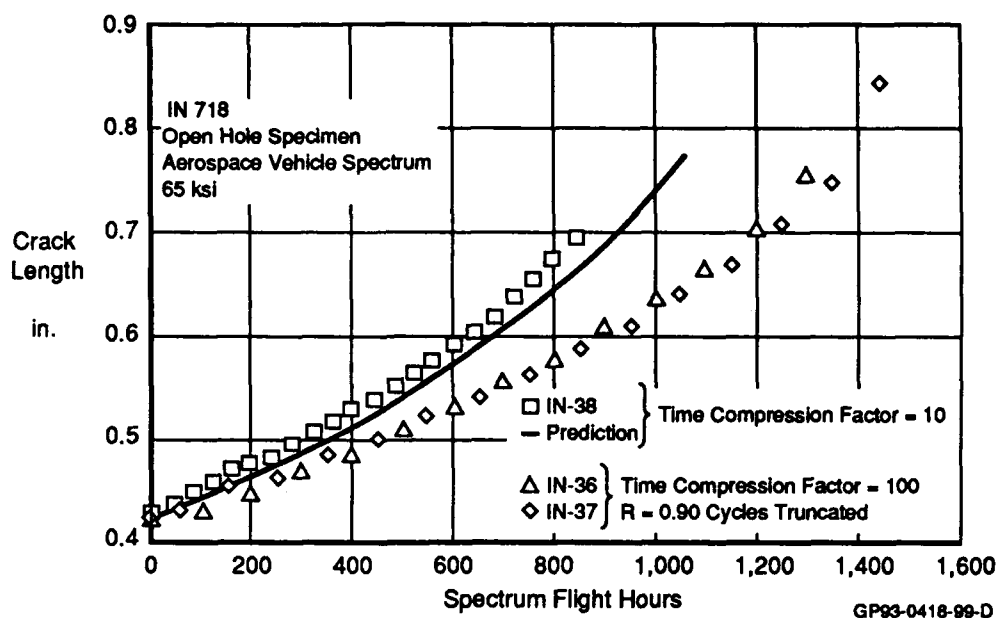
**Figure 113. Verification Tests for IN 718 Open Hole Specimens
(Aerospace Vehicle Spectrum, Time Compression Factors = 10, 100)**

Crack growth in the 100 hour compressed spectrum tests is predicted accurately by DAMAGE (Figure 114). The crack growth predictions were based on a different stress intensity solution than used in the other open hole test predictions because a crack grew out of only one side of the open hole for both tests. The final crack growth prediction exceeds the test data simply because both tests were stopped before failure because of time limitations.

The data from the 10 hour compressed spectrum test displays the same behavior as the center cracked test data discussed in Section VI-6c. Crack growth is greatly accelerated compared to the 100 hour compressed spectrum tests (Figure 115). Direct comparison of these results can be made because only one crack grew out of the open hole in all three tests. The same conclusions from the center cracked test apply here as well. Crack growth was apparently accelerated by crack growth property degradation after long exposure times and the 3000 additional R=0.90 cycles which were not applied in the 100 hour compressed spectrum tests. The predicted crack growth curve is not sensitive to these specific effects, and therefore is unconservative.
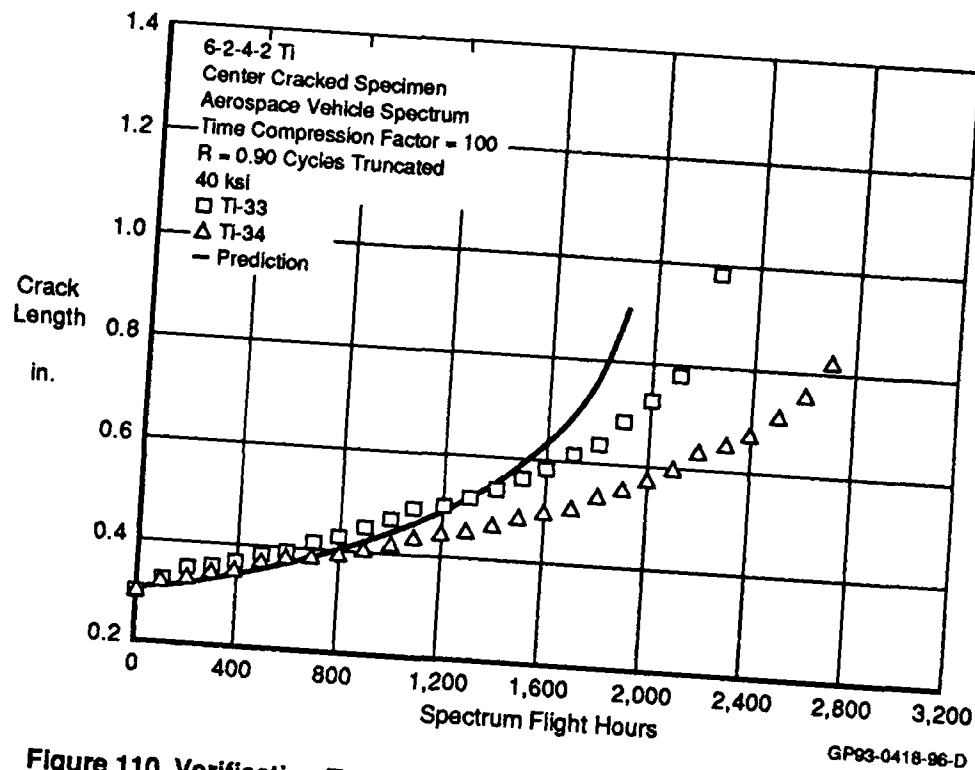
129
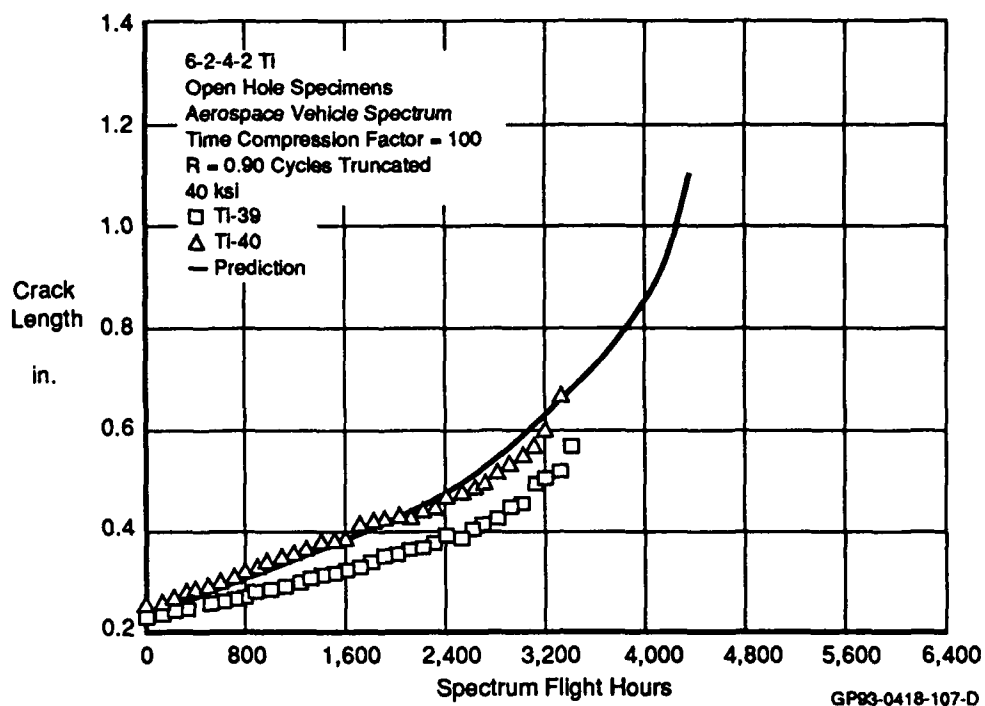
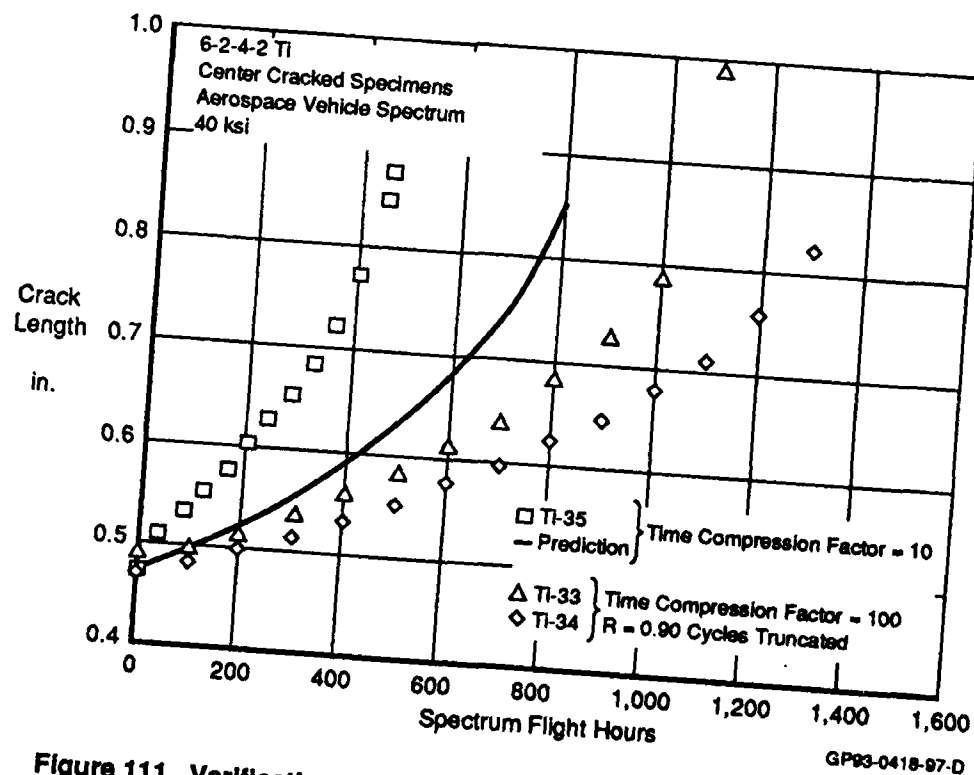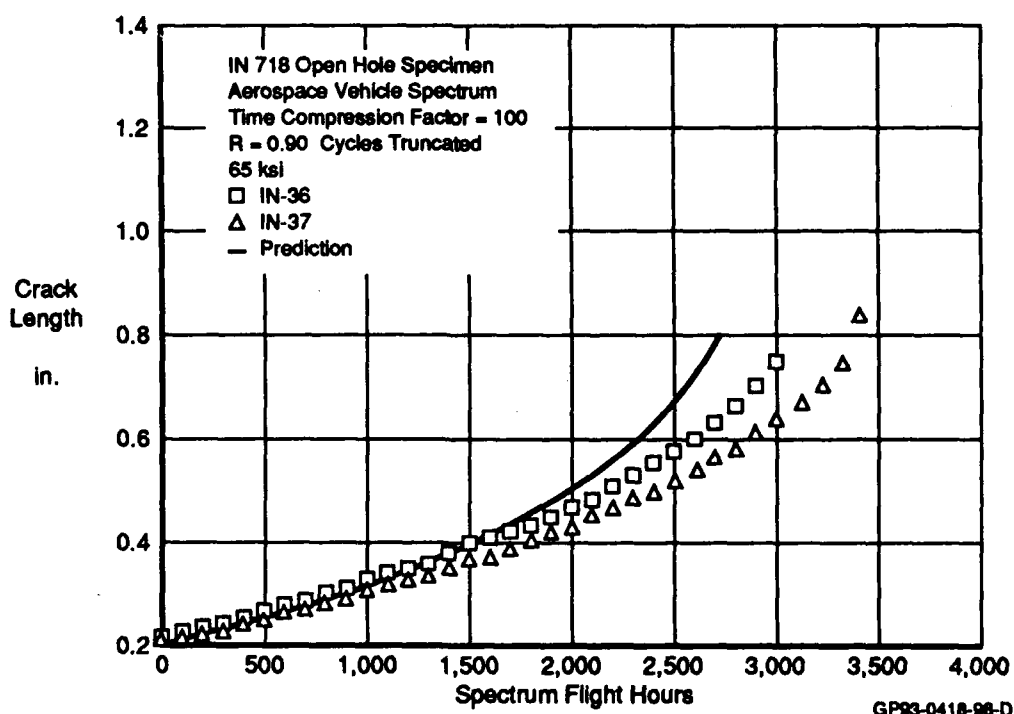**Figure 114. Verification Tests for 6-2-4-2 Ti Open Hole Specimens (Aerospace Vehicle Spectrum, Time Compression Factor = 100)**
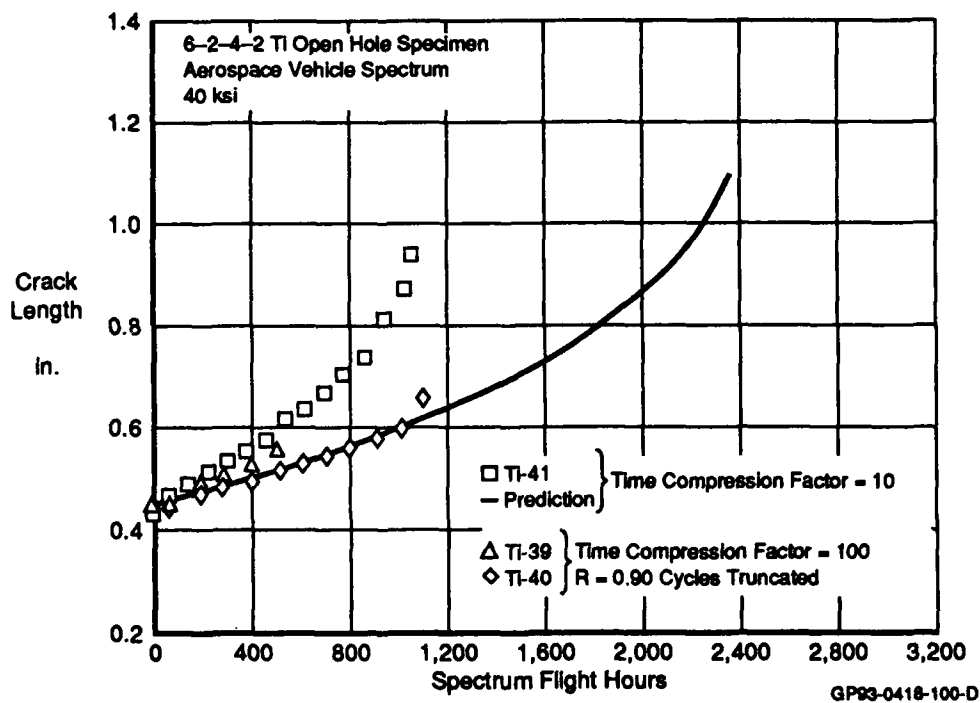
Figure 115. Verification Tests for 6-2-4-2 Ti Open Hole Specimens (Aerospace Vehicle Spectrum, Time Compression Factors = 10, 100)

130

SECTION VII

ADDITIONAL TESTING - 14AL-21NB TITANIUM

1.   <u>Testing Summary</u> - Concurrent with this contract, MCAIR was independently conducting a similar test program on a third material. This material was an ingot metallurgy titanium aluminide 14-21 Ti. These materials are of interest because they maintain their strengths at high temperatures better than typical titanium alloys.

Whereas 6-2-4-2 Ti and IN 718 were chosen for model development due to their vastly different material behavior at elevated temperatures, titanium aluminide materials are of interest because of their high potential in a variety of elevated temperature applications. They are also being considered as candidate matrix materials for metal matrix composites. In other Air Force contracts, titanium aluminide matrix composites are being consolidated and will be tested under thermomechanical fatigue conditions.

2.   <u>Material Selection</u> - The ingot metallurgy titanium aluminide selected for testing was 14Al-21Nb titanium (14-21 Ti). The material was purchased in ingot form from The Duriron Company in Dayton Ohio. The ingots were cast and hot isostatically pressed (HIP). The ingot diameter was 3.2 inches.

The ingots were then extruded to achieve the material properties typical of plate or sheet product forms. One obvious limitation of using this process to simulate rolling is that the grain structure is being modified only in the extrusion direction. This results in high longitudinal properties and lower transverse properties than rolled product forms. This process was used because the amount of material was too small to allow rolling. The extrusion was performed by Nuclear Metals of Concord Massachusetts. Two types of extrusion dies were used to obtain two product forms: 3/4 inch diameter rod and 3/4 inch x 2 inch rectangular bar.

3.   Specimen Configuration - Two specimen configurations were required for testing. Static tension specimens were made out of the 3/4 inch diameter bar. The static tension specimen was the same as that used in the main program. A round bar tensile specimen with a 2 inch gage length and a 0.50 inch diameter was used (Figure 9).

Compact tension specimens were required for fatigue crack growth tests. The specimen configuration is detailed in Figure 116. This specimen differs in size from those used for 6-2-4-2 Ti and IN 718 specimens tested under the contracted effort at Georgia Tech.

Note: All dimensions in inches.

Notch Detail - Straight Thru
GP93-0418-101-D
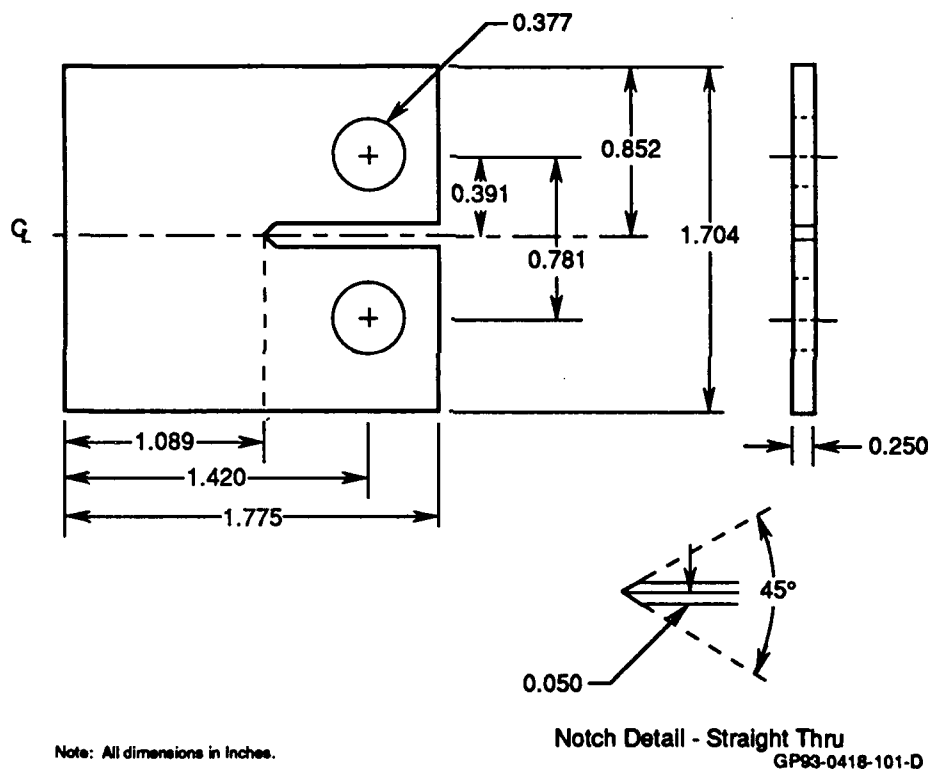
Figure 116. Compact Tension Specimen (CT)

4.   Test Program - Testing of the 14-21 Ti was performed by two contractors. The complete test matrix is shown in Figure 117.

The static tests were performed by Georgia Tech. Tests were conducted at room temperature, 700°F, and 1400°F. Two strain rates were used to determine the effect of time at temperature on the strength.

132

Fatigue crack propagation tests were performed by the University of Dayton through the Wright Research and Development Center Materials Lab at Wright-Patterson Air Force Base (Reference 19). The purpose of this testing was to examine the effects of temperature and hold time on the crack growth rate of the material (Figure 117).

a. __Static Tension Tests__ - The ingot based 14-21 Ti was not as strong as the 6-2-4-2 Ti material (Figures 118 and 119). The room temperature ultimate

Static Tension Tests (Georgia Tech)

Temperature (°F)	Strain Rate	
	0.50%/min	50.0%/min
Room Temperature	2	2
700	2	2
1,400	2	2

Fatigue Crack Propagation Tests (WRDC/MLLN)
R = 0.02

Temperature (°F)	Frequency (Hz)	Hold Time @ Peak (sec)	No. of Tests
Room Temperature	10	0	2
1,200	10	0	2
	0.1	10	2
1,500	10	0	2
	0.1	10	2

GP93-0418-9-T

Figure 117. 14-21 Ti Test Program

strength of the 14-21 Ti was 56 percent of the 6-2-4-2 Ti room temperature strength. Similarly, the 700°F ultimate strength of the 14-21 Ti was 78 percent of the 6-2-4-2 Ti strength. The percentage difference in the yield strengths are nearly the same as for the ultimate strengths.

Although weaker than 6-2-4-2 Ti, 14-21 Ti maintains its strength much better (Figure 120). At 700°F, the 14-21 Ti material lost only 3 percent of its room temperature strength. Conversely, the 6-2-4-2 Ti experienced a 28 percent loss in strength.

133

Elevated temperature strengths of 14-21 Ti decreased as the strain rate decreased. 14-21 Ti is extremely brittle at room temperature, and its ductility improves with an increase in temperature. However, the ductility decreases the longer the material is exposed to elevated temperatures. The 14-21 Ti tests were conducted at two strain rates: 0.50 and 50.0 percent/minute. Slightly higher yield and ultimate strengths were obtained at the 50.0 percent/minute strain rate (Figures 118 and 119).

The increase in ductility with increasing temperature is evident from the elongation results obtained at the three test temperatures (Figure 121). Elevated temperature elongations at 700°F and 1400°F and at a strain rate of 0.5 percent/minute increased by factors of 2.2 and 21.8, respectively, over room temperature elongations. The effect of strain rate on elongation is also significant. At 700°F, a decrease in the strain rate from 50.0 percent/minute to 0.50 percent/minute decreased the elongation by a factor of 2.25. Similarly, at 1400°F, the same decrease in strain rate produced a 1.5 factor decrease in elongation.

b. __Fatigue Crack Growth Tests__ - Crack growth rates were higher in the ingot based 14-21 Ti material than in the 6-2-4-2 Ti (Figure 122). This was true at room and elevated temperatures. The brittle room temperature 14-21 Ti produced a very steep crack growth rate curve. Crack growth rates were greater at higher temperatures in the 14-21 Ti, despite the increase in ductility observed in the static tests.

The environmental sensitivity of 14-21 Ti increases at elevated temperatures. Environment interaction decreased the threshold stress intensity dramatically at 1200°F and 1500°F as compared to room temperature values.

A minimal effect of environment and hold time at peak load on crack growth rate was seen at 1200°F (Figure 123). Sustained load crack growth was studied by comparing crack growth rates at a high frequency (10 Hz) with no hold times to those at a low frequency (0.1 Hz) with a 10 second hold time at peak load. In addition, environmental sensitivity was examined by comparing data from tests conducted in lab air to data from tests conducted in an argon atmosphere.
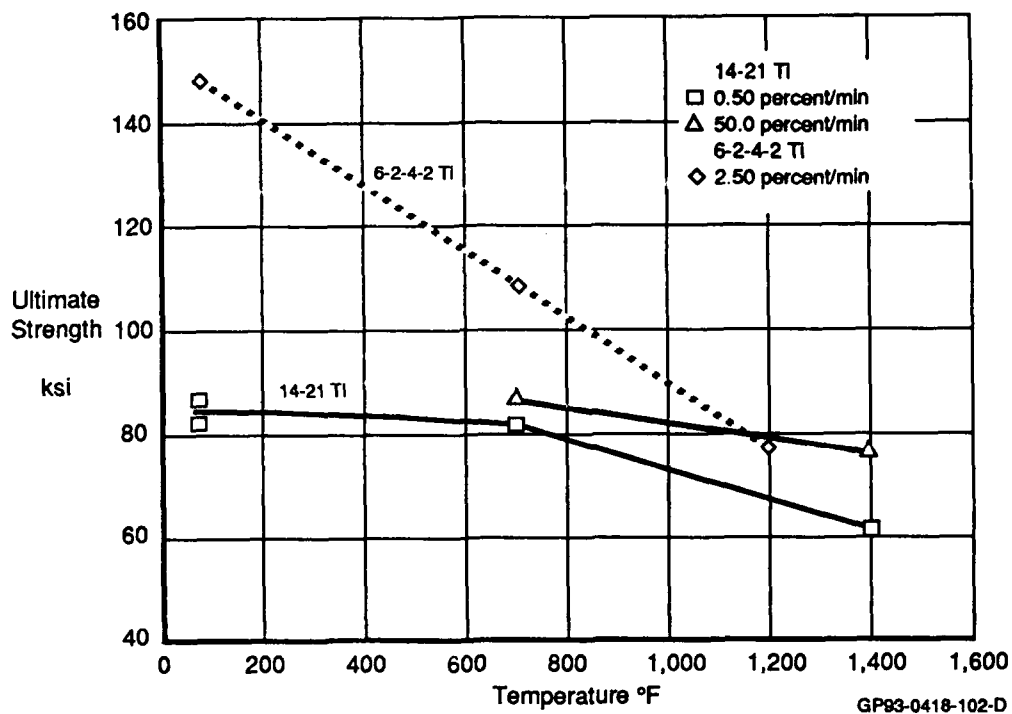
Figure 118. Ultimate Strength vs Temperature and Strain Rate for 14-21 Ti and 6-2-4-2 Ti
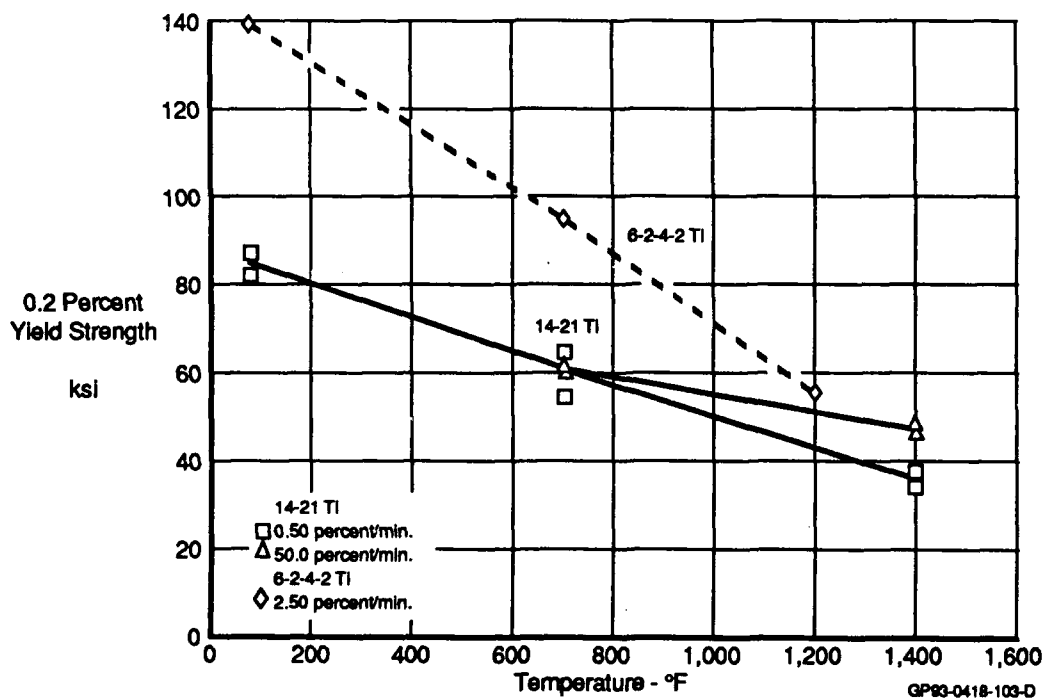
Figure 119. Yield Strength vs Temperature and Strain Rate for 14-21 Ti and 6-2-4-2 Ti

135
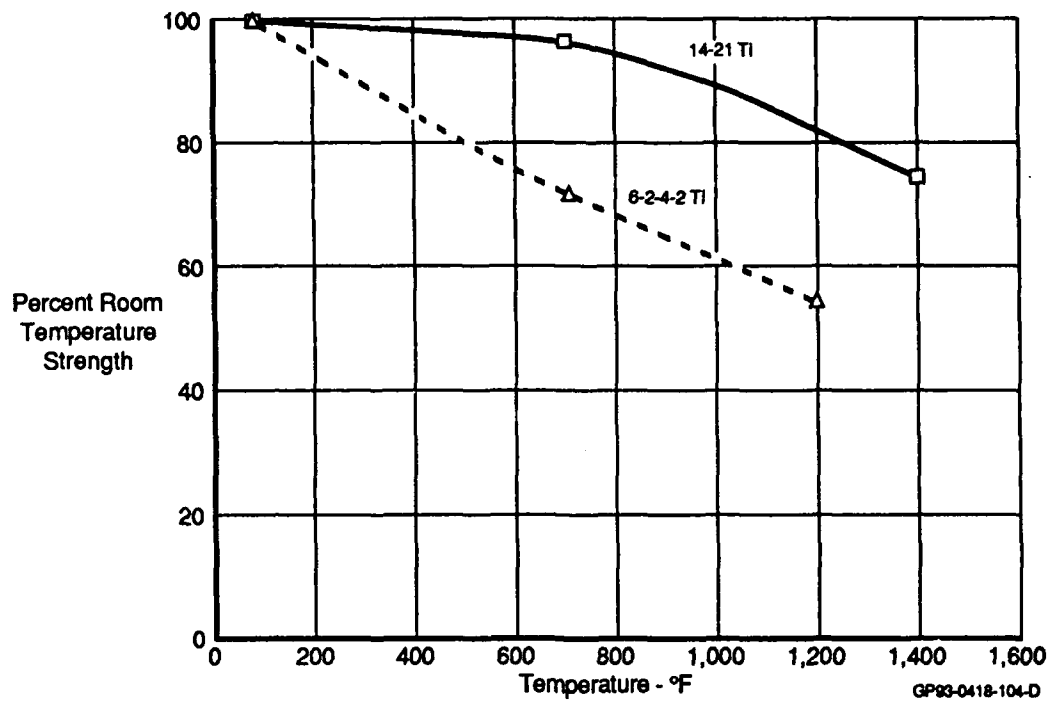
Figure 120. Strength Reduction at Temperature
for 14-21 Ti and 6-2-4-2 Ti
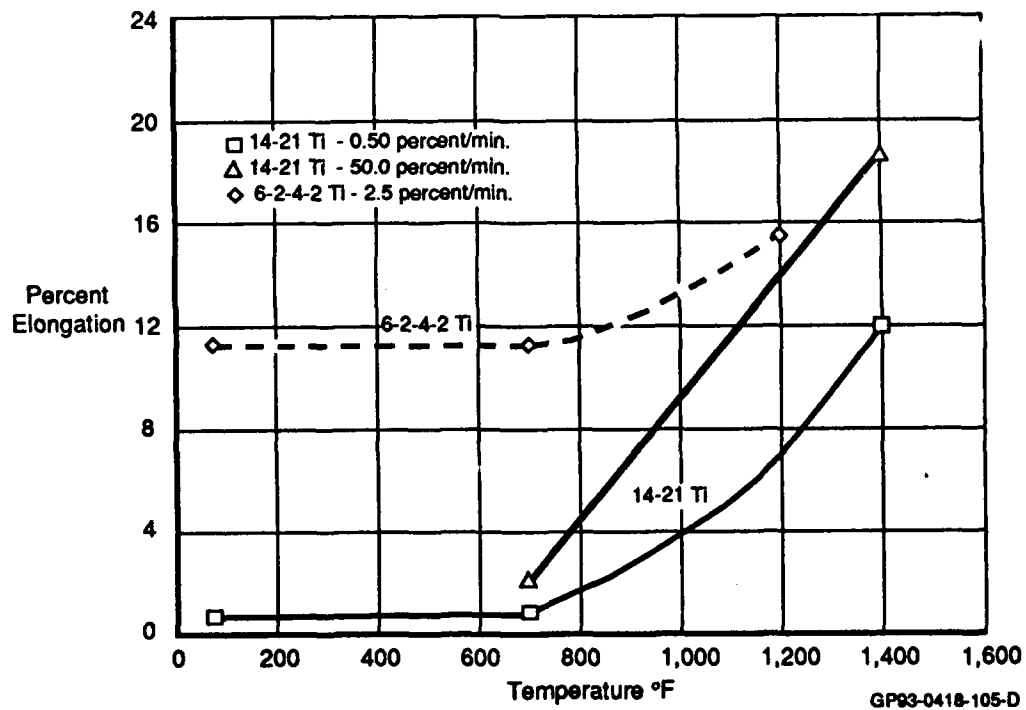
Figure 121. Elongation vs Temperature for 14-21 Ti and 6-2-4-2 Ti

136
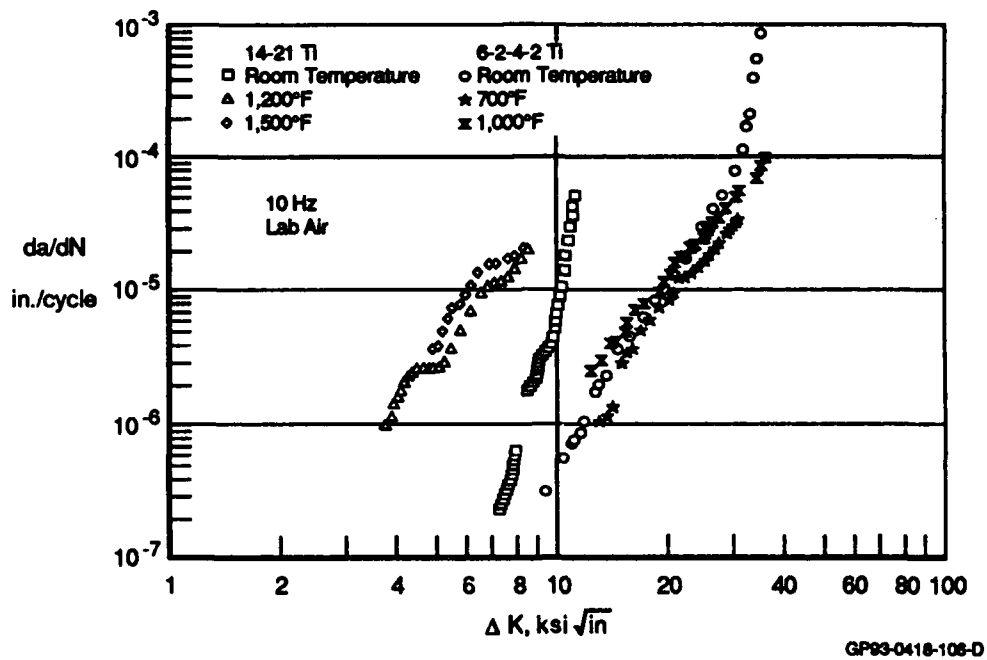
Figure 122. Crack Growth in 14-21 Ti and 6-2-4-2 Ti
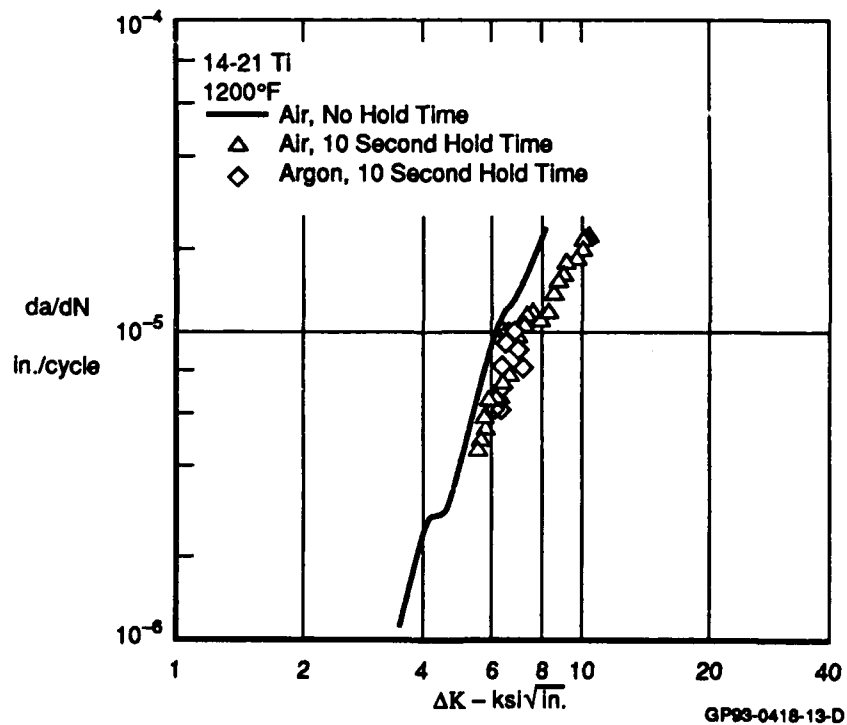
Figure 123. Sustained Load Crack Growth in 14-21 Ti at 1200°F

137

The crack growth behavior of 14-21 Ti is different at 1500°F than at 1200°F. Sustained loads at 1500°F retard crack growth (Figure 124). In addition, lab air accelerates crack growth compared to an argon environment. The effect of the oxidized environment is more pronounced at 1500°F than 1200°F.

This limited data indicates that in 14-21 Ti crack growth acceleration caused by the environment is more a function of temperature than time at temperature. In fact, sustained loads decreased the crack growth rates.
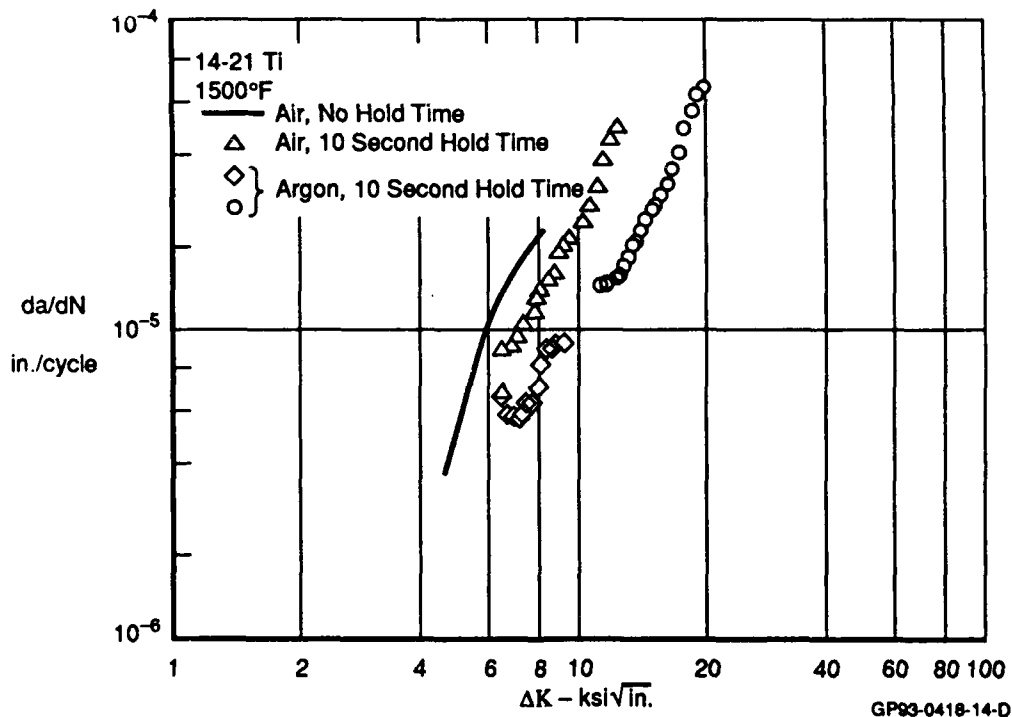
Figure 124. Sustained Load Crack Growth in 14-21 Ti at 1500°F

SECTION VIII

CONCLUSIONS AND RECOMMENDATIONS

1. <u>Contract Summary</u> - A fracture mechanics based life prediction procedure has been developed for hypersonic airframes subjected to combined mechanical and thermal load profiles. This analysis models crack growth behavior in metals and accounts for the effects of temperature on yield strength and fracture toughness. It also accounts for the effects of the environment and sustained load at elevated temperatures on crack growth rate.

A FORTRAN computer code performs the life prediction. This code is called DAMAGE, <u>D</u>amage <u>A</u>nalysis of <u>M</u>etals subjected to <u>AG</u>gressive <u>E</u>nvironments. This code was based on a room temperature code developed by Rockwell known as CRKGRO. DAMAGE models the high frequency crack growth rate using the Modified Walker and Chang equations. Load interaction effects are accounted for by the Generalized Willenborg model for tensile overloads, and the Chang acceleration scheme for compressive underloads.

DAMAGE includes modular routines to specifically account for elevated temperature crack growth analysis. These routines include:

1) a temperature dependent Modified Walker equation for fitting crack growth data
2) a Wei-Landes method for sustained load crack growth
3) the use of Larson-Miller data which will determine the effective yield strength
4) a reduction in yield strength with temperature
5) the effects of temperature on fracture toughness
6) a temperature dependent overload shut-off ratio for calculating retardation effects caused by overloads.

DAMAGE will analyze crack growth in specimens with part-through or through cracks emanating from open holes or slots. Stress intensity solutions were also added to DAMAGE to account for out-of-plane bending

moments on crack growth. Components may be subjected to axial loads and/or out-of-plane bending moments.

In addition, DAMAGE was made extremely user-friendly for the interactive user. Error traps were incorporated into the code to prevent premature termination of an analysis session. The user is prompted for revised data whenever input data is found to be erroneous. The code was commented and streamlined to make both the baseline code and the additions more easily deciphered. All of these enhancements are fully documented in the User's Manual, Reference 1.

The development of the elevated temperature life prediction code was based on model development testing of two materials: Inconel 718 (IN 718) and 6Al-2Sn-4Zr-2Mo titanium (6-2-4-2 Ti). IN 718 and 6-2-4-2 Ti were selected because they can be used at temperatures up to 1000°F, and because they exercise different aspects of the crack growth model. Yield strength reduction and creep at elevated temperature are much subtler for IN 718 than for 6-2-4-2 Ti. IN 718 is much more sensitive to environmental crack growth acceleration at high temperatures than is 6-2-4-2 Ti, according to the literature.

In this test program, however, the IN 718 material did not show the type of crack growth acceleration at elevated temperatures that was evidenced in the literature. The IN 718 material used in this testing was initially found to be under-strength (probably underaged). Additional aging was performed on all of the test specimens to bring the material up to specifications. This was desirable because previous experience at MCAIR with under-strength steels showed that environmental sensitivity is sometimes greatly reduced in under-strength material. It was also felt that under-strength material did not represent the type of material that would normally be used for airframes. Whether the crack growth behavior of this aged, under-strength material is representative of standard IN 718 material remains uncertain, but all of the room temperature mechanical and chemical properties of this material were within specifications.

Two load-temperature-time profiles were developed for verification testing. One was based on expected usage of an advanced fighter aircraft. This profile has a maximum temperature of 800°F. This spectrum was developed by defining a typical mission scenario for a Mach 3.5 fighter, and by using the exceedance curve of a current Air Force fighter. The second spectrum was developed for an aerospace vehicle. The maximum temperature in this spectrum is 1200°F. The load profile was developed by tailoring the exceedance curve to match that of a typical transport aircraft. These spectra were developed with the help of MCAIR's Advanced Design and NASP teams. They are completely generic spectra, and do not infringe on the limits of national security.

The two load and temperature spectra were significantly different. The advanced fighter spectrum was characterized by high temperatures during supersonic cruise and dash, and high loads during quick low temperature combat maneuvers. The aerospace vehicle spectrum experiences its highest temperatures during atmospheric exit and re-entry. It experiences high temperatures and long load durations while performing atmospheric maneuvers.

The advanced fighter and aerospace vehicle spectra were used for verification of the life prediction analysis. Tests were performed on IN 718 and 6-2-4-2 Ti specimens with cracks growing out of centered EDM slots and open holes. To conduct the tests within time limitations, it was necessary to compress the load profiles such that either 10 or 100 flight hours occurred within one real hour. The temperature profiles were not modified.

The DAMAGE routine was used to predict crack growth lives within ±20 percent of test lives for 67 percent of the tests. DAMAGE was very successful in modeling crack growth behavior in tests which used a load profile compressed 100 times. Conversely, the least accurate crack growth estimates were obtained in the tests using the 10 hour compressed spectrum. This is not surprising because the later tests had to be conducted on the upper portion of the material crack growth rate curve where the analysis is extremely sensitive to slight differences in any variable, such as stress level or initial crack length. These tests had 10 times fewer load cycles per unit time than the 100 hour compressed spectrum and, therefore required more time to achieve the same amount of crack growth. The only way to conduct these tests in a reasonable

amount of time was to run them starting at crack lengths approaching the critical crack length.

While the majority of the predictions matched the test lives within 20 percent, trends in the correlation demonstrate that the simple techniques incorporated within this routine cannot be used to extrapolate the test data extensively. For instance, the real time elevated temperature tests at very high stress levels will give somewhat shorter lives than those predicted from truncated test spectrum data. As long as the test data available represent the extremes of temperature, hold time, and stress levels as predicted by the model, the predictions that interpolate this data should be accurate. In other words, the model is best used to interpolate rather than extrapolate data.

2. Analysis Procedures - The work performed under this contract was limited to relatively simple methods to account for the effects of temperature, sustained loads, and the environment on crack growth behavior. Numerous areas require improvements and/or further work. This includes modifying and enhancing some of the analytical methods used for life prediction, as well as performing additional testing.

a. Crack Growth Rate - The crack growth rate of any material depends upon several variables. These include frequency (including hold times), stress ratio, temperature, and environment. The Modified Walker and Chang equations used in CRKGRO and DAMAGE linearly or bi-linearly model high frequency crack growth data for any given stress ratio and temperature. Crack growth rate predictions at temperatures or stress ratios other than those provided as input are interpolated. As long as the applied spectrum does not exceed the limits defined by the input data, the interpolated value will be reasonably accurate.

Linear and bi-linear crack growth rate models do not always accurately represent the crack growth behavior of a material. The engine community has developed comprehensive crack growth rate models which more closely resemble the trends seen in the data. The Hyperbolic Sine Model developed by Pratt & Whitney and the Modified Sigmoidal Equation Model developed by General

Electric have shown promise. These models directly account for frequency, stress ratio, and temperature, and therefore interpolation is not required. However, these models require significantly more constant amplitude data than that generated herein to determine the required empirical parameters.

Any crack growth rate model is heavily dependent on input data. A successful model obtains accurate predictions for crack growth rate without interpolation and requires a minimum amount of input data.

b. Creep - Materials which are sensitive to creep experience a retardation in crack growth. This is caused by a blunting of the crack tip due to the increased plasticity around the crack tip. DAMAGE accounts for crack growth retardation by enlarging the plastic zone size. However, this model has serious limitations.

Crack growth retardation occurs as long as the current plastic zone size falls within the previous plastic zone. If the plastic zone size does not change from cycle to cycle, then the crack growth rate will not be retarded. Similarly, since the plastic zone size is inversely proportional to the effective yield stress, the crack growth will not retard if the effective yield stress does not change from cycle to cycle. The effective yield stress depends upon temperature, sustained load level, and the length of hold time. In constant amplitude spectra with identical load cycles, the effective yield stress does not change, and therefore the crack growth rate is not affected. Retardation will best be predicted in cases where the effective yield stress is constantly changing.

A creep method is required which models the crack tip. This model would characterize crack tip blunting, and therefore model crack growth retardation more accurately.

c. Sustained Loads - Sustained load crack growth is determined in DAMAGE using the Wei-Landes model, which integrates the creep crack growth rate with respect to time. Sustained load crack growth is calculated during the load-up and hold time portion of each cycle regardless of temperature.

143

However, tests recently conducted by Heil, Nicholas, and Haritos have indicated that sustained load growth is only a contributing factor if the creep rate increases with load and temperature (Reference 20). These tests included thermomechanical fatigue tests of IN 718. A combined constant amplitude load cycle was applied with a constant amplitude thermal cycle varying between 800°F and 1200°F. Tests were conducted in-phase (0°), out-of-phase (180°), and at two other phase angles: 90° and 270°.

Crack growth predictions were made in which it was assumed that sustained load growth only occurred during the mechanical loading portion of a cycle regardless of temperature. The 0°, 90°, and 180° phase angle data agreed well with the predictions. However the prediction for the 270° phase angle over-estimated crack growth. Although the crack growth rate increases with increased load and temperature, it does not appear to increase with increased load and decreased temperature, as is the case with a 270° phase angle.

d. <u>Load Interaction</u> - DAMAGE uses the Generalized Willenborg model to account for load interaction effects. This model examines the size of the interaction zone for each load cycle. If the current zone size is smaller than for the previous overload cycle, then the crack growth rate is reduced for that load cycle. DAMAGE also includes the Chang acceleration scheme in which the plastic zone size is reduced after the application of a compressive underload, thereby increasing the crack growth rate.

A number of researchers have shown that a crack closure (or crack opening) model may accurately represent load history effects on the crack growth behavior under various thermal and chemical environments. Such a model accounts for the previous load history effects and current load and temperature effects on crack opening displacements and thus on crack growth. Evaluation of such a closure model was, however, outside the scope of this contract. There was no time within this program to explore such a technique even though MCAIR has previously developed such a model for room temperature crack growth prediction.

3. <u>Testing</u> - Testing is an extremely important part of any model development program. The testing performed in this contract included high and low frequency crack growth subjected to various temperatures. Tests were performed in lab air and in a vacuum. As with any test program, however, complications did arise. Additional testing was performed whenever possible.

a. <u>Environmental Tests</u> - The IN 718 material tested in this program did not show any environmental sensitivity. It would be interesting to find out if properly heat treated IN 718 material would be as insensitive to hold time at load and temperature as the material used in this program.

In addition, further testing of other environmentally sensitive materials would help identify weaknesses in the Wei-Landes model incorporated into DAMAGE.

b. <u>Phasing Tests</u> - A phasing test is one in which both load and temperature profiles are constant amplitude, and both are run at the same frequency. Phasing tests can be considered simplified spectrum tests with no random loads or temperatures. These tests introduce only thermal cycling to an elevated temperature fatigue test.

Phasing tests were not performed in this test program. However, phasing tests would provide additional understanding of the material behavior. They would be useful before performing variable profile load and temperature spectrum tests.

c. <u>Spectrum Tests</u> - The spectra developed for the verification testing were significantly different. Other variations of these spectra, however, could prove useful. For example, hold time effects on spectrum crack growth could be examined by randomly inserting hold time load cycles in the spectrum.

DAMAGE predictions were not sufficiently sensitive to load spectrum time compression. Real time spectrum and compressed spectrum tests are required to further verify the analysis procedures.

In summary, the analysis techniques included in DAMAGE can be used to interpolate constant amplitude and combined thermal and mechanical load history data to predict fatigue lives within ±20 percent. However, much additional work is required to create a model capable of extrapolating simple constant amplitude isothermal crack growth data to obtain a more accurate prediction of crack growth under arbitrary thermomechanical load histories.

REFERENCES

1. Harmon, D. M. and Saff, C. R., "Damage Analysis for Manned Hypervelocity Vehicles, Volume II - Software User's Manual," Report No. WRDC-TR-89-3067, September 1989.

2. Chang, J. B., Szamossi, M., and Liu, K. W., "A User's Manual for a Detailed Level Fatigue Crack Growth Analysis Computer Code, Volume 1 - The CRKGRO Program," Report No. AFWAL-TR-81-3093, November 1981.

3. Willenborg, J., Engle, R. M., and Wood, H. A., "A Crack Growth Prediction Model Using an Effective Stress Concept," Report No. AFFDL-TM-71-1-FBR, 1971.

4. Fuchs, H. O. and Stephens, R. I., Metal Fatigue in Engineering, John Wiley & Sons, New York, 1980, pp. 208-209.

5. Wei, R. P. and Shih, T. T., "Delay in Fatigue Crack Growth," _International Journal of Fracture_, Volume 10, No. 1, March 1974, pp. 77-85.

6. Probst, E. P. and Hillberry, B. M., "Fatigue Crack Delay and Arrest Due to Single Peak Tensile Overloads," AIAA Paper 73-325, AIAA Dynamics Specialists Conference, Williamsburg, Va., March 19-20, 1973.

7. Gallagher, J. P. and Hughes, T. F., "Influence of Yield Strength on Overload Affected Fatigue Crack Behavior in 4340 Steel," Report No. AFFDL-TR-74-27, March 1974.

8. Chang, J. B., Hiyama, R. M., and Szamossi, M., "Improved Methods for Predicting Spectrum Loading Effects - Final Report, Volume I - Technical Summary," Report No. AFWAL-TR-81-3092, November 1981.

9. Johnson, H. H., "Calibrating the Electrical Potential Method for Studying Slow Crack Growth," _Materials Research and Standards_, Vol. 5, No. 9, September 1965, pp. 442-445.

10. Aerospace Structural Metals Handbook, 1987, Code 3718 - Titanium 6Al-2Sn-4Zr-2Mo, Code 4103 - Inconel 718.

11. Larsen, J. M. and Nicholas, T., "Cummulative-Damage Modeling of Fatigue Crack Growth in Turbine Engine Materials," _Engineering Fracture Mechanics_, Vol. 22, No. 4, pp. 713-730, 1985.

12. Wallace, R. M., Annis, C. G. Jr., and Sims, D. L., "Application of Fracture Mechanics at Elevated Temperatures," Final Report No. AFML-TR-76-176 Part II, April 1977.

13. Dill H. D. and Saff, C. R., "Environment-Load Interaction Effects on Crack Growth," Report No. AFFDL-TR-78-137, November 1978.

14. Newman, J. C. and Raju, I. S., "Stress Intensity Factor Equations for Cracks in Three Dimensional Finite Bodies Subjected to Tension and Bending Loads," NASA Tech Memorandum 85793, April 1984.

15. Newman, J. C., "Predicting Failure of Specimens With Either Surface Cracks or Corner Cracks at Holes," NASA TN D-8244, June 1976.

16. Tada, H., Paris, P., and Irwin, G., "The Stress Analysis of Cracks Handbook," Del Research,1973.

17. Rooke, D. P. and Cartwright, D. J., "Compendium of Stress Intensity Factors," 1976.

18. Abelkis, P. R., "Effect of Transport/Bomber Loads Spectrum on Crack Growth," Report No. AFFDL-TR-78-134, November 1978.

19. Ruschau, J. J., "Fatigue Crack Growth Rate Testing of Titanium-Aluminide, Ti-14Al-21Nb Under Combinations of Time/Temperature/Environment," University of Dayton Technical Memorandum UDR-TM-89-11, July 1989.

20. Heil, M. L., Nicholas, T., and Haritos, G. K., "Crack Growth in Alloy 718 Under Thermal-Mechanical Cycling," <u>Thermal Stress, Material Deformation, and Thermo-Mechanical Fatigue</u>, PVP-Vol,. 123, H. Sehitoglu and S. Y. Zamrik - Editors, American Society of Mechanical Engineers, 1988.

APPENDIX

LITERATURE LISTING

1. Analysis Methods

1. Nikbin, K. M., Webster, G. A., and Turner, C. E., "A Comparison of Methods of Correlating Creep Crack Growth," Advances in Research on the Strength and Fracture of Materials - Vol. 2A, D. M. R. Taplin (Ed.), Fourth International Conference on Fracture, University of Waterloo, Canada; June 1977; 1978, pp. 627-634.

With the use of materials under increasingly arduous conditions at elevated temperatures, increasing attention has been devoted recently to establishing the circumstances under which cracks could be extended by creep. Correlations are made between creep crack growth and the parameters K (stress intensity factor) and C*.

2. Corten, Herbert T., Finn, Joseph M., and Readey, William B., "Study to Determine the Suitability of Compressing the Time of Mission Profile During Elevated Temperature Fatigue Testing on Large or Full Scale Vehicles," Report No. FDL-TDR-64-52; McDonnell Aircraft Corporation; St. Louis, Missouri; September 1964.

A general method is presented for compressing the elevated temperature fatigue test time of supersonic aircraft, gust or maneuver critical, in the Mach 2 to 5 range. The problem is approached by dividing creep diagrams into realms of material behavior, which are used, in conjunction with mission characteristics, to define basic environments for which time compression criteria are developed. These individual "building blocks" are then combined to reproduce complex supersonic aircraft missions and to compress the time required for testing.

3. Cervay, Russell R., "An Empirical Model for Load Ratio and Test Temperature Effects on the Fatigue Crack Growth Rate of Aluminum Alloy

151

2024-T351," Interim Report No. AFWAL-TR-82-4025; University of Dayton, Research Institute; Dayton, Ohio; April 1982.

Constant amplitude loading fatigue crack growth rate test data were generated for aluminum alloy 2024-T351 at 20 test conditions: the combination of five load ratios (0.01, 0.1, 0.3, 0.5, 0.6) and four test temperatures (72°F, 200°F, 300°F, 400°F). A mathematical model of the shift in the linear data region with the variation in test temperature and/or load ratio was formulated.

Using the model, a predictive equation was formulated for an unexplored test condition, R = 0.35 and 250°F. Following the generation of data at the test-case load ratio/test temperature, the best fitting equation to the linear region of the test case data set was then calculated. This best fitting equation was found to agree very well with the predictive equation formulated beforehand.

4. Hirschberg, M. H., "Elevated Temperature Fatigue Testing of Metals," NASA TM 82745; Lewis Research Center; Cleveland, Ohio; December 1981.

The major technology areas needed to perform a life prediction of an aircraft turbine engine hot section component are discussed and the steps required for life prediction are outlined. These include a) the determination of the operating environment; b) the calculation of the thermal and mechanical loading of the component; c) the cyclic stress-strain and creep behavior of the material required for structural analysis; d) the structural analysis to determine the local stress-strain-temperature-time response of the material at the critical location in the component; and e) from a knowledge of the fatigue, creep, and failure resistance of the material, a prediction of the life of the component.

5. Haritos, G. K., Nicholas, T., and Painter, G. O., "Evaluation of Crack Growth Models for Elevated Temperature Fatigue," Eighteenth National Symposium on Fracture Mechanics, ASTM STP XXX, R. P. Reed, Ed., American Society for Testing and Materials, 1985.

Crack growth tests on Inconel 718 were performed at 649°C. The data from these tests were used to assess the predictive and interpolative characteristics of two crack growth models : 1) the SINH model - developed by Pratt and Whitney Aircraft which utilizes a hyperbolic sine equation and 2) the modified sigmoidal equation (MSE model) - developed by General Electric Co. The test covered variations in frequency, stress ratio, and hold time.

6. Larsen, James M. and Nicholas, Theodore, "Cummulative-Damage Modeling of Fatigue Crack Growth in Turbine Engine Materials," Engineering Fracture Mechanics, Vol. 22, No. 4, pp. 713-730,1985.

This paper reviews the modified sigmoidal equation (MSE) and the hyperbolic sine equation (SINH) as methods for crack growth prediction for metals under a variety of load conditions and in different environments. A comparison of the two methods is also presented.

7. Liu, H. W. and McGowan, J. J., "A Kinetic Analysis of High Temperature Fatigue Crack Growth," Final Report No. AFWAL-TR-81-4036; Syracuse University, Syracuse, NY; University of Alabama, University, AL; June 1981.

The increased fatigue crack growth rate at high temperature is primarily caused by environmental effects. The amount of the environmental effect depends on the penetration rate of the detrimental chemical element relative to the crack growth rate. Depending upon the relative chemical penetration rate, there can either be no, partial, or full environmental effects. In both cases of no or full environmental effects, the crack growth rate is not sensitive to cyclic frequency and temperature. In the case of partial environmental effect, the crack growth rate is controlled by the rate of the transport of the detrimental chemical element to the crack tip, and the crack growth rate is both frequency and temperature dependent. Crack growth rate data of IN 100, Waspaloy, and 304 stainless steel were analyzed. The data seem to support the analysis.

8. Nicholas, T., Weerasooriya, T., and Ashbaugh, N. E., "A Model for Creep/Fatigue Interactions in Alloy 718," Fracture Mechanics: Sixteenth

153

Symposium, ASTM STP 868, M. F. Kanninen and A. T. Hopper, Eds.,American Society for Testing and Materials, Philadelphia, 1985, pp.167-180.

An experimental investigation was conducted to evaluate the crack growth rates in Inconel 718 at 649°C under symmetric and unsymmetric triangular waveshapes and triangular waves with hold times at maximum load. An analytical model is developed which predicts crack growth rate from an integration of the sustained load crack growth rates over the cycle when time-dependent behavior is dominant. The data show that the loading portion of a cycle is the major contributor to the time-dependent crack growth behavior. At low unloading frequencies or high load ratios, however, the unloading portion of the cycle is found to become increasingly important. The model utilizes minimum baseline data and is proposed for predictions of crack growth rate over a variety of loading cycle types.

9.   Dill, H. D., and Newman, J. A., "Experimental Verification of the Suitability of Compressing the Time of Mission Profile During Elevated Temperature Fatigue Testing," Report No. FDL-TDR-64-52.

A method for compressing the elevated temperature fatigue test time of supersonic aircraft, while maintaining the true time damage level, is experimentally investigated. The problem is approached by dividing the flight mission into several separate environments, defined by material temperature and the rate of change of temperature with time. Five basic environments are defined, treated separately, and then combined to obtain a general test time compression method.

10.   Haritos, G. K., Miller, D. L., and Nicholas, T., "Sustained-Load Crack-Growth in Inconel 718 Under Nonisothermal Conditions," Journal of Engineering Materials and Technology, Vol. 107, April 1985.

Sustained-load crack-growth experiments were conducted under isothermal and non-isothermal conditions. Temperature cycling was conducted between 537°C and 647°C. Hold times at minimum and/or maximum temperature were included in the temperature profiles. An analytical model was developed to predict crack-growth rates based solely on isothermal data. The linear

154

cumulative damage model was able to predict crack-growth rates in Inconel 718 for all the temperature profiles investigated including a proof test.

11. Chang, J. B., Hiyama, R. M., and Szamossi, M. "Improved Methods for Predicting Spectrum Loading Effects," Volume 1 - Technical Summary, Final Report No. AFWAL-TR-81-3092; Rockwell International, Los Angeles, California; November 1981.

This report presents the technical details of improved methods for predicting the load interaction effects on crack growth under flight spectrum loading developed in a research effort sponsored by the USAF. These include the cycle-by-cycle crack-growth prediction method used in the detail design stage, the flight-by-flight crack growth analysis method for individual aircraft tracking usage, and preliminary design trade-off studies. Results of the experimental verification program are also presented in this document.

12. Wilson, Dale, A. (P&W) and Walker, Kevin, P. (H, K, S, Inc), "Constitutive Modeling of Engine Materials," Final Report No. AFWAL-TR-84-4073, Pratt & Whitney, West Palm Beach Florida; Hibbit, Karlsson, Sorensen, Inc., Providence, Rhode Island; July 1984.

This investigation examines the capability to predict the growth of cracks in critical structural components operating at elevated temperatures where time-dependent behavior occurs. A viscoelastic constitutive model for IN 718 was developed to determine this behavior in the area of the crack tip. The model constants were obtained from monotonically increasing cyclic and sustained loading. Therefore, the model has the capability to account for load history effects as well as material damage accumulation. Theoretical predictions are compared to the experimental results.

13. Wilson, D. A. and Warren, J. R., "Thermal Mechanical Fatigue Crack Growth - An Application for Fracture Mechanics Analyses of Gas Turbine Engine Disks," Interim Report No. AFWAL-TR-84-4185; United Technologies Corporation - Pratt & Whitney, West Palm Beach, Florida; March 1985.

155

The capability of the existing Hyperbolic Sine Model to accurately or conservatively predict the crack growth in engine components subject to thermal mechanical fatigue (TMF) was investigated. It was determined that existing empirical crack growth models adequately predict TMF crack growth under conditions tested, which reflect the current gas turbine engine Retirement for Cause requirements/applications.

14. Kaufman, Albert and Hunt, Larry E., "Elastic-Plastic Finite-Element Analyses of Thermally Cycled Double-Edge Wedge Specimens," NASA Technical Paper 1973, Lewis Research Center, Cleveland, Ohio, March 1982.

Three-dimensional elastic and elastic-plastic stress-strain analyses using the MARC nonlinear, finite-element program were performed for double-edge wedge specimens subjected to thermal cycling in fluidized beds. Elastic analysis results from the MARC program were in good agreement with previous results of elastic analyses from the NASTRAN and ISO3DQ finite-element programs.

15. Dill, H. D. and Saff, C. R., "Effects of Fighter Attack Spectrum on Crack Growth," Final Report No. AFFDL-TR-76-112; McDonnell Douglas Corporation, McDonnell Aircraft Company, St. Louis, Missouri; March 1977.

The Willenborg and Contact Stress Models are used to study the effects of spectrum loading on crack growth. Over 100 spectra variations were generated. Tests were conducted on 7075-T7351 Aluminum.

16. Wallace, R. M., Annis, C. G. Jr., and Sims, D. L., "Application of Fracture Mechanics at Elevated Temperatures," Final Report No. AFML-TR-76-176 Part II; United Technologies Corporation, Pratt & Whitney, West Palm Beach, Florida; April 1977.

The applicability of linear elastic fracture mechanics to predict crack growth at elevated temperatures is investigated. The interactive effects of stress, temperature, time, and environment on the crack growth of IN-100 are described with an interpolative empirical model based on the hyperbolic sine.

17. Abelkis, P. R., "Effect of Transport/Bomber Loads Spectrum on Crack Growth," Final Report No. AFFDL-TR-78-134; McDonnell Douglas Corporation, Douglas Aircraft Company, Long Beach, California; November 1978.

   Analytical and experimental studies were performed to study the effects of transport/bomber load spectra on crack growth. Tests were performed on 7475-T7651 aluminum. The Linear and Generalized Willenborg crack growth models were used to study the data.

18. Saff, C. R., "Environment-Load Interaction Effects on Crack Growth in Landing Gear Steels," Final Report No. NADC-79095-60; McDonnell Douglas Corporation, McDonnell Aircraft Company, St. Louis, Missouri; December 1980.

   Chemical environment-load interaction effects on crack propagation were investigated in 300M and HP-9-4-0.30 steels. Crack growth predictions were made using the Generalized Willenborg model.

19. Laflen, J. H., "Advanced Cumulative Damage Modeling," Final Report for Contract No. F33615-84-C-5032; GE Aircraft Engines, Cincinnati, Ohio.

   The objective of this contract was to develop a mathematical model for predicting crack growth in nickel-base superalloys under operating conditions that produce time-dependent and cycle-dependent effects. Tests were conducted which studied the effects of hold time, test frequency, stress ratio, and overpeak ratio on crack growth. Time-dependent crack growth models studied included interpolative models, superposition models, and retardation models.

20. Nicholas, T., Haritos, G. K., Heil, M. L., "Crack Growth in Alloy 718 Under Thermal-Mechanical Cycling," Materials Laboratory, Wright-Patterson Air Force Base, Ohio; May 1988.

   A linear cumulative damage model was developed which sums cycle-dependent and time-dependent crack damage terms to predict thermal-mechanical fatigue crack growth rates. It was observed that time-dependent damage only occured during the increasing load portion of a cycle. Testing was performed on Inconel 718.

2. Test Data

1. Sadananda, K. and Shahinian, P., "Crack Growth Under Creep and Fatigue Conditions," Creep-Fatigue-Environment Interactions, R. M. Pelloux and N. S. Stoloff, Eds., Fall Meeting of The Metallurgical Society of AIME, Milwaukee, WI; September 18-19 1979; 1980, pp. 86-112.

High temperature crack growth behavior of several structural alloys under cyclic, static and combined loads is examined. Alloys included are Alloy 718, Udimet 700, and stainless steel 304 and 316. Some of the conclusions are :

a) Crack growth under high temperature cyclic load could be due to cycle-dependent processes or time-dependent processes or a combination of the two,

b) The cycle-dependent process generally is less sensitive to micro-structure and temperature than the time-dependent process,

c) Hold time effects were dependent on applied stress intensity,

d) Time dependent crack growth is due to both creep effects and environmental effects and is very sensitive to microstructure,

e) Time dependent crack growth can be improved by changing microstructure.

2. Scarlin, R. B., "Effects of Loading Frequency and Environment on High Temperature Fatigue Crack Growth in Nickel-Base Alloys," Advances in Research on the Strength and Fracture of Materials - Vol. 2B, D. M. R. Taplin (Ed.), Fourth International Conference on Fracture, University of Waterloo, Canada; June 1977; 1978, pp. 849-858.

Nimonic 105 and In 738 LC were tested to determine the effects of frequency of fatigue loading on the crack growth rates in air and vacuum.

3. Gasc, C., Petit, J., Bouchet, B., and DeFouquet, J., "A Contribution to the Study of the Influence of Environment on Crack Growth Rate of High Strength Aluminum Alloys in Fatigue," Advances in Research on the Strength and Fracture of Materials - Vol. 2B, D. M. R. Taplin (Ed.), Fourth International Conference on Fracture, University of Waterloo, Canada; June 1977; 1978, pp.867-872.

Crack propagation results are presented for three aluminum alloys - A-U4, A-U4G1, and A-U2GN. Experiments were made on compact testing size specimens in tension tension loading and sinusoidal load-time variation, inside a vacuum chamber where pressure may get down to 10^{-3}Pa. The air vacuum effects on crack growth rate have been studied for medium rates and low or very low rates, i.e., about threshold below which fatigue crack growth will not occur.

4. Hillberry, B. M. and Crandall, C. M., "Effect of Stress Level on Fatigue Crack Delay Behavior," Advances in Research on the Strength and Fracture of Materials - Vol. 2B, D. M. R. Taplin (Ed.), Fourth International Conference on Fracture, University of Waterloo, Canada; June 1977; 1978, pp.1009-1016.

Effects of overloads and underloads on crack growth are examined in aluminum alloy 2024-T3 loaded parallel to the direction of rolling.

5. Pao, P. S., Gao, M., and Wei, R. P., "Environmentally Assisted Fatigue Crack Growth in 7075 and 7050 Aluminum Alloys," MDRL 84-67; McDonnell Douglas Research Laboratories; St. Louis, Missouri; March 1984.

Fatigue crack growth in high strength aluminum alloys has been shown to be significantly accelerated by water vapor. The effect of moisture on fatigue crack growth is strongly dependent on the frequency of load fluctuations and water vapor pressure. Results of a study of the influences of yield strength and microstructure on environmentally assisted fatigue crack growth are presented.

6. Sastry, S. M. L., "High Temperature Titanium Alloys," Memorandum MDRL-3626; McDonnell Douglas Research Laboratories; St. Louis, MO; April 9, 1985.

This is a summary of mechanical properties of conventional titanium alloys, titanium aluminides, and rapid solidification technology (RST) titanium alloys.

7. Weerasooriya, T. and Nicholas, T., "Overload Effects in Sustained Load Crack Growth in Inconel 718," Interim Report No. AFWAL-TR-85-4121, Jan. 85 - Oct. 85, University of Dayton, Dayton, Ohio; November 1985.

Crack growth rate experiments were conducted on CT specimens of Inconel 718 at 649°C. The loading spectrum consisted of a single 1 Hz cycle at R=0.1 and a hold time. The ratio of the amplitude of the hold time load to the maximum load amplitude of the fatigue cycle, R_{in}, was 1.0, 0.9, 0.8, and 0.5 with hold times from 0 to 200 seconds. Tests were performed under computer controlled constant K conditions using values of the maximum of the fatigue cycle of 40 MPa $m^{1/2}$. Data show that for R_{in} = 1.0, a linear summation model works well, while at R_{in} = 0.9 there is a measurable retardation effect on the crack growth during hold time. For values of R_{in} less than 0.8, the sustained load crack growth is almost completely retarded. A simple retardation model is proposed which can fit the experimental data and is based on the concept of an overload plastic zone being produced by the fatigue cycles. It is concluded that the hold times do not contribute to crack growth in this material unless their amplitude is at or near the maximum amplitude of the adjacent fatigue cycles.

8. Hinnerichs, T. D., Palazotto, A. N., and Nicholas, T., "Evaluation of Creep Crack Growth in IN-100 at Elevated Temperature," AIAA, 81-0540; 1981.

This paper presents an evaluation of a number of crack growth rate criteria from numerical computations of simulated creep crack growth experiments. A finite element computer program was utilized to calculate the various parameters. Both near-field or local as well as far-field criteria were examined. The results indicate that environment plays a major role in crack growth in IN-100 at 1350°F and that time effects must be considered in modeling crack growth using local criteria. Stress intensity and net-section stress were found to be adequate as correlating parameters but were unable to model observed transient phenomena.

9. Weerasooriya, T. and Nicholas, T., "Hold-Time Effects in Elevated Tempera-
ture Fatigue Crack Propagation," Interim Report, AFWAL-TR-84-4184;
University of Dayton, Dayton, Ohio; March 1985.

An experimental investigation was conducted to evaluate the effects of
hold-times on the fatigue crack growth rate of Inconel 718 at 649°C using
compact tension specimens. Tests were run under computer controlled constant
K conditions using compliance to determine crack length. Hold-times ranging
from 5 to 50 seconds were applied at maximum, minimum, and intermediate load
levels. The data show that hold-times greater than 5 seconds led to purely
time-dependent crack growth behavior which was predictable from sustained load
data using K as a correlating parameter. Hold-times at minimum or intermedi-
ate load levels had little or no effect on crack growth rate. A linear
cumulative damage model based solely on fatigue and sustained load data was
found to be adequate for spectrum loading as long as the hold-times were at
maximum load.

10. Sadananda, K. and Shahinian, P., "Effect of Specimen Thickness on Crack
Growth Behavior in Alloy 718 Under Creep and Fatigue Conditions," Naval
Research Laboratory; Washington, D.C.

Effect of specimen thickness on the high temperature crack growth
behavior in Alloy 718 has been studied under cyclic and static loads. For the
thickness variation from 6.3 to 25.4 mm, the crack growth rates under cyclic
load at 650°C were found to be independent of thickness. Likewise under
static load, for the range of 2.6 to 25.4 mm, there was no thickness effect on
the crack growth rates. However, at stress intensities close to the threshold
value, decreasing thickness decreases the growth rates and appears to increase
the threshold stress intensity as well. The observed thickness effects are
compared with those published in the literature on other materials and the
results are discussed in terms of thickness criteria for plane strain under
fatigue and in terms of micromechanisms of crack growth.

11. Harrod, D. L. and Manjoine, M. J., "Stress Controlled Creep-Fatigue Tests
on 304 SS in Air and Vacuum," ASME-MPC Symposium on Creep-Fatigue Inter-
action, R. M. Curran (Ed.), ASME, New York NY, 1976, pp. 87-101.

Mechanical data and metallographic results are presented from load controlled continuous cycle, tension hold time and creep tests on 304 SS at 1200°F in both air and vacuum environments. The results in both environments were roughly similar and showed a pronounced time dependence. The time dependence is interpreted as being due to creep effects, with the environment (oxidation) being of relatively minor importance. The deformation and fracture mode varied markedly, but systematically, throughout the wide range of test conditions.

12. Shahinian P. and Sadananda K., "Crack Growth Behavior Under Creep-Fatigue Conditions in Alloy 718," ASME-MPC Symposium on Creep-Fatigue Interaction, R. M. Curran (Ed.), ASME, New York NY, 1976, pp. 365-391.

Crack-growth behavior under static, cyclic, and combined loads were studied at 1000°F, 1200°F, and 1400°F. Application of the linear cumulative damage rule to the creep-fatigue data showed that the lives, based on fractional damage, were less than predicted, and also that the actual crack growth rates were higher than the predicted rates.

13. Michel, D. J. and Smith, H. H., "Effect of Hold Time on Elevated Temperature Fatigue Crack Propagation in Types 304 and 316 Stainless Steel," ASME-MPC Symposium on Creep-Fatigue Interaction, R. M. Curran (Ed.), ASME, New York NY, 1976, pp. 391-417.

The effect of combined cyclic and static loading on crack propagation in thermally aged and unaged Types 304 and 316 stainless steel was investigated at 800 and 1100°F. Results were evaluated on the basis of possible time-dependent deformation processes and the influence of thermal aging on relative strength of the steels.

14. Stubbington, C. A. and Pearson, S., "Effect of Dwell on the Growth of Fatigue Cracks in Ti-6Al-4V Alloy Bar," Royal Aircraft Establishment - Technical Report 76040, March 1976.

The growth of cracks in Ti-6Al-4V alloy was studied in fatigue tests in which the maximum load in each cycle was held constant for a chosen dwell-

time, and the results were compared with those obtained using sinusoidal stressing. The implications of the results are discussed for aircraft components, for example, pressure cabins, gas turbine discs etc., subjected to in-service cyclic loads such that each flight is broadly simulated by a stress pattern having a dwell-time at maximum load.

15. Bensussan, Philippe L. and Pelloux, Regis M., "Creep Crack Growth in 2219-T851 Aluminum Alloy: Applicability of Fracture Mechanics Concepts," MIT Industrial Liason Program Report 9-53-84, Massachusetts Institute of Technology, Cambridge, MA, 1984.

   Creep crack growth rate data measured in 2219-T851 aluminum alloy at 175°C in air are reported.

16. Venkataraman, S., "Elevated Temperature Crack Growth Studies of Advanced Titanium Aluminides," Final Report No. AFWAL-TR-87-4103; Systran Corporation, Dayton, Ohio; September 1987.

   Ti$_3$-Al alloyed with niobium (Ti-16Al-10Nb) was tested in air and vacuum environments at temperatures ranging from room temperature to 1200°F.

17. Rich, D. L., "Evaluation of Fracture and Crack Growth Characteristics of Titanium Alloy - Ti-6Al-2Sn-4Zr-2Mo," Report No. MDC A2388; McDonnell Douglas Corporation, McDonnell Aircraft Company, St. Louis, Missouri; June 1973.

   Residual strength tests and crack growth tests were conducted on Ti-6-2-4-2 at room temperature after exposure to temperatures of 1000°F, 1100°F, and 1200°F. The test results indicate that thermal exposure has a significant effect on room temperature residual strength and crack growth properties.

3. Test Methods

1. Larsen, J. M., Jira, J. R., and Weerasooriya, T., "Crack Opening Displacement Measurements on Small Cracks in Fatigue," ASTM 18th National Symposium on Fracture Mechanics, Boulder CO, June 1985.

A computerized interferometric displacement gage was used to monitor the crack mouth opening behavior of naturally initiated small fatigue cracks in the high strength alloy Ti-6Al-2Sn-4Zr-6Mo. An excellent correlation between crack mouth opening compliance and surface crack length was demonstrated, and the data were shown to agree with an analytical expression for part-through surface cracks. In general, the interferometric method proved to be very effective and demonstrated unique capability to monitor the behavior of very small fatigue cracks.

2.   Wilkowski, G. M. and Maxey, W. A., "Review and Application of the Electric Potential Method for Measuring Crack Growth in Specimens, Flawed Pipes, and Pressure Vessels," Fracture Mechanics - Fourteenth Symposium, Volume II: Testing and Applications, J. C. Lewis and George Sines (Eds.), ASTM Special Technical Publication 791, ASTM, Philadelphia, PA, 1981.

This paper recommends D.C. electric potential drop method for monitoring crack growth at elevated temperatures and specifies how measuring crack opening displacement can be used to account for crack tip blunting and crack initiation under monotonic or sustained loading.